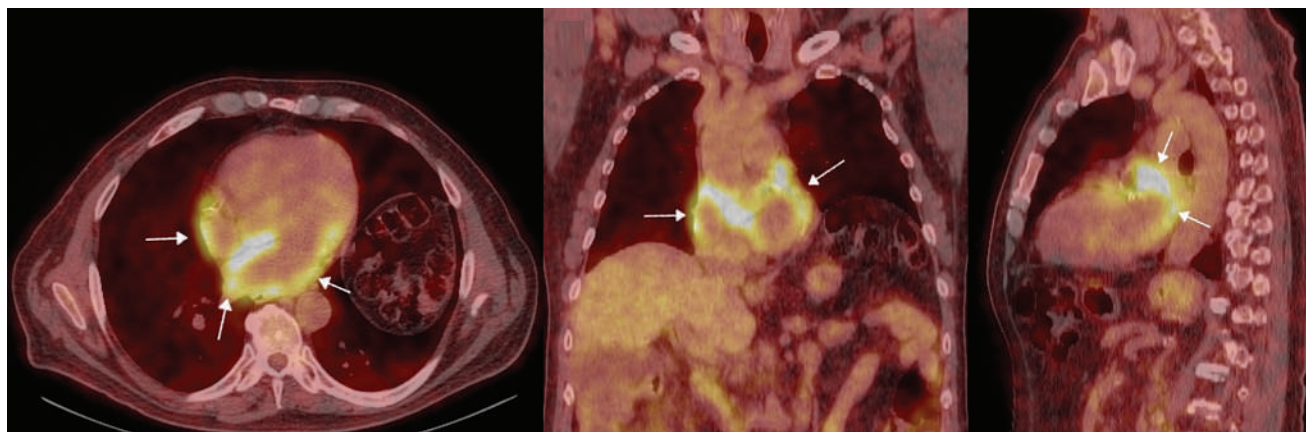


# JNM<sup>TM</sup>

Journal of Nuclear Medicine Technology

## FEATURED IMAGE

<sup>18</sup>F-FDG PET/CT Imaging Features of Cardiac Arrhythmia in a Patient Treated with Panitumumab. Pokhraj Suthar et al. See page 360.



# YOUR SOURCE FOR SODIUM IODIDE I-131

SODIUM IODIDE I-131 kit for the preparation of Iodine I-131 capsules and solution USP, Therapeutic – Oral

- The ONLY U.S. Produced Source of Sodium Iodide I-131
- Outstanding Quality
- Flexible Ordering and Delivery
- Calibrated for Date of Receipt

FDA approved and manufactured under full GMP controls.

Exceptional personalized customer service.

To find out more or to place your order please contact International Isotopes Inc. customer service at [iodineinfo@intisoid.com](mailto:iodineinfo@intisoid.com) or by calling (208) 524-5300

**Indications and Usage:** Sodium Iodide I-131 is a radioactive therapeutic agent indicated for the treatment of hyperthyroidism and selected cases of carcinoma of the thyroid.



**International Isotopes Inc.**

4137 Commerce Circle Idaho Falls, ID 83401

Toll Free: (800) 699-3108  
[www.intisoid.com](http://www.intisoid.com)

1 The product is offered in a fixed concentration of 1000 mCi/mL. In addition to the bulk solution of SODIUM IODIDE I-131 each order may include at least one carton of capsules which contains two blister packs with five empty Size 1 capsules and five dibasic sodium phosphate filled Size 2 capsules per blister (a total of 10 empty & 10 filled capsules). Larger order sizes may contain an increased number of capsule packages.

## HIGHLIGHTS OF PRESCRIBING INFORMATION

These highlights do not include all the information needed to use SODIUM IODIDE I-131 SOLUTION safely and effectively. See full prescribing information for SODIUM IODIDE I-131 SOLUTION.

**SODIUM IODIDE I-131 SOLUTION** (for the preparation of sodium iodide I-131 solution or sodium iodide I-131 capsules), therapeutic, for oral use. Initial U.S. Approval:

## INDICATIONS AND USAGE

Sodium Iodide I-131 Solution is a radioactive therapeutic agent indicated for the treatment of hyperthyroidism and selected cases of carcinoma of the thyroid. (1)

## DOSAGE AND ADMINISTRATION

- The concentrated sodium iodide I-131 solution provided must be diluted. (2.2)
- See Full Prescribing Information for important administration instructions and dilution and preparation instructions for sodium iodide I-131 capsules or oral solution. (2.2, 2.4)
- The recommended dose is based on the thyroid gland uptake as well as the size of the gland:
- Treatment of Hyperthyroidism: Recommended dosage is 148 MBq to 370 MBq (4 mCi to 10 mCi). (2.3)
- Treatment of Thyroid Carcinoma: Recommended dosage is 1,110 MBq to 3,700 MBq (30 mCi to 100 mCi). (2.3)

## DOSAGE FORMS AND STRENGTHS

Vials: Sodium Iodide I-131 Solution (with a radioconcentration pF 37,000 MBq/mL (1000 mCi/mL) at the time of calibration) for the preparation of sodium iodide I-131 capsules, therapeutic or sodium iodide I-131 solution, therapeutic. (3)

## CONTRAINDICATIONS

- Patients with vomiting and diarrhea. (4)
- Patients with thyroid malignancies shown to have no iodide uptake. (4)
- Patients receiving concurrent anti-thyroid therapy. (4)
- Pregnancy. (4)
- Lactation. (4)

## WARNINGS AND PRECAUTIONS

- Radiation-induced thyroiditis may cause or worsen hyperthyroidism. Consider pre-treatment with anti-thyroid medications. (5.1)
- Multiple non-thyroid radiation toxicities, including hematopoietic suppression: Individualize dose and monitor for toxicity. (5.2)
- Hypersensitivity Reactions: Hypersensitivity reactions including anaphylaxis may occur in patients who receive sodium iodide I-131. (5.3)
- Embryo-Fetal toxicity: May cause severe and irreversible hypothyroidism in the neonate. Verify pregnancy status in females of reproductive potential prior to initiating treatment. Females and males of reproductive potential should use effective contraception. (5.4)
- Radiation exposure to breast tissue with lactation: Sodium iodide I-131 concentrates in the breast of lactating women. Discontinue breast feeding at least 6 weeks prior to therapy. (5.5)

- Transient Infertility: Transient dose-related impairment of testicular function in men and transient ovarian insufficiency in women has been reported after sodium iodide I-131 therapy. (5.6)
- Radiation Exposure to Other Individuals: Patients should avoid close contact with others, especially pregnant women and children, and take care to avoid contamination of other persons or the environment with body fluids. Sodium Iodide I-131 Solution contributes to a patient's overall long-term cumulative radiation exposure, which is associated with an increased risk of cancer. (5.7)
- Risk of Decreased Effectiveness of Therapy: Certain food or drugs may alter the thyroid uptake of sodium iodide I-131 and diminish its effectiveness. (5.8)

## ADVERSE REACTIONS

Common adverse reactions reported with therapeutic doses of sodium iodide I-131 include local swelling, radiation sickness, sialadenitis, salivary gland dysfunction, bone marrow depression, lacrimal gland dysfunction, hypothyroidism, hyperthyroidism, thyrotoxic crisis. (6)

To report SUSPECTED ADVERSE REACTIONS, contact International Isotopes Inc. at 1-800-699-3108 or FDA at 1-800-FDA-1088 or [www.fda.gov/medwatch](http://www.fda.gov/medwatch).

## DRUG INTERACTIONS

Many pharmacologic agents are known to interact with radioiodide. See Full Prescribing Information complete list. (5.8, 7)

## USE IN SPECIFIC POPULATIONS

- Pregnancy. (4)
- Lactation. (4)
- Females and Males of Reproductive Potential: May impair fertility in females and males. (5.6, 8.3)

See 17 for PATIENT COUNSELING INFORMATION.

"V" Vial Size (mL)	Minimum (mCi)	Maximum (mCi)
1	250	750
2	400	1500
3	400	2250

# Pass the NMTCB CT Exam. We GUARANTEE it!

Because MIC is all about outcomes.

Our  
30<sup>th</sup>  
Year!

**We guarantee you'll pass the NMTCB CT Exam or *your money back!***

- Technologists must complete 35 hours of didactic education related to CT during the 3 year period prior to applying for the CT Exam.
- NMTCB has approved MIC's **CT Registry Review Program** along with **Sectional Anatomy & Imaging Strategies** to **completely satisfy that 35-hour CT didactic requirement!**
- Excellent companion for technologists in hybrid imaging.

There's no better time  
to participate in

**MIC's Self-Study CE**

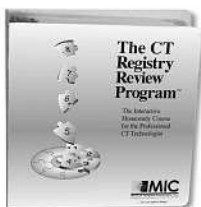
- Prepare for **CT certification**
- Satisfy NMTCB's **prerequisite**
- Ensure the **highest standards**

**Ask for the CNMT discount when you enroll in both courses!**

Technologists and their managers agree:  
**"MIC's courses really work!"**

## The CT Registry Review Program™

**Pass the CT Exam after  
completing this course  
or we will refund your  
entire tuition!**

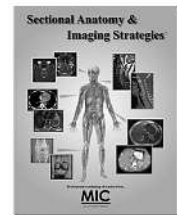


- Learn **essential** and **advanced** topics on the NMTCB and ARRT CT Exam.
- Prior training in CT is recommended.
- Pass the NMTCB or ARRT Exam in CT or your money back!
- 22 Credits      • 8 StudyModules

**5th  
Ed!**

## Sectional Anatomy & Imaging Strategies™

**Learn the essentials  
of sectional imaging in  
a convenient self-study  
format!**



- Patient positioning, artifact reduction, image orientation, slice thickness, etc., for each clinical area.
- Explains sectional imaging with over 1,000 images and figures. The perfect companion to **The CT Registry Review Program**.
- 18 Credits      • 6 StudyModules

A Proud Member of...

**SNMMI**

Call today for your  
**Free Info Kit**  
**800-589-5685**  
or visit [www.MICinfo.com](http://www.MICinfo.com)



Medical Imaging Consultants, Inc.  
1037 US Highway 46, Suite G2 • Clifton, NJ 07013 • 800-589-5685  
...for your perfect image.™

As a Gold Standard  
professional, you want  
to continually



THE AMERICAN REGISTRY  
OF RADIOLOGIC  
TECHNOLOGISTS®

# IMPROVE YOUR SKILLS

"The process was easy  
to navigate and a much  
needed refresher."



CQR helps  
you become  
even better.

Questions about CQR?

Visit ARRT's CQR Resource Center at [arrt.org/cqr](https://arrt.org/cqr)



# JNMT

Volume 49, Number 4 • December 2021

## EDITOR'S PAGE

- 295** A Constellation of NMTs Celebrate Nuclear Medicine Week  
*Kathy S. Thomas*

## CONTINUING EDUCATION

- 297** SNMMI Clinical Trials Network Research Series for Technologists: Introduction  
*Sarah Frye, Regan Butterfield, and John M. Hoffman*
- 303** SNMMI Clinical Trials Network Research Series for Technologists: Ethical Issues and Regulations in the Medical Workplace  
*Sarah Frye, Regan Butterfield, and John M. Hoffman*

## PRACTICAL PROTOCOL TIP

- 311** Technegas Lung Ventilation  
*Geoffrey M. Currie*

## CONTINUING EDUCATION

- 313** A Technical Overview of Technegas as a Lung Ventilation Agent  
*Geoffrey M. Currie and Dale L. Bailey*

## IMAGING

- 320** Lung Perfusion Scintigraphy Early After COVID-19: A Single-Center Retrospective Study  
*Sajal De, Mudalsha Ravina, Tinu Lukose, Ranganath T. Ganga, and Dibakar Sahu*
- 324** Immune Checkpoint Inhibitor–Related Adverse Effects and  $^{18}\text{F}$ -FDG PET/CT Findings  
*Jan-Henning Schierz, Ismet Sarikaya, Uwe Wollina, Leonore Unger, and Ali Sarikaya*
- 330** Can the Diagnostic Accuracy of Bone Scintigraphy Be Maintained with Half the Scanning Time?  
*Valeria M. Moncayo, Sebastine Chimafor, Elizabeth Lulaj, John A. Malko, and Raghuveer Halkar*

## RADIATION SAFETY

- 334** Occupational Radiation Exposure of Radiopharmacy, Nuclear Medicine, and Surgical Personnel During Use of [ $^{99\text{m}}\text{Tc}$ ]Tc-PSMA-I&S for Prostate Cancer Surgery  
*Else A. Aalbersberg, Desiree Verwoerd, Chelvi Mylvaganan-Young, Hilda A. de Barros, Pim J. van Leeuwen, Mariska Sonneborn-Bols, and Maarten L. Donswijk*
- 339** Establishing a Local Diagnostic Reference Level for Bone Scintigraphy in a Nigerian Tertiary Hospital  
*Musa Y. Dambele, Sikiru G. Bello, Umar F. Ahmad, Maryam Jessop, Nasiru F. Isa, and Kenneth K. Agwu*

## QUALITY & PRACTICE MANAGEMENT

- 344** Decay Correction for Quantitative Myocardial PET Perfusion in Established PET Scanners: A Potentially Overlooked Source of Errors  
*Robert Bober*

## QUALITY CASE STUDIES

- 350** Root Cause Analysis of  $\text{Na}^{131}\text{I}$  Contamination  
*Jitesh Dhingra, Cesar Santana, John Harvey, Amelia Miller, Ariel Benton, Meguewell Childs, and Raghuveer Halkar*

## TEACHING CASE STUDIES

- 354** A Case of  $^{177}\text{Lu}$ -DOTATATE Therapy Without the Use of Antiemetics  
*Justin G. Peacock, Brendan O'Sullivan, and Michael R. Povlow*
- 356** Artifact from  $^{131}\text{I}$ -Contaminated Mask in Postradioiodine Therapy Scintigraphy  
*Francesca Betti, Luca Antonacci, and Duccio Volterrani*
- 358** Rare Multisystem Histiocytic Sarcoma on  $^{18}\text{F}$ -FDG PET/CT  
*Matthew Harwood, Fiona E. Craig, and Ming Yang*
- 360**  $^{18}\text{F}$ -FDG PET/CT Imaging Features of Cardiac Arrhythmia in a Patient Treated with Panitumumab  
*Pokhraj P. Suthar, Jagadeesh S. Singh, and Khushboo Gupta*
- 362** Bone Scanning Findings in a Patient with Heat Stroke–Induced Rhabdomyolysis  
*Jitesh Dhingra and Yoram Baum*

## DEPARTMENTS

- 8A** Message from the President
- 349** Erratum

# JNMT Journal of NUCLEAR MEDICINE TECHNOLOGY

The Official Publication of **SNMMI-TS**

## Publications Committee

### Chairperson

JESSICA WILLIAMS, CNMT, RT(N), FSNMMI-TS

### Ex-Officio Member

TINA M. BUEHNER, PhD, CNMT, FSNMMI-TS

DANNY A. BASSO, MS, CNMT, NCT,  
FSNMMI-TS

ERIN B. BELOIN, CNMT, RT(CT)

AMANDA COFFEY, CNMT

GEOFFREY M. CURRIE, PHD BPHARM  
MMRS CNMT

MARY BETH FARRELL, MS, CNMT, NCT,  
FSNMMI-TS

KRYSTLE W. GLASGOW, CNMT, NMTCB(CT),  
NMAA

TOMMY LIEU, RTNM, CNMT

ELEANOR S. MANTEL, CNMT, RT(N),  
FSNMMI-TS

MATTHEW C. McMAHON, MS, CNMT, RT(CT)

FRANCES L. NEAGLEY, BA, CNMT, FSNMMI-TS

CYBIL J. NIELSEN, MBA, CNMT, FSNMMI-TS

LISA L. PATRICK, RT(N), NCT, CT, PET

KIMBERLY RAMOS, CNMT

PAUL S. RILEY, Jr., MPH, CNMT

ELIZABETH C. ROMERO, RT(N)(CT), FSNMMI-TS

KIRAN K. SOLINGAPURAM SAI, PHD

KATHY S. THOMAS, MHA, CNMT, PET,  
FSNMMI-TS

JOYCE K. ZIMMERMAN, CNMT, MBA,  
FSNMMI-TS

## Associate Director of Communications

SUSAN ALEXANDER

## Senior Publications & Marketing Service Manager

STEVE KLEIN

## Senior Copyeditor

SUSAN NATH

## Editorial Production Manager

PAULETTE MCGEE

## Editorial Project Manager

MARK SUMIMOTO

## Director of Communications

REBECCA MAXEY

## CEO

VIRGINIA PAPPAS

The *JOURNAL OF NUCLEAR MEDICINE TECHNOLOGY* (ISSN 0091-4916 [print]; ISSN 1535-5675 [online]) is published quarterly by the SNMMI, 1850 Samuel Morse Dr., Reston, VA 20190-5316; phone: (703) 708-9000; fax: (703) 708-9018. Periodicals postage paid at Reston, VA, and at additional mailing offices.

**POSTMASTER:** Send address changes to the *Journal of Nuclear Medicine Technology*, 1850 Samuel Morse Dr., Reston, VA 20190-5316.

**EDITORIAL COMMUNICATIONS** should be sent to the editor, Kathy S. Thomas, MHA, CNMT, PET, FSNMMI-TS, JNMT Office, SNMMI, 1850 Samuel Morse Dr., Reston, VA 20190-5316; phone: (703) 326-1185; fax: (703) 708-9018. To submit a manuscript, go to <http://submit-tech.snmjournals.org>.

**BUSINESS COMMUNICATIONS** concerning permission requests should be sent to the publisher, SNMMI, 1850 Samuel Morse Dr., Reston, VA 20190-5316; phone: (703) 708-9000; home page address: <http://tech.snmjournals.org>. Subscription requests, address changes, and missed issue claims should be sent to Membership Department, SNMMI, at the address above. Notify the Society of change of address and telephone number at least 30 days before date of issue by sending both the old and new addresses. Claims for copies lost in the mail are allowed within 90 days of the date of issue. Claims are not allowed for issues lost as a result of insufficient notice of change of address. For information on advertising, contact Team SNMMI (Kevin Dunn, Rich Devanna, and Charlie Meitner; (201) 767-4170; fax: (201) 767-8065; [TeamSNMMI@cunnasso.com](mailto:TeamSNMMI@cunnasso.com)). Advertisements are subject to editorial approval and are restricted to products or services pertinent to nuclear medicine. Closing date is the 25th of the second month preceding the date of issue.

**INDIVIDUAL SUBSCRIPTION RATES** for the 2021 calendar year are \$237 within the United States and Canada; \$252 elsewhere. CPC IPM Sales Agreement No. 1415131. Sales of individual back copies are available for \$58 at <http://www.snmmt.org/subscribe> ([subscriptions@snmmi.org](mailto:subscriptions@snmmi.org); fax: (703) 667-5134). Individual articles are available for sale online at <http://tech.snmjournals.org>.

**MISSION:** SNMMI-TS is dedicated to the advancement of molecular and nuclear medicine technologists by providing education, advocating for the profession, and supporting research to achieve clinical excellence and optimal patient outcomes. **VISION:** To be recognized as the leader in molecular imaging and therapy. To be dedicated to the advancement of the profession through adoption of emerging technologies.

COPYRIGHT © 2021 by the Society of Nuclear Medicine and Molecular Imaging, Inc. All rights reserved. No part of this work may be reproduced or translated without permission from the copyright owner. Individuals are asked to fill out a permission-request form at <http://tech.snmjournals.org/misc/permission.dtl>. Because the copyright on articles published in the *Journal of Nuclear Medicine Technology* is held by the Society, each author of accepted manuscripts must sign a statement transferring copyright (available for downloading at <http://tech.snmjournals.org/site/misc/ifora.xhtml>).

The ideas and opinions expressed in *JNMT* do not necessarily reflect those of the SNMMI or the Editors of *JNMT* unless so stated. Publication of an advertisement or other product mentioned in *JNMT* should not be construed as an endorsement of the product or the manufacturer's claims. Readers are encouraged to contact the manufacturer with any questions about the features or limitations of the products mentioned. The SNMMI does not assume any responsibility for any injury or damage to persons or property arising from or related to any use of the material contained in this journal. The reader is advised to check the appropriate medical literature and the product information currently provided by the manufacturer of each drug to be administered to verify the dosage, the method and duration of administration, and contraindications.



# Achieve the True Mark of **Quality & Safety** for Your Facility with IAC

A leader in accreditation for 30 years and counting, **IAC accreditation clearly indicates a 'seal of approval'** to current and prospective patients — proof that the facility has undergone a rigorous evaluation, by clinical experts, of all aspects of the operations deemed relevant to providing quality patient care.

IAC's quality solutions and resources provide facilities with a foundation to create and achieve realistic patient care goals:



The **IAC Quality Improvement (QI) Tool** allows facilities to assess their case studies and final reports, receive a quantitative report targeting opportunities for continuous improvement and satisfy a component of the MIPS Improvement Activity score.



Free access to the IAC **Online Accreditation** application including the capability to upload cases to a HIPAA-compliant, secure medical image sharing service. Trained, clinical staff are dedicated to guiding you through the process via phone, live chat or e-mail.



The IAC website offers **helpful resources** including a robust calendar of CE courses and free access to live special topic webinars, accreditation webinars and webcasts offering CE credit. Plus sample and guidance documents, accreditation checklist and more!

What can **IAC accreditation** do for ***your*** facility?

VASCULAR TESTING  
ECHOCARDIOGRAPHY  
NUCLEAR/PET  
MRI . CT . DENTAL CT



CAROTID STENTING  
VEIN CENTER  
CARDIAC ELECTROPHYSIOLOGY  
CARDIOVASCULAR CATHETERIZATION

# JNM<sup>T</sup> Journal of NUCLEAR MEDICINE TECHNOLOGY

---

## Editor

**Kathy S. Thomas, MHA, CNMT, PET, FSNMMI-TS**

*Battle Ground, Washington*

## Associate Editors

Sarah A. Frye, MBA, CNMT, PET, NCT, CCRP  
*St. Louis University  
St. Louis, Missouri*

Sara G. Johnson, MBA, CNMT, NCT,  
FSNMMI-TS  
*VA Hospital San Diego  
San Diego, California*

Sara L. Johnson, MEd, CNMT, NMTCB (RS),  
ARRT(N)(CT)  
*Hillsborough Community College  
Tampa, Florida*

April Mann, MBA, CNMT, NCT, RT(N),  
FSNMMI-TS  
*Hartford Healthcare Corporation  
Hartford, Connecticut*

Jennifer Prekeges, MS, CNMT, FSNMMI-TS  
*Bellevue College  
Bellevue, Washington*

Jessica Williams, CNMT, RT(N), FSNMMI-TS  
*HCA Healthcare  
London, England*

## Associate Editor, Continuing Education

Mary Beth Farrell, MS, CNMT, NCT, FSNMMI-TS  
*Intersocietal Accreditation Commission  
Langhorne, Pennsylvania*

## Associate Editor, Book Reviews

Frances L. Neagley, BA, CNMT, FSNMMI-TS  
*San Francisco, California*

## Consulting Editors

Norman Bolus, MSPH, MPH, CNMT,  
FSNMMI-TS  
*University of Alabama  
Birmingham, Alabama*

Patrick M. Colletti, MD  
*University of Southern California  
Los Angeles, California*

George H. Hinkle, RPh, MS, BCNP  
*The Ohio State University  
Columbus, Ohio*

Carl K. Hoh, MD  
*University of California San Diego  
San Diego, California*

Alexander W. Scott, II, PhD, DABR,  
DABSNM  
*Cedars-Sinai Medical Center  
Los Angeles, California*

Michael E. Spieth, MD  
*Rochester General Hospital  
Rochester, New York*

Jennifer R. Stickel, PhD  
*Colorado Associates in Medical Physics  
Golden, Colorado*

Alan D. Waxman, MD  
*Cedars-Sinai Medical Center  
Los Angeles, California*

## Consulting Editors (International)

Geoffrey M. Currie, BPharm,  
MMedRadSc (NucMed),  
MAppMngt (Hlth), MBA, PhD  
*Charles Sturt University  
Wagga Wagga, Australia*

John D. Thompson, PhD, MSc, BSc (HONS)  
*University of Salford  
Greater Manchester, United Kingdom*



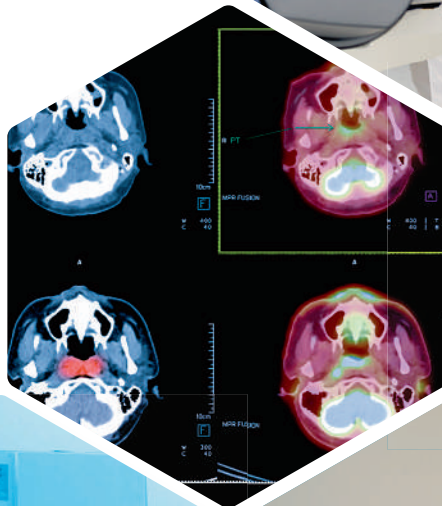


**MIRION**  
TECHNOLOGIES

# RADIATION SAFETY, EXPERTISE AND INNOVATION

Powered by an unstoppable drive for discovery. Backed by 60+ years of radiation measurement, innovation, and science expertise. Mirion's trusted family of brands and industry-leading products and services are helping to advance human health around the world.

- *Nuclear Medicine Devices*
- *Radiation Shielding and Accessories*



*Driving Innovation, Together:*



**CAPINTEC, INC.**  
Part of Mirion Technologies



**BIODEX**  
Part of Mirion Technologies

Visit [capintec.com](http://capintec.com) to learn how we can support your unique requirements.

Mirion, the Mirion logo, and other trade names of Mirion products listed herein are registered trademarks or trademarks of Mirion Technologies, Inc. or its affiliates in the United States and other countries.

BIO-331 - 11/2021

## Update on Advocacy

Dusty M. York, CNMT, PET, RT(N)(CT)

**F**all 2021 holds many exciting things for SNMMI-TS, particularly in the area of advocacy. The Scope of Practice (SOP) Committee, Technologist Advocacy Group (TAG), and Advocacy Committee hit the ground running at the start of the 2021–2022 year.

### The Model Practice Act

At the June meeting of the SNMMI-TS Executive Board, the second edition of the Model Practice Act (MPA) was approved. The MPA is a legislative tool that equips our TAG representatives, state legislators, and other technologist state advocates with the information they need to help ensure that nuclear medicine technology is administered by qualified professionals. Since improper administration of ionizing radiation and radiopharmaceuticals can lead to harmful effects for individual patients and the public, it is essential to educate legislatures about nuclear medicine technology and about what certified and licensed nuclear medicine technologists do. For example, before legislation is introduced, we work with our partners at the American Registry of Radiologic Technologists and the American Society of Radiologic Technologists to make sure the draft includes pertinent nuclear medicine definitions, recommendations on the composition of a medical board, and other critical information.

This second edition of the MPA went through three rounds of review and voting within the SOP Committee. It was also reviewed by Advocacy Committee members, who had additional input. Additions included the definition of the *nuclear medicine advanced associate* (NMAA) and the explicit statement that “a nuclear medicine technologist is a medical professional.” We found this statement to be imperative to establish public awareness that the nuclear medicine technologist is a medical professional and an essential part of the nuclear medicine care team. Other changes to the MPA included refining the definition of an *Authorized User* and streamlining the patient care management section (for nuclear medicine technologists and NMAAs) to refer to the patient care management section of the Scope of Practice and Standards document. The second edition of the MPA may be found at <http://ow.ly/pEff30rYjHk>.

### State Advocacy

At this point in the year, Michigan and Pennsylvania are the only states left that have active legislative sessions (since their sessions are year-long). Our very own Pennsylvania TAG representative, Janice Van Dolsen, represented the society

in an informational meeting on October 6 for H.B. 1440, the licensure bill. The bill is now moving forward. Michigan is also waiting for an informational meeting; Michigan TAG representative Melissa Snody will represent the society when it occurs. Michigan’s bill is not a licensure requirement; rather, House Bill 5116 will enable the Department of Labor and Economic Opportunity to certify nuclear medicine technologists who meet the requirements for registration and certification for nuclear medicine technology under the ARRT, Nuclear Medicine Technology Certification Board (NMTCB), and/or equivalent standards. Grassroots efforts are underway.

Various other states are gearing up for legislative sessions that begin in January. Alabama’s bill will be reintroduced. Although Georgia’s bill does not yet have regulatory buy-in, it does have the governor’s approval; now it must be presented to the composite medical board for feedback. A grassroots campaign for Missouri licensure will likely begin this December. A public relations campaign is underway to bring awareness to the lack of medical imaging operators standards.

### The FIND Act

For the first time since SNMMI and its partners (MITA and CORAR) began advocating for the separate reimbursement of diagnostic radiopharmaceuticals in the hospital outpatient setting, we have a bicameral bill. H.R. 4479 was introduced in the House on July 16, and S. 2609 was introduced in the Senate weeks after. Before introduction, SNMMI held 3 dozen virtual fly-ins. Recently, the society has participated in numerous fly-ins as a coalition.

It has been all hands on deck for SNMMI-TS members! Various nuclear medicine technologists from the Advocacy Committee, TAG, and SOP Committee represented the society and voiced their concerns on CMS’s packaging policy—and in the past few months, SNMMI members have sent more than 400 letters of support to their members of Congress. As a result, the House bill now has 17 co-sponsors, and more are joining every week. More work needs to be done to secure co-sponsors on the Senate side, and we will look to our nuclear medicine technologists to assist us with those fly-ins. Although passage by the end of the year seems unlikely at this point due to the current political climate, we are confident in its passage next year.



Dusty M. York, CNMT,  
PET, RT(N)(CT)

# A Constellation of NMTs Celebrate Nuclear Medicine Week

Kathy S. Thomas, MHA, CNMT, PET, FSNMMI-TS

Editor, *JNMT*

It's early fall, and a "constellation of nuclear medicine technologists" (an innovative term coined by a fellow technologist, Geoff Currie, in Australia) worldwide is raising the flag of professional pride to celebrate all aspects of nuclear medicine and molecular imaging during Nuclear Medicine Week. The concept of a constellation of nuclear medicine technologists plays on the idea of scintillation and reinforces that we are all a bunch of stars that shine brightly on a dim background! Nuclear Medicine Week allows us to share our commitment to our patients and reinforce how nuclear medicine and molecular imaging continue to transform medicine and improve lives.

In this issue, a new article category is being launched: Quality Case Studies. A quality case study is an institution's internal review process using standard quality assessment tools (e.g., a root cause analysis using Lean or Six Sigma methodology) to assess a significant issue or problem and identify solutions, with the ultimate goal of preventing and solving underlying issues. For example, the study presented in this issue is related to a therapeutic administration of  $^{131}\text{I}$  that resulted in significant contamination of the department and personnel (1). The subsequent quality analysis of the problem explored all variables, identified a corrective action, and verified the effectiveness.

Has your hospital or clinic performed a recent quality case study that can help other nuclear medicine professionals? Consider sharing your information so others may benefit from your findings. The template for presenting this information is very straightforward: a brief, unstructured abstract followed by 4 sections—an introduction (a detailed description of the event, answering the questions what, how, when, where, and who), a "Quality Analysis" section (repeatedly asking the question why until a solution to the error is found), a "Corrective Action" section, and a "Verification of Effectiveness" section. Sharing your information is the first step in helping others improve the quality of the services provided and, perhaps, avoid a brewing problem.

Three continuing education articles are included in this issue. I am excited to announce the launch of the SNMMI Clinical Trials Network research series for technologists, which will provide fundamental clinical research information for both experienced and new nuclear medicine technologists

working in academic or research settings or interested in a potential new career pathway. This series will help bridge the instruction gaps in nuclear medicine technologist programs or on-the-job training. Technologists will learn the common language of clinical trials, examine ethical and regulatory considerations, and review the different types of clinical studies involving imaging and radiopharmaceutical therapy agents. The first 2 articles in this series are included in this issue. The first article serves

as an introduction to the topic as a whole (2). The second introduces the concept of ethical issues and the regulatory agencies that maintain best practices in clinical research (3). Rounding out our continuing education articles for 2021 is an introduction to Technegas (Cyclomedica) lung ventilation studies (4). This topic may seem like old news to the international community; however, in the United States, Technegas has yet to be approved. Thus, an educational offering is required in anticipation of its approval in 2022. A practical protocol tip (5) on Technegas ventilation is included to complement the Technegas continuing education article and can be added to the department's procedure manual and incorporated into clinical practice on approval.

Complications associated with COVID-19 patients continue to challenge health-care professionals worldwide. Sajal De et al. present an interesting discussion on the incidence of thromboembolic complications and the risk factors for mismatched perfusion defects (6).

PSMA-based image-guided surgery is used to prevent incomplete resection and improve intraoperative detection and clearance of nodal metastasis. Else Aalbersberg et al. discuss the estimation and measurement of occupational radiation exposure for all personnel involved in the production, administration, imaging, and surgery associated with this technique (7).

Finally, don't miss the remaining teaching case studies and scientific articles offering diverse topics of interest.

The December issue concludes my fourth year as *JNMT* editor. The support and input from my associate and



**Kathy S. Thomas,  
MHA, CNMT, PET,  
FSNMMI-TS**

consulting editors and the patience and dedication of the SNMMI publication staff continue to improve *JNMT* content. However, your input is also essential in helping *JNMT* meet the technical needs of the nuclear medicine community. If you have comments or suggestions, please contact me at [ksthomas0412@msn.com](mailto:ksthomas0412@msn.com).

Wishing you all the happiest of holidays and a safe and healthy new year.

## REFERENCES

1. Dhingra J, Santana C, Harvey J, et al. Root cause analysis of Na<sup>131</sup>I contamination. *J Nucl Med Technol.* 2021;49: 350–353.
2. Frye S, Butterfield R, Trembath L, Hoffman JM. SNMMI Clinical Trials Network research series for technologists: introduction. *J Nucl Med Technol.* 2021; 49: 297–302.
3. Frye S, Butterfield R, Trembath L, Hoffman JM. SNMMI Clinical Trials Network research series for technologists: ethical issues and regulations in the medical workplace. *J Nucl Med Technol.* 2021;49: 303–310.
4. Currie GM, Bailey DL. A technical overview of Technegas as a lung ventilation agent. *J Nucl Med Technol.* 2021;49: 311–317.
5. Currie GM. Technegas lung ventilation. *J Nucl Med Technol.* 2021;49: 318–319.
6. De S, Ravina M, Lukose T, et al. Lung perfusion scintigraphy early after COVID-19: a single-center retrospective study. *J Nucl Med Technol.* 2021;49: 320–323.
7. Aalbersberg EA, Verwoerd D, Mylvaganan-Young C, et al. Occupational radiation exposure of radiopharmacy, nuclear medicine, and surgical personnel during use of [<sup>99m</sup>Tc]Tc-PSMA-I&S for prostate cancer surgery. *J Nucl Med Technol.* 2021;49: 334–338.



# SNMMI Clinical Trials Network Research Series for Technologists: Introduction

Sarah Frye<sup>1</sup>, Regan Butterfield<sup>2</sup>, and John M. Hoffman<sup>2,3</sup>

<sup>1</sup>Department of Clinical Health Sciences, St. Louis University, St. Louis, Missouri; <sup>2</sup>Center for Quantitative Cancer Imaging, Huntsman Cancer Institute, University of Utah, Salt Lake City, Utah; and <sup>3</sup>Huntsman Cancer Institute, University of Utah School of Medicine, Salt Lake City, Utah

**CE credit:** For CE credit, you can access the test for this article, as well as additional JNMT CE tests, online at <https://www.snmlearningcenter.org>. Complete the test online no later than December 2024. Your online test will be scored immediately. You may make 3 attempts to pass the test and must answer 80% of the questions correctly to receive 1.0 CEH (Continuing Education Hour) credit. SNMMI members will have their CEH credit added to their VOICE transcript automatically; nonmembers will be able to print out a CE certificate upon successfully completing the test. The online test is free to SNMMI members; nonmembers must pay \$15.00 by credit card when logging onto the website to take the test.

The field of nuclear medicine and molecular imaging has grown tremendously over the past several years with the approval of new imaging agents, diagnostic radiopharmaceuticals, and radiopharmaceutical therapies. Clinical research continues to expand within nuclear medicine and molecular imaging departments. Working as a nuclear medicine technologist on a clinical trial or with investigational radiopharmaceuticals can be quite different from working in an approved-drug setting in the clinic. Nuclear medicine technologists involved in clinical trials can be at the front line of following rigorous trial requirements and ensuring good-quality data. The details of working in clinical research are often not taught in nuclear medicine technologist programs. As such, there is an emerging need for education about clinical research for both experienced and new nuclear medicine technologists, particularly for those working with investigational radiopharmaceuticals. This article is an introduction to the SNMMI Clinical Trials Network Research Series for Technologists. This series of articles aims to provide education on working in the context of a clinical trial within the nuclear medicine department. The following 7 topics will be addressed in the series: ethical issues in clinical research, application of good clinical practice to clinical research in medical imaging, contract research organizations with application in clinical imaging, a clinical research primer on the regulatory process for how and when radiopharmaceuticals can be used and the role of the institutional review board, use of imaging agents in therapeutic drug development and approval, imaging agent trials, and imaging agents with radiopharmaceutical therapies in clinical trials. Other topics may be added over the course of the development of the series.

**Key Words:** clinical research; FDA; good clinical practice; protocol; clinical trial

**J Nucl Med Technol 2021; 49:297–302**

DOI: 10.2967/jnmt.121.263099

Received Aug. 28, 2021; revision accepted Oct. 4, 2021.  
For correspondence or reprints, contact Sarah Frye ([sarah.frye@health.slu.edu](mailto:sarah.frye@health.slu.edu)).

COPYRIGHT © 2021 by the Society of Nuclear Medicine and Molecular Imaging.

An important goal for this series of articles is to provide clinical research education to nuclear medicine technologists and information to those in our community interested in the use of molecular imaging as a biomarker and in the development, regulatory, and approval process for new, investigational molecular imaging diagnostic and therapeutic radiopharmaceuticals. Various sources of information are available and valuable to review (1–4). The Society of Nuclear Medicine and Molecular Imaging (SNMMI) created the Clinical Trials Network (CTN) in 2008 to advance the use of molecular imaging and therapeutic radiopharmaceuticals in clinical trials. Through the work of its committees (a database committee, a committee that validates scanners and qualifies sites, an education committee, a gallium users group/committee for access to nonproprietary radiopharmaceuticals, and a radiopharmaceutical manufacturers committee), the CTN fulfills its mission of facilitating the effective use of diagnostic and therapeutic molecular imaging and radiopharmaceuticals in clinical trials in many ways. One way is by maintaining a searchable database of molecular imaging and radiopharmaceutical production sites to assist clinical trial sponsors with site selection for their studies. Another is by validating PET/CT scanners with the CTN proprietary chest oncology phantom to ensure that the scanners are producing accurate quantitative data, as well as providing harmonized reconstruction parameters across multiple centers. In addition, the CTN characterizes and calibrates SPECT/CT scanners to ensure that they are producing accurate quantitative data, to assist with dosimetry measurements for radiopharmaceutical therapy dose determinations. The CTN also audits investigational radiopharmaceuticals produced for clinical trials under investigational-new-drug applications to help ensure the safety, consistency, and purity of the drugs being administered to study patients, as well as assisting with trial design and protocol development for molecular imaging and radiopharmaceutical therapy clinical trials. Finally, the CTN develops

educational programs for live meetings, webinars, and online courses, including imaging interpretation training sessions that help nuclear medicine professionals learn about working in clinical research and about translating clinical trial experience into the clinical implementation of new tracers and radiopharmaceutical therapies after approval (5).

The nuclear medicine field has experienced a decade of growth in Food and Drug Administration (FDA) approvals from 2011 to 2021 (Table 1), with 2 SPECT imaging agents, 8 PET oncology imaging agents, 5 PET brain imaging agents, and 3 radiopharmaceutical therapy agents approved (6,7). These approved radiopharmaceuticals are being used as biomarkers in clinical trials of therapeutic drugs to assess response.

Because of the growth in radiopharmaceutical approvals (6), there is also more interest in, and a greater need for, education about clinical research, the process and challenges for approvals, and implementation of new imaging agents and radiopharmaceutical therapies into the clinic. With recent approvals and anticipated future approvals of radiopharmaceutical therapies, the SNMMI CTN therapy toolkit was created to provide educational tools, including a therapy implementation checklist, and to help sites establish a successful radiopharmaceutical therapy program (8). Working in a clinical trial context can create a set of challenges different from those in an approved-drug setting. Nuclear medicine technologists must learn new terms and acronyms that are common language in clinical trials, understand the complexities of a protocol, and be able to follow rigorous clinical trial requirements to provide quality data. Since most nuclear medicine technology programs do not address these details, the CTN has provided this series of articles to help meet the educational needs of nuclear medicine technologists working in clinical research. This introductory article begins with an overview of some basic terms and concepts included in clinical trials and then summarizes the subsequent set of articles in the series.

## OVERVIEW OF BASIC TERMS, CONCEPTS, AND PHASES OF CLINICAL TRIALS

There are many terms, acronyms, and concepts involved in clinical trials that may be new to nuclear medicine technologists. Learning the language of clinical trials is important for nuclear medicine technologists to be able to understand instructions within a protocol, provide high-quality data, and communicate with the sponsor and research team. The CTN currently has a couple of courses in the SNMMI Learning Center that provide an overview of research team members, study documents, phases of clinical trials, and common terms and acronyms used in clinical research: “CTN Course 102: The Language of Clinical Trials” (9) and “CTN Course 116: Imaging in Clinical Research—Elements for Success” (10). Definitions are

given below for many of the common terms (in alphabetical order):

- Adverse drug reaction: An unintended reaction to a drug taken at normal doses (11).
- Adverse event: Any untoward medical occurrence in a study subject who has been administered a pharmaceutical product; it does not necessarily need to have a causal relationship with this treatment (11).
- Blinding (masking): The process thorough which study subjects, the investigator, or other involved parties in a clinical trial are kept unaware of the treatment assignments of study subjects (11).
- Case history: The investigator’s subject source documents and case report forms for a trial (11).
- Case report form: A record of pertinent information collected on each subject based on the protocol during a clinical trial (11).
- Clinical research associate (monitor): A sponsor monitor who visits sites periodically during a study to monitor data and assess study progress (11).
- Clinical research coordinator (study coordinator, research coordinator): A person at the investigational site who manages the daily operations of a clinical investigation and reports to the investigator (11). An individual can become a certified clinical research coordinator by having 2 or more years of experience and passing an exam (11).
- Clinical trial (clinical study, clinical investigation): Any experiment that involves a test article (drug, device, biologic) and one or more human subjects (11).
- Code of Federal Regulations: Organization of rules published by the U.S. federal government departments and agencies; divided into 50 titles (12).
- Contract: A written, dated, and signed agreement between 2 or more parties that lays out any arrangements or delegation and distribution of tasks and obligations, including, if appropriate, on financial matters (11).
- Contract research organization (CRO): A person or organization with which the sponsor contracts to perform one or more of the sponsor’s trial-related duties and functions (11).
- Control group: A group of subjects who are not treated with the investigational product; this group is compared with the treatment group (11).
- Data management: The process of handling the data generated and collected during a clinical trial, usually including data entry and data management (11).
- Double-blind: The design of a study in which neither the investigator nor the subjects know which treatment the subject is receiving (11).
- Drug: An article (other than food) intended for use in the diagnosis, cure, mitigation, treatment, or prevention of disease in humans or animals (11).
- Essential documents: Documents that individually and collectively permit evaluation of the conduct of a study and the quality of the data produced (11).
- FDA form 1572: A legally binding, signed agreement between the principal investigator and the FDA that the former will conduct the study in accordance with the protocol (10).
- Good clinical practice (GCP): The regulations and guidelines that specify the responsibilities of sponsors, investigators, monitors, and institutional review boards (IRBs) involved in clinical

**TABLE 1**  
FDA-Approved Molecular Imaging and Therapeutic Radiopharmaceuticals from 2011 to 2021 (6,7)

Year of approval	Drug	Indication	Modality
2011	<sup>123</sup> I-ioflupane (DaTscan; GE Healthcare)	Parkinson disease	Single-photon imaging
2012	<sup>18</sup> F-florbetapir (Amyvid; Eli Lilly)	Alzheimer disease	PET brain imaging
2012	<sup>11</sup> C-choline (Mayo Clinic)	Prostate CANCER	PET oncology
2013	<sup>123</sup> I-MIBG iobenguane (Progenics)	Pheochromocytoma, paraganglioma	Single-photon imaging
2013	<sup>223</sup> Ra-dichloride (Xofigo; Bayer Healthcare)	Prostate cancer	Radiopharmaceutical therapy
2013	<sup>18</sup> F-flutemetamol (Vizamyl; GE Healthcare)	Alzheimer disease	PET brain imaging
2014	<sup>18</sup> F-florbetaben (Neuraceq; Piramal)	Alzheimer disease	PET brain imaging
2016	<sup>18</sup> F-fluciclovine (Axumin; Blue Earth)	Prostate cancer	PET oncology
2016	<sup>68</sup> Ga-DOTATATE (Netspot; AAA/Novartis)	Neuroendocrine cancer	PET oncology
2018	<sup>177</sup> Lu-DOTATATE (Lutathera; AAA/Novartis)	Neuroendocrine cancer	Radiopharmaceutical therapy
2018	<sup>131</sup> I-MIBG iobenguane (Azedra; Progenics)	Pheochromocytoma, paraganglioma	Radiopharmaceutical therapy
2019	<sup>68</sup> Ga-DOTATOC (University of Iowa)	Neuroendocrine cancer	PET oncology
2019	<sup>18</sup> F-fluorodopa (Feinstein Institute)	Parkinson disease	PET brain imaging
2020	<sup>18</sup> F-fluoroestradiol (Cerianna; Zionexa)	Breast cancer	PET oncology
2020	<sup>18</sup> F-flortaucipir (Tauvid; Lilly)	Alzheimer disease	PET brain imaging
2020	<sup>64</sup> Cu-DOTATATE (Detectnet; RadioMedix-Curium)	Neuroendocrine cancer	PET oncology
2020	<sup>68</sup> Ga PSMA-11 (UCSF-UCLA)	Prostate cancer	PET oncology
2021	<sup>18</sup> F-DCFPyL or <sup>18</sup> F-piflufolastat (Pylarify; Lantheus)	Prostate cancer	PET oncology

trials. They are meant to protect the safety, rights, and welfare of subjects while ensuring the accuracy of data collected (11).

- Human subject (study subject, study participant): An individual who participates in research, either as a recipient of the test article or as a control (11).
- Imaging manual: A document that contains detailed information on the scanning requirements for a clinical trial, such as patient preparation, dose, uptake time, acquisition and reconstruction parameters, deidentification, and image transmittal requirements (10).
- Inclusion and exclusion criteria: The characteristics that must be present (inclusion) or absent (exclusion) for a subject to qualify for a clinical trial, as per the protocol for the trial (11).
- Informed consent: The process by which a subject, after reviewing the clinical trial procedures, voluntarily provides a signature to confirm willingness to participate (11).
- IRB: Any board, committee, or group formally designated to review biomedical research involving human subjects, approve the initiation of such research, and periodically review it (11).
- IRB approval: The determination of an IRB that a clinical investigation may be conducted within the constraints set by the IRB and applicable regulations (11).
- International Conference on Harmonization: A conference that promotes public health safety through international harmonization (13).
- Investigational-new-drug application: The application submitted to the FDA per regulations within title 21, part 312, of the *Code of Federal Regulations* to start clinical testing of a new drug or biologic in humans (11).
- Investigator (clinical investigator, principal investigator): An individual who conducts a clinical investigation—that is, under whose immediate direction the test article is dispensed or, in the case of an investigation conducted by a team of individuals, who is the responsible team leader (11).
- Investigator brochure: A compilation of all information known to date about the test product, including chemistry and formulation information and preclinical and clinical data. It is updated at least annually. Once the product is marketed, it is replaced by the package insert for the product (11).
- Legally authorized representative: An individual, a judicial body, or another body authorized under applicable law to consent on behalf of a potential subject to the subject's participation in research (11).
- Minimal risk: A term indicating that the probability and magnitude of harm or discomfort anticipated in the research are not greater than those ordinarily encountered in daily life or routine medical care (11).
- New-drug application: The marketing application for a new drug submitted to the FDA under the requirements of title 21, part 314, of the *Code of Federal Regulations*. The new-drug application contains all nonclinical, clinical, pharmacologic, pharmacokinetic, and stability data required by the FDA (11).
- Placebo: An inactive substance designed to resemble the drug being tested (11).
- Quality assurance: Systems and procedures designed to ensure that a study is being performed in accordance with GCP guidelines and that the data being generated are accurate (11).
- Radioactive drug research committee: A committee that reviews research protocols that include the use of radioactive drugs and approves those protocols once a certain list of requirements is met (14).
- Randomization: A method by which study subjects are randomly assigned to treatment groups. It helps to reduce bias in a trial by ensuring that there is no pattern in the way subjects are assigned to treatment groups (11).
- Regulatory coordinator: A member of the research team who is responsible for submitting protocol documents to the IRB and maintaining regulatory files (9).

- Scientific review committee: A committee that reviews research protocols for scientific merit to determine whether involvement of human subjects is justified (10).
- Serious adverse event: After administration of any dose of a drug, any untoward medical occurrence that results in death, is life-threatening, requires hospitalization, or results in persistent or significant disability or incapacity; a serious adverse event can also be a congenital anomaly or birth defect (11).
- Source document: Original documents and records including, but not limited to, hospital records, clinical and office notes, laboratory notes, subjects' diaries or evaluation checklists, pharmacy records, copies of transcripts, images, and subject files (11).
- Sponsor: A person or entity who initiates a clinical investigation but does not actually conduct the investigation (11).
- Standard operating procedures: Official written instructions for the management and conduct of clinical trial processes, ensuring that they are performed consistently and efficiently (11).
- Study protocol: The formal plan for carrying out a clinical investigation.
- Study protocol amendment: Planned changes to the protocol that must be approved by the review boards before being applied to the participants.
- Study protocol deviations: Any change, divergence, or departure from the study design or procedures defined in the protocol (15).
- Study protocol exception (planned protocol deviation): A temporary protocol deviation that is preapproved by the funding agency.
- Study protocol violation (important protocol deviation): A change, divergence, or departure from the study requirements, whether by the subject or the investigator, that resulted in a subject's withdrawal from study participation (15).
- Subinvestigator (coinvestigator): An individual who performs critical clinical trial-related procedures or makes important decisions and is supervised by the investigator (9).
- Unanticipated event: A problem involving risks to human subjects or others participating in a clinical research study. These events need to be collected and reported (11).

Clinical trials involve active participation of people to test the safety and efficacy of new medical treatments (16). Clinical trials are divided into phases (Table 2); the different phase numbers serve as markers or milestones in the drug development process and are not necessarily distinct consecutive periods (16). The regulatory aspects of a clinical trial for an approved agent being studied in a therapeutic drug trial can differ from those for a new diagnostic radiopharmaceutical being studied for eventual approval. The drug development process can be further complicated by the fact that the approved agent may still be carefully monitored, particularly if the trial is a response assessment. Having a knowledge of the basic terms described above will increase one's understanding of the topics that will be discussed in the series.

## **SERIES TOPIC 1: ETHICAL ISSUES IN CLINICAL RESEARCH**

To understand what it means to conduct ethical medical studies and work in clinical research, it is important to be

familiar with the historical context of why current enforceable policies exist in clinical practice and in clinical trial regulations. This first topic in the series will review several agencies, mostly in the United States, that oversee both clinical and research policies in medical practice. Some of the agencies and their responsibilities discussed in this article include the FDA (which ensures the safety, efficacy, and security of human and veterinary drugs, biologic products, and medical devices (17)), the Nuclear Regulatory Commission (which ensures that radioactive materials are used safely (18)), the Joint Commission (which encourages excellence and quality while evaluating health-care organizations (19)), the Office for Human Research Protection (which provided leadership for protecting human subjects in research (20)), and the World Health Organization (which helps ensure healthy lives and the well-being of all peoples (21)).

This article moves into a discussion of the ethical requirements for humans involved in clinical research. It explores the historical examples of medical mistreatment in research and the main regulations developed to guide current researchers in informed research studies. Some of these ethical principles and laws that have shaped clinical research practices include the U.S. *Code of Federal Regulations*, the Nuremberg Code, the Declaration of Helsinki, and the Belmont Report. These all work together to help manage the applicable ethical and scientific quality standards included in GCP, which outlines the responsibilities of the investigator, sponsor, and institution involved in human subject research, as well as the design of clinical trials (22).

## **SERIES TOPIC 2: APPLICATION OF GCP TO CLINICAL RESEARCH IN MEDICAL IMAGING**

After understanding the context of the development of current clinical trial regulations, it is important to know the meaning of those regulations, the language used in clinical trials, and how the regulations and language all apply toward GCP. The objective of this second topic in the series includes the importance of GCP and the relationship between GCP and federal regulations that govern human subject research in the United States. The article will describe good documentation practices for collection and recording of raw and processed data; define source material, source documents, and the differences between them; characterize the critical role of technologists in mitigating key risks to data standardization in trials that rely on imaging endpoints; and describe how to read and follow a sponsored research protocol while relying on key supplemental documents such as an imaging charter.

The article also provides other material useful for readers, including the use of documentation tools such as a delegation log and drug accountability log; definitions and descriptions of adverse event; the role of the medical imaging provider in reporting adverse events to the sponsor; and the need to work together with the sponsor, investigator,



**TABLE 2**  
Phases of Clinical Trials (16)

Phase	Primary purpose	Study participants
Preclinical	Collect data to determine basic physical, chemical, and biologic characteristics of new compound	Cell studies and animal studies
I	Safety in humans	Healthy volunteers or people with the disease or condition (usually 20–100 participants)
II	Efficacy in target/disease condition; determination of dose	People with the disease or condition (usually a few hundred participants)
III	Efficacy and monitoring of adverse events; comparison to current standard treatment	People with the disease or condition (often thousands of participants)
IV	Safety and efficacy over time, usually after FDA approval	People with the disease or condition (usually thousands of participants)

and study coordinator to produce high-quality, reproducible, and audit-ready data.

### **SERIES TOPIC 3: CROS WITH APPLICATIONS IN CLINICAL IMAGING**

CROs can play a major role in ensuring safe and ethical clinical trials, which help in the development of new drugs and medical devices that benefit millions of patients worldwide (23). Sponsors contract with imaging CROs, which assume the responsibility of performing services or managing the imaging portion of the trial. These aspects often include writing imaging manuals, reviewing image charters, qualifying and training sites, collecting and performing quality control of study images, and performing image analysis. Clinical research conducted by CROs increased 40% from 2008 to 2014 and is expected to reach over \$45 billion a year by 2022 (23). This third topic of the CTN series will discuss, in detail, clinical trial management and tasks performed by an imaging CRO, common primary and secondary endpoints tied to imaging in clinical trials, centralized image review with response assessment criteria, potential safety assessments measured during clinical trials, and the use of nuclear medicine and molecular imaging in drug development.

Finally, the article will discuss how an imaging CRO can serve as a gateway to a research-focused career for nuclear medicine technologists.

### **SERIES TOPIC 4: CLINICAL RESEARCH PRIMER—REGULATORY PROCESSES, PARTS I AND II (HOW AND WHEN RADIOPHARMACEUTICALS CAN BE USED AND THE ROLE OF THE IRB)**

Regulatory processes are developed to ensure patient safety, patient privacy, and data integrity while conducting effective research. This fourth topic in the series will familiarize the reader with the regulatory process for clinical research involving radiopharmaceuticals by providing a basic understanding of how and when radiopharmaceuticals can be used. This focus will identify and explain the role of the IRB or ethics committee in protecting human subjects. It will continue to define terms, exemptions, and processes

that are specific to the clinical research environment. This topic will describe the importance of a clinical trial and how the protocol needs to be written and interpreted to comply with the objectives of the research being performed.

### **SERIES TOPICS 5–7: USE OF IMAGING AGENTS IN THERAPEUTIC DRUG DEVELOPMENT AND APPROVAL, IMAGING AGENT TRIALS, AND IMAGING AGENTS WITH RADIOPHARMACEUTICAL THERAPIES IN CLINICAL TRIALS**

Molecular imaging agents used as a biomarker in clinical trials can provide sponsors of therapeutic agents, such as a chemotherapy for cancer, with valuable information to determine eligibility, efficacy, and response. This can be done by showing either the presence or lack of disease, by confirming whether the drug would bind to a particular target, and by predicting or showing a patient's response to therapy. The last 3 topics in this series will review the use of imaging in clinical trials and discuss many aspects of clinical research, including inclusion and exclusion criteria, biomarkers, surrogate endpoints, test–retest variability, radiolabeling of a drug, biodistribution, monitoring and audit processes, clinical and research lab assessments, dosimetry, tumor response assessments, protocol deviations and violations, adverse event reporting, common documents in clinical trials, administration techniques, and attention to details in following the imaging parameters in the protocol.

Each topic will further examine the types of studies, namely phase 1 through phase 4. The fifth topic will focus on the use of an imaging agent in a study designed to help develop and approve a nonradioactive therapeutic drug. The sixth topic will examine clinical research on an imaging agent. The seventh topic will review the use of an imaging agent along with a radiopharmaceutical therapy in a clinical trial, such as a theranostic study. This last topic will also discuss use of positive scan findings to qualify a patient for therapy, the administration of concomitant medications, and posttherapy imaging.

### **CONCLUSION**

The radiopharmaceutical market is expected to grow from \$5.9 billion in 2021 to over \$10.5 billion in 2026,

nearly doubling in 5 y (24). This expansion represents the lives of actual patients who are impacted because of a diagnosis or therapy that nuclear medicine can provide (24). The phases of drug development, the investigational-new-drug application requirements, and the clinical research process can be difficult to navigate in the clinical setting. Recent advances in  $\beta$ -amyloid therapies in Alzheimer disease, immune modulation therapy for cancer, and radiopharmaceutical therapies have increased the demand for highly trained research personnel with nuclear medicine expertise to assist in the design, conduct, and analysis of clinical trial data and results. The SNMMI CTN recognized the need to develop a committee to ensure the advancement and development of new radiopharmaceuticals and clinical trials. The CTN has a variety of resources to assist the nuclear medicine community involved in research, including scanner validation programs, educational opportunities, a therapy toolkit, a database of molecular imaging and radiopharmaceutical production sites to assist clinical trial sponsors with site selection, and assistance with trial design and protocol development. Clinical trial education will help advance not only the career of a nuclear medicine technologist but also the entire field of medicine.

## DISCLOSURE

No potential conflict of interest relevant to this article was reported.

## ACKNOWLEDGMENTS

We thank Amanda Abbott, MS, CNMT, RT(N)(CT), PET, from the SNMMI Clinical Trials Network, for her organization for this paper and the series and her willingness to add information and input. We also thank LisaAnn Trembath, FSNMT, CNMT, MHA, from Avid Radiopharmaceuticals, for her subject matter expertise and input on the CE questions.

## REFERENCES

- Covington MF, Schwarz SW, Hoffman JM. The regulatory process for imaging agents and devices. In: Ross B, Gambhir S, eds. *Molecular Imaging: Principles and Practice*. 2nd ed. Academic Press; 2021:1643–1661.
- Schwarz SW, Dick D, VanBrocklin HF, Hoffman JM. Regulatory requirements for PET drug production. *J Nucl Med*. 2014;55:1132–1137.
- Marcus CS. How should the FDA review diagnostic radiopharmaceuticals? *J Nucl Med*. 2018;59:868–870.
- Schwarz SW, Clarke B. Perspective on how the FDA should review diagnostic radiopharmaceuticals. *J Nucl Med*. 2018;59:865–867.
- Clinical trials network. SNMMI website. <http://www.snmmi.org/Research/ClinicalTrialsNetwork.aspx?ItemNumber=6831&navItemNumber=748>. Accessed October 13, 2021.
- FDA approves second PSMA-targeted PET imaging drug for men with prostate cancer. U.S. Food and Drug Administration website. <https://www.fda.gov/drugs/drug-safety-and-availability/fda-approves-second-psma-targeted-pet-imaging-drug-men-prostate-cancer>. Updated May 27, 2021. Accessed October 13, 2021.
- Sunderland J, McConathy J. Molecular imaging 2020: year in review. SNMMI website. [https://s3.amazonaws.com/rdeems-snmmi/files/production/public/FileDownloads/CTN/CTN\\_Pathways\\_Newsletter\\_January2021.pdf](https://s3.amazonaws.com/rdeems-snmmi/files/production/public/FileDownloads/CTN/CTN_Pathways_Newsletter_January2021.pdf). Published January 2021. Accessed October 13, 2021.
- Pathways January 2021. SNMMI website. <http://www.snmmi.org/NewsPublications/NewsletterIssue.aspx?ItemNumber=37614>. Published January 2021. Accessed October 13, 2021.
- CTN course 102: the language of clinical trials. SNMMI website. <https://www.snmmilearningcenter.org/lms/activity?@curriculum.id=1&@activity.id=2017104&@activity.bundleActivityId=-1>. Published June 1, 2021. Accessed October 13, 2021.
- CTN course 116: imaging in clinical research—elements for success. SNMMI website. <https://www.snmmilearningcenter.org/lms/activity?@curriculum.id=1&@activity.id=2016901&@activity.bundleActivityId=-1>. Published October 1, 2013. Accessed October 13, 2021.
- Sather S. Appendix B: glossary. In: *The CRC's Guide to Coordinating Clinical Research*. 4th ed. CenterWatch; 2019:227–232.
- Code of Federal Regulations (CFR), 1996 to present. Govinfo website. <https://www.govinfo.gov/help/cfr/#about/>. Updated March 17, 2021. Accessed October 13, 2021.
- Overview of ICH. ICH website. [https://admin.ich.org/sites/default/files/2021-06/OverviewOfICH\\_2021\\_0614.pdf](https://admin.ich.org/sites/default/files/2021-06/OverviewOfICH_2021_0614.pdf). Published June 2021. Accessed October 13, 2021.
- What are the responsibilities of the RDRC? U.S. Food and Drug Administration website. <https://www.fda.gov/drugs/science-and-research-drugs/what-are-responsibilities-rdrc>. Updated September 27, 2017. Accessed October 13, 2021.
- E3 structure and content of clinical study reports: questions and answers (R1). U.S. Food and Drug Administration website. <https://www.fda.gov/regulatory-information/search-fda-guidance-documents/e3-structure-and-content-clinical-study-reports-questions-and-answers-r1>. Updated August 24, 2018. Accessed October 13, 2021.
- Sather S. An overview of product development. In: *The CRC's Guide to Coordinating Clinical Research*. 4th ed. CenterWatch; 2019:33–46.
- What does FDA regulate? U.S. Food and Drug Administration website. [www.fda.gov/about-fda/fda-basics/what-does-fda-regulate](http://www.fda.gov/about-fda/fda-basics/what-does-fda-regulate). Updated June 24, 2021. Accessed October 13, 2021.
- About NRC.U.S. Nuclear Regulatory Commission website. <https://www.nrc.gov/about-nrc.html>. Updated November 25, 2020. Accessed October 13, 2021.
- History of The Joint Commission. The Joint Commission website. <https://www.jointcommission.org/about-us/facts-about-the-joint-commission/history-of-the-joint-commission/>. Accessed October 13, 2021.
- About OHRP. U.S. Department of Health and Human Services website. <https://www.hhs.gov/ohrp/about-ohrp/index.html>. Reviewed February 12, 2016. Accessed October 13, 2021.
- The U.S. Government and the World Health Organization. KFF website. <https://www.kff.org/coronavirus-covid-19/fact-sheet/the-u-s-government-and-the-world-health-organization/>. Published January 25, 2021. Accessed October 13, 2021.
- Sather S. Regulations and good clinical practice. In: *The CRC's Guide to Coordinating Clinical Research*. 4th ed. CenterWatch; 2019:21–31.
- The value of clinical research and technology organizations. ACRO website. <https://www.acrohealth.org/value-of-clinical-research-organizations/>. Published 2021. Accessed October 13, 2021.
- Global radiopharmaceutical market size and share 2021: industry analysis by trends, key findings, future demands, growth factors, emerging technologies, leading players updates and forecast till 2026. GlobeNewswire website. <https://www.globenewswire.com/news-release/2021/04/25/2216440/0/en/Global-Radiopharmaceutical-Market-Size-and-Share-2021-Industry-Analysis-By-Trends-Key-Findings-Future-Demands-Growth-Factors-Emerging-Technologies-Leading-Players-Updates-and-Forec.html>. Published April 25, 2021. Accessed October 13, 2021.

---

---

# SNMMI Clinical Trials Network Research Series for Technologists: Ethical Issues and Regulations in the Medical Workplace

Sarah Frye<sup>1</sup>, Regan Butterfield<sup>2</sup>, and John M. Hoffman<sup>3</sup>

<sup>1</sup>Department of Clinical Health Sciences, St. Louis University, St. Louis, Missouri; <sup>2</sup>Center for Quantitative Cancer Imaging, Huntsman Cancer Institute, University of Utah, Salt Lake City, Utah; and <sup>3</sup>Huntsman Cancer Institute, University of Utah School of Medicine, Salt Lake City, Utah

**CE credit:** For CE credit, you can access the test for this article, as well as additional JNMT CE tests, online at <https://www.snmmilearningcenter.org>. Complete the test online no later than December 2024. Your online test will be scored immediately. You may make 3 attempts to pass the test and must answer 80% of the questions correctly to receive 1.0 CEH (Continuing Education Hour) credit. SNMMI members will have their CEH credit added to their VOICE transcript automatically; nonmembers will be able to print out a CE certificate upon successfully completing the test. The online test is free to SNMMI members; nonmembers must pay \$15.00 by credit card when logging onto the website to take the test.

---

Ethical principles and laws have developed as medical practice and research have grown. This article discusses regulatory policies in patient care and the governing bodies that provide oversight. These include but are not limited to the Food and Drug Administration, Office for Human Research Protection, *Code of Federal Regulations*, Nuclear Regulatory Commission, Joint Commission, Health Insurance Portability and Accountability Act, Occupational Safety and Health Administration, World Health Organization, and International Conference on Harmonization. This article reviews ethical requirements in clinical research and provides examples of medical mistreatment that forced the development of these rules and regulations. Some include the Nuremberg Code, Declaration of Helsinki, and Belmont Report; good clinical practice; and the Common Rule. Several specific research documents are discussed further in this continuing education series. These guiding documents and principles are important because every patient and research subject deserves a safe environment with safe products and protection of privacy. Individuals deserve to understand their role in medicine and clinical research, have the right to refuse care, make informed decisions, know the risks and benefits included, and ultimately have their individual choices respected.

**Key Words:** ethics; ethical regulation; clinical research; informed consent

**J Nucl Med Technol 2021; 49:303–310**

DOI: 10.2967/jnmt.121.263100

---

Medical professionals follow their own principles, which develop from a combination of values, personality, education, upbringing, and the philosophy of where and sometimes when those professionals work. *Ethics* derives

from the Greek word *ethos*, meaning custom or character, and is defined as “the discipline dealing with what is good and bad and with moral duty and obligation” (1). Ethics is not the same as morality. Morality must specify which codes from a society or group count as moral (2). In another sense, morality refers to a code of conduct that would be accepted by anyone who meets certain intellectual conditions, almost always including the condition of being rational (2). Morality frequently relates to upbringing, culture, personality, and other factors. Ethics brings an added layer to morality that is more systematic (2). Ethics is the systematic study of values by which the determination of what is right and wrong is made (2).

Many individuals would not be where they are today without a strong opinion of right and wrong. How is this professional code established? How do we abide by similar ethical codes for our patients? Why are these rules and regulations in place in patient care? There are enforceable laws followed in our workplace, with regulations coming from governing and regulating bodies. This article summarizes the most prominent in the United States, as well as how each evolved, and discusses additional requirements for individuals involved in research studies. Many principles followed today were developed because of medical experiments and atrocities performed on unknowing participants in the past. Some of these codes and guidelines include the Nuremberg Code, the Declaration of Helsinki, and the Belmont Report. This article reviews the basics of these, how each evolved, how they are applied, and the historical context for their creation. Further articles in this research series will elaborate on these topics.

## REGULATORY AGENCIES

This section discusses the agencies involved in the formation and execution of clinical patient regulations, with a

---

Received Aug. 28, 2021; revision accepted Sep. 21, 2021.  
For correspondence or reprints, contact Sarah Frye ([sarah.frye@health.slu.edu](mailto:sarah.frye@health.slu.edu)).  
COPYRIGHT © 2021 by the Society of Nuclear Medicine and Molecular Imaging.

**TABLE 1**  
Regulatory Policies and Governing Bodies

Name	Responsibilities
U.S. FDA	Protects public health by ensuring safety, efficacy, and security of human and veterinary drugs, biologic products, and medical devices
CFR	Organizes rules published by U.S. federal government departments and agencies; is divided into 50 titles
NRC	Ensures safe use of radioactive materials
Joint Commission	Sets standards and accredits health-care organizations in United States
HIPAA	Provides data privacy and security for safeguarding medical information
OSHA	Sets and enforces workplace safety
OHRP	Protects human subjects and provides leadership in biomedical and behavioral research
WHO	Promotes healthy lives and well-being for all people
ICH	Promotes public health safety through international harmonization

focus on those most applicable in the United States (Table 1).

### U.S. Food and Drug Administration (FDA)

The U.S. FDA is responsible for protecting public health by ensuring the safety, efficacy, and security of human and veterinary drugs, biologic products, and medical devices (3). The FDA is responsible for protecting public health by ensuring that foods are safe, wholesome, sanitary, and properly labeled and that human and veterinary drugs, vaccines, and other biologic products and medical devices intended for human use are safe and effective (3). The FDA is also responsible for protecting the public from electronic product radiation, ensuring that cosmetics and dietary supplements are safe and properly labeled, regulating tobacco products, and advancing public health by helping to speed product innovations (3).

The FDA can trace its origins back to the creation of the agricultural division in the patent office in 1848. Its origins as a federal consumer protection agency began with the 1906 Pure Food and Drugs Act (4). Not all products undergo review of safety and effectiveness by FDA experts or receive agency approval before being marketed (5). In some cases, the FDA's enforcement efforts focus on products after they are already for sale (5). When FDA approval is not required before a product is sold, the agency has regulatory authority to act when safety issues arise (5).

### The U.S. Code of Federal Regulations (CFR)

The CFR annual edition is the codification of the general and permanent rules published in the *Federal Register* by the U.S. federal government (6). It is divided into 50 titles that represent broad areas subject to federal regulations (6). Each title is divided into chapters, and each chapter is subdivided into parts or subparts that cover regulatory areas (6). Various parts of the CFR are important to imaging technologists. For technologists who participate in research studies with human subjects, title 21, part 312, governs the use of investigational materials, whereas part 50 provides regulations for protections of human subjects via the role of

the institutional review board and part 361.1 includes information on radioactive drugs for certain research uses and includes how to report research use of radioactive drugs (7). Title 45, part 164, includes HIPAA requirements. Title 10, parts 19, 20, and 30 – 37, have to do with worker safety, radiation protection, and byproduct material (8).

Before the *Federal Register* Act was established in 1935, the U.S. executive branch agencies and the office of the president would each publish its own regulations in separate publications (8). This excessive number of authoritative documents made it difficult to determine where a U.S. regulation was found, when it was issued, and whether it had been altered or revoked (8). Congress passed the *Federal Register* Act in 1935, which empowered the archivist of the United States to establish a division within the National Archives to be responsible for the publication of a daily *Federal Register* (8). This act required that the *Federal Register*, begun on March 14, 1936, be the federal government's comprehensive documentation for publishing all agency rules, regulations, and executive orders (8).

### The U.S. Nuclear Regulatory Commission (NRC)

The U.S. NRC was created as an independent agency by Congress in 1974 to ensure the safe use of radioactive materials for beneficial civilian purposes while protecting people and the environment (9). The NRC regulates commercial nuclear power plants and other uses of nuclear materials, including nuclear medicine, through licensing, inspection, and enforcement of its requirements (9). Before the NRC was created, nuclear regulation was the responsibility of the Atomic Energy Commission (AEC), which Congress established in the Atomic Energy Act of 1946 (10). Congress later replaced the Atomic Energy Act of 1946 with the Atomic Energy Act of 1954, which made the development of commercial nuclear power possible (10). The AEC functioned by encouraging the use of nuclear power and regulating its safety (10). The AEC's regulatory programs ensured protection of public health from the hazards of nuclear power without imposing excessive requirements that would inhibit the growth of the industry (10). By 1974,



the AEC's regulatory programs had come under attack, so Congress decided to abolish the agency (10). The Energy Reorganization Act of 1974 created the Nuclear Regulatory Commission, which began in January 1975 (10).

The NRC regulates all persons and organizations that receive an NRC license to use nuclear materials or operate nuclear facilities (11). Today, the NRC's regulatory activities are focused on reactor safety oversight and reactor license renewal of existing plants, materials safety oversight and materials licensing, and waste management of high-level waste and low-level waste (10). The NRC (like the AEC before it) focuses on several broad radiation issues that are essential to protecting public safety. There are 39 agreement states in the United States as of August 2021 (12). Agreement states have entered NRC agreements that give them authority to license and inspect byproduct, source, or special nuclear materials used or possessed within their borders (12). Agreement state regulations must be as strict as NRC regulations.

### **The Joint Commission**

The Joint Commission is an independent, not-for-profit organization that seeks to "improve health care for the public, in collaboration with other stakeholders, by evaluating health care organizations and inspiring them to excel in providing safe and effective care of the highest quality and value" (13). Founded in 1951, The Joint Commission accredits more than 22,000 U.S. health-care organizations and programs (13). It is the United States' oldest and largest standards-setting and accrediting body in health care (13). To earn and maintain The Gold Seal of Approval from The Joint Commission, an organization must undergo an on-site survey at least every 3 y, with laboratories surveyed every 2 y (13). The Joint Commission's vision is that all people always experience the safest, highest-quality, best-value health care (14).

### **Health Insurance Portability and Accountability Act (HIPAA)**

HIPAA is U.S. legislation that provides data privacy and security provisions for safeguarding medical information (15). This is in title 45 of CFR with the primary purpose of helping people carry their health insurance between companies and streamline the movement of medical records between institutions (16). Title I is "Health Care Access, Portability, and Renewability," which deals with health-care plans and policies (16). Title II is "Preventing Health Care Fraud and Abuse" and comprises the privacy rule, the transactions-and-code-sets rule, the security rule, unique identifiers or the national provider rule, and the enforcement rule (16). Medical practices can use a specialized electronic medical record for managing individual records in a larger electronic health records system (16). The law has emerged into greater prominence in recent years with the proliferation of health data breaches caused by cyberattacks on health insurers and providers (17).

Although the law itself was passed in 1996, there have been major additions to HIPAA over the past 25 y with the introduction of the privacy rule, security rule, breach notification rule, and omnibus final rule (18). HIPAA is a living document that attempts to change with the times, and serious penalties can ensue from a HIPAA breach (18). The HIPAA privacy rule deals with protected health information, and the HIPAA security rule deals with electronic protected health information. HIPAA is used daily in patient care and helps keep medical information private and secure.

### **Occupational Safety and Health Administration (OSHA)**

OSHA is part of the U.S. Department of Labor (19). The Occupational Safety and Health Act of 1970 was passed to prevent workers from being killed or seriously harmed at work (19). This act sets and enforces protective workplace safety and health standards (19). OSHA provides information, training, and assistance to employers and workers (19). Under the Occupational Safety and Health Act, employers have the responsibility to provide a safe workplace. OSHA standards describe the methods employers are legally required to follow to protect their workers (19). Before OSHA can issue a standard, it must go through an extensive process that includes substantial public engagement, notice, and comment (19). OSHA offers help for employers, with free confidential advice (19). Several programs and services help employers identify and correct job hazards and improve their injury and illness prevention programs (19).

Workplaces and employees in the United States must comply with OSHA standards (19). Examples of OSHA standards include requirements to provide fall protection, prevent exposure to some infectious diseases, ensure the safety of workers who enter confined spaces, put guards on machines, provide safety equipment, and provide training for certain dangerous jobs (19). OSHA inspections are initiated without notice and performed by highly trained compliance officers (19). OSHA and the NRC both have radiation dose limits for radiation workers. Radiation produced by machines is overseen by OSHA. Radiation from radionuclides is overseen by the NRC. OSHA and the NRC have the same yearly whole-body radiation exposure limits for occupational workers. OSHA's goal is to keep a safe work environment in the United States.

### **Office for Human Research Protections (OHRP)**

OHRP provides leadership in the protection of the rights, welfare, and well-being of human subjects involved in research conducted or supported by the U.S. Department of Health and Human Services (20). OHRP also provides guidance, develops educational programs, and maintains regulatory oversight issues in biomedical and behavioral research (20). OHRP was created in June 2000 to lead the Department of Health and Human Services' efforts to protect human subjects in research and to provide leadership for federal agencies that conduct or support human

subject research under the Federal Policy for the Protection of Human Subjects, also known as the Common Rule (20). OHRP replaced the Office for Protection from Research Risks, which was created in 1972 and was part of the National Institutes of Health. OHRP has oversight in more than 13,000 institutions in the United States and worldwide that conduct Department of Health and Human Services–supported nonexempt human subject research (20).

### **The World Health Organization (WHO)**

The WHO was founded in 1948 with a broad mandate to act as a coordinating authority on international health issues (21). Its mission is “attainment by all peoples of the highest possible level of health” (21). The U.S. government has been actively engaged with WHO, providing financial and technical support and participating in its governance structure (21). The WHO’s primary concern since January 2020 has been the worldwide response to the COVID-19 global pandemic (21). It supports its mission through activities such as providing technical assistance to countries, setting international health standards, providing guidance on health issues, coordinating and supporting international responses to health emergencies, and advocating for better global health (21). WHO is made up of 194 member states, with an executive board comprising 34 members technically qualified in the health field (21). The WHO is headquartered in Geneva, Switzerland, and has a worldwide network of representatives (21).

The WHO successfully achieved initiatives but faces many challenges. Its objective from 2019 to 2023 is to ensure healthy lives and promote well-being for all (21). The WHO has 3 strategic priorities: helping 1 billion people benefit from universal health coverage, ensuring that 1 billion more people are protected against health emergencies, and helping 1 billion more people enjoy better health and well-being (21).

### **The International Council for Harmonization of Technical Requirements for Pharmaceuticals for Human Use (ICH)**

The ICH is unique in coordinating technical drug registration guidelines with the engagement of regulators and industry (22). The purpose is promotion of public health through international harmonization that contributes to prevention of unnecessary duplication of clinical trials, to development and registration of new medicines, and to reduction of unnecessary animal testing (22). The ICH’s mission is to achieve greater worldwide harmonization to ensure that safe, effective, and high-quality medicines are developed in a resource-efficient manner (23). Harmonization is achieved through a process of scientific consensus with experts to develop ICH guidelines (23). In 2021, the ICH Association has continued its harmonization, defined strategic priorities, and identified new topics for harmonization (24).

These regulatory organizations guide interactions with medical practitioners regarding patient care. Adding clinical research to the discussion includes another layer of scrutiny on regulatory and ethical guidance. Historically, medical mistreatment under the guise of clinical research contributed to the change in the culture of health care and caused people to be fearful of interactions with health-care providers.

### **HISTORICAL EXAMPLES OF MISTREATMENT**

Regulations that govern human subject research have evolved because of errors and faulty research practices, including deliberate exploitation of specific populations (usually based on race, religion, mental status, age, socioeconomic status, or sex). With the evolution of digital medicine and Internet-based technology, these regulations are continually adjusted to protect individuals’ rights. The examples of targeted mistreatment of discriminated populations have made individuals and communities skeptical of medical treatment and research.

The various examples listed were performed on individuals unaware of the repercussions of this medical treatment. One notable case of mistreatment occurred between 1932 and 1972, when more than 400 African American men were observed to study the natural course of untreated syphilis (25). The study was originally called the “Tuskegee Study of Untreated Syphilis in the Negro Male” (now referred to as the “U.S. Public Health Service Syphilis Study at Tuskegee”) (25). Participants’ informed consent was not obtained, and participants were told they were being treated for “bad blood” (24). The study continued even after penicillin became the treatment of choice for syphilis in 1943, and participants were not offered this treatment (25). Another case, which began in 1956 and lasted 14 y, included mentally disabled children intentionally injected with hepatitis (26). The study goal was to track development of the viral infection to determine the effectiveness of  $\gamma$ -globulin injections (26). The researchers of this study justified their deliberate infections and exposures by claiming that the high rate of infection in the institution made it practically inevitable that the children would become infected (26).

In 1962, a physician in Brooklyn injected live cancer cells into 22 elderly cancer patients after being rebuffed by his institution, Sloan-Kettering (27). The goal was to learn whether people who were debilitated by cancer could reject cancer cells (27). Study participants were not informed about the risks and were not informed that the experiment involved injecting live cancer cells (27). Three whistleblowers refused to participate in the experiment and brought attention to the hospital board, which eventually accused the original physician of fraud and unprofessional conduct (27).

Of note to imaging technologists, radiation research was not exempt from examples of medical mistreatment. The Advisory Committee on Human Radiation Experiments appointed by President Clinton published an executive

**TABLE 2**  
Research Ethical Standards

Standard	Description
Nuremberg Code	Set of research ethical principles for human experimentation from Nuremberg trials
Declaration of Helsinki	General guiding principles for researchers when working with human subjects
Belmont Report	Basic ethical guidelines on human subject research (respect for persons, beneficence, and justice)
GCP	Description of clinical trial design and responsibilities of investigator, sponsor, and institution
Common Rule (title 45 of CFR, part 46, subpart A)	Rule for creating uniform regulations across U.S. agencies involved in human subject research

summary that found over 4,000 human radiation experiments sponsored by the U.S. federal government between 1944 and 1974 (28). After the discovery of radiation, the discovery of radiation side effects quickly occurred. Individuals were looking for opportunities to understand more about radiation effects on the body. Researchers wanted to advance medical understanding, but there were physicians who did not appreciate the rights of the individuals included in these studies (28). The advisory committee from the Alliance for Human Research Protection found at least 27 experiments that exposed pregnant or nursing mothers and their babies to radiation in nontherapeutic research between 1944 and 1974 (25). One case in the 1940s included a radiation exposure experiment funded by the U.S. Public Health Service that involved 820 poor pregnant White women who were given radioactive iron in a cocktail drink (29). The women were not informed about the contents of the drink or that they were in an experiment (29). The goal of the radiation portion of the experiment was to study the absorption of iron during pregnancy (29). It was later discovered that a higher number of malignancies occurred among the offspring of those that received this cocktail than among the offspring of a control group of similar size (29).

Another case from the 1940s included 18 terminally ill patients injected with plutonium. Starting in 1945, doctors working with the Manhattan Project initially injected plutonium into 18 men, women, and children (30). The doctors in this study did not obtain consent, and the injections were not given with therapeutic intent (30). The goal was to study the toxic effects of plutonium on selected groups so that physician-scientists would know how to protect American researchers, soldiers, and citizens exposed to atomic weapons (30). In the 1950s, another research study, conducted by Harvard University and the Massachusetts Institute of Technology, gave developmentally disabled boys radioactive calcium and iron in their breakfast cereal (31). From 1946 to 1956, these boys consumed radioactive food to help the researchers better understand the human digestive process, exposing the boys to the radiation-equivalent of at least 50 chest radiographs (31). Parents were never informed that radioactive elements were involved in the tests (31). In a different experiment that ended in 1971, 88 poor, uneducated, and mostly African American patients

with incurable cancers were exposed to heavy doses of experimental full-body irradiation (28). Many subjects died hours after treatment and were not provided palliatives against the side effects of nausea and vomiting because the researchers did not want the drugs to interfere with their data collection (28). These cases show that much of the current understanding of radiation effects was collected at the very high cost of devastating experiments on vulnerable individuals without their knowledge or consent.

## ETHICAL CODES

Table 2 summarizes the ethical codes.

### The Nuremberg Code

The Nuremberg Code is a set of research ethics principles for human experimentation resulting from the Nuremberg trials at the end of the Second World War (32). In August 1947, the International Medical Tribunal in Nuremberg, Germany, delivered its verdict in the trial of 23 doctors and bureaucrats accused of war crimes and crimes against humanity for their roles in cruel and often lethal concentration camp medical experiments (32). The Nazi doctors performed twin experiments, freezing experiments, sterilizations, and epidemic jaundice experiments. As part of the tribunal's judgment, the Nuremberg Code was introduced articulating 10 principles for the conduct of human experiments (32). Among other requirements, the code called for the "voluntary consent" of the human research subject, an assessment of risks and benefits, and assurances of competent investigators (32). There has been debate about the code's authorship, scope, and legal standing; however, the Nuremberg Code was a monumental milestone in the history of medical research ethics used worldwide (32).

The main points to take home from the Nuremberg Code are that voluntary consent is essential, research risks must be minimized and be relative to the anticipated benefits of the research, research must benefit society, poorly designed human subject research is unethical from its inception, research must be based on preclinical studies on animals and knowledge of the condition under study, subjects have the right to end their participation in research, proper planning and measures should be taken to protect the subject,

and the experiment should be conducted only by scientifically qualified persons (33).

### **The Declaration of Helsinki**

The Declaration of Helsinki is a document that considers the evolving nature of scientific research. It was developed from 10 principles stated in the Nuremberg Code and further incorporated elements from the 1948 Declaration of Geneva, a statement of the ethical duties of physicians (34). It was adopted by the World Medical Assembly in 1964 and has been revised 7 times, with the most recent being in 2013 (35). The Declaration of Helsinki developed as a statement of ethical principles to provide guidance to physicians and other participants in medical research involving human subjects (34). Medical research involving human subjects includes research on identifiable human material or identifiable data (35). The Declaration of Helsinki includes general guiding principles that are the foundation for the ethical standards, including protecting patient health; not allowing knowledge to trample rights; considering the risks, burdens, and benefits of research; protecting vulnerable populations; following scientific requirements and research protocols; using research ethics committees; maintaining privacy and confidentiality; obtaining informed consent; using placebos; making posttrial provisions; regulating and publishing the research; and not using unproven interventions in clinical practice (34).

The guidelines from the Declaration of Helsinki help inform ethical decisions based on medical research. The purpose is to ensure that the well-being of subjects takes precedence over the interests of science and society (34). Some populations are vulnerable and require special protection. Experimental procedures involving vulnerable populations must be detailed in a protocol and submitted to an ethical review committee. Subjects must be informed volunteers. If they are unable to give consent for themselves, a legally authorized representative must consent on their behalf (34). Informed consent (including the process) must be documented (34). The context of obtaining informed consent is as important as the information typed in the document itself.

### **The Belmont Report**

“The Belmont Report: Ethical Principles and Guidelines for the Protection of Human Subjects of Research,” was written by the National Commission for the Protection of Human Subjects of Biomedical and Behavioral Research (36). The commission, created because of the National Research Act of 1974, was charged with identifying the basic ethical principles that should be included in biomedical and behavioral research involving human subjects and in the development of guidelines to ensure that such research is conducted in accordance with those principles (36). Informed by discussions that spanned almost 4 y and an intensive 4 d of deliberation in 1976, the commission published, in 1976, what became known as the Belmont Report, which identified basic guidelines that address

ethical issues arising from the conduct of human subject research (36). The 3 basic principles of the Belmont Report are respects for persons, beneficence, and justice.

Respect for persons is demonstrated by the informed consent process and in safeguards for vulnerable populations (37). Other important concerns are privacy and confidentiality (37). Beneficence has 2 general characteristics: do no harm and maximize benefit while minimizing risk (37). Beneficence is expressed in the use of good research design, competent investigators, and a favorable risk-to-benefit ratio (37). Justice implies fairness and is displayed in the equitable selection of research subjects, ensuring that no group of people is chosen unfairly on the basis of factors unrelated to the research (37). This equitability means that there must be appropriate inclusion and exclusion criteria and a fair system of recruitment (36). The Belmont Report built the foundation for ethical treatment of human subjects in clinical research and associated laws in the United States (37).

### **Good Clinical Practice (GCP)**

GCP is a set of quality standards for the design, conduct, recording, and reporting of clinical research trials involving human subjects (37). Published by the ICH as a report entitled “E6(R2): Good Clinical Practice,” this document describes the responsibilities of the investigator, sponsor, and institution; what should be included in a clinical trial protocol; how research sites should be monitored; and how the investigational product should be controlled (37). GCP is in alignment with federal regulations for conducting research on human subjects, and research sponsors require that investigators and research staff be trained in GCP and conduct their work in accordance with the quality standards. A detailed discussion of GCP and how it impacts medical imaging research is provided later in this series. GCP includes some of the laws previously discussed, local laws, institutional policy, and study-specific requirements. This is not one document; individuals must interpret what GCP means for their specific study, and these interpretations can differ depending on the individual. The ICH assists with some aspects of GCP; the ICH was structured to provide opportunities for standardization of regulatory GCP initiatives (37). The latest revision of ICH E6, released in 2016, focused on the industry changes related to performing trials with more risk-based approaches and provides some clarification on GCP requirements (37). Members of the ICH have updated this standard into their own GCPs (37).

### **The Common Rule**

The Common Rule was originally adopted in 1991 and revised in 2017 for 17 U.S. agencies and departments involved in human clinical research (37). The rule, published in title 45 of CFR, part 46, subpart A, and entitled “Federal Policy for the Protection of Human Subjects” (37), serves to create a uniform body of regulations across various U.S. agencies involved in human subject research (37). As with other regulatory and ethical guidelines, the

Common Rule is based on historical documents (including the Nuremberg Code, the Declaration of Helsinki, and the Belmont Report) and several international bioethics codes (30). Compliance with the Common Rule is a requirement for federal funding of research activities.

The 2017 Common Rule revision included improving the process of documenting informed consent. This improvement included requiring that consent forms for certain federally funded clinical trials be publicly available, requiring review by a single institutional review board for cooperative research for some studies, allowing the use of broad consent for future research for secondary studies on stored identifiable data or identifiable biospecimens, eliminating continuing review for certain minimal-risk research, establishing new exempt categories of research based on risk posed to subjects, and adopting a definition of *clinical trial* that includes behavioral health–related outcomes. The Common Rule is further reviewed later in this continuing education series. Noncompliance can result in penalties to individuals and institutions and loss of a license to practice.

## DISCUSSION

The ethics, values, and regulations that guide medical practitioners' interactions with individuals and research subjects have evolved as the understanding of individual rights has evolved. Current laws and ethical guidance for patient care and research in the United States came directly from regulatory agencies mentioned in this article. Sadly, numerous changes resulted directly from medical atrocities that occurred on specific groups throughout recent U.S. and world history. Laws and guidelines should and will change as understanding, culture, technology, and systems in health care change. Further articles in this series will highlight GCP, the research regulatory environment, and other details about clinical research in medical imaging.

## CONCLUSION

Technologists and other health-care providers should be familiar with the regulatory agencies' ethical guidelines that govern patient care and research. It is important to respect every patient's safety, autonomy, and privacy and to give all patients an informed understanding of their participation in clinical care and research studies. It is imperative that the reader become familiar with these laws and question those that have moral ambiguity. These guiding documents and principles are vital, as individual patients and those participating in clinical trials deserve a safe environment with safe products and confidentiality. Individuals deserve to understand their role in medicine and clinical research and have the right to refuse care, make informed decisions about their care, know the risks and benefits of proposed procedures or interventions, and have their individual choices respected. Critical lessons from past egregious research practices should guide care so that individuals, especially those from targeted and vulnerable populations, are not subjected to

medical mistreatment disguised as health care or legitimate clinical research.

## DISCLOSURE

No potential conflict of interest relevant to this article was reported.

## ACKNOWLEDGMENTS

We thank Amanda Abbott, MS, CNMT, RT(N)(CT), PET, from the SNMMI Clinical Trials Network, for her organization for this paper and the series and her willingness to add information and input. We also thank LisaAnn Trembath, FSNMT, CNMT, MHA, from Avid Radiopharmaceuticals, for her subject matter expertise and input on the CE questions.

## REFERENCES

1. Ethic. Merriam-Webster website. <https://www.merriam-webster.com/dictionary/ethic>. Accessed September 27, 2021.
2. The definition of morality. Stanford Encyclopedia of Philosophy website. <https://plato.stanford.edu/entries/morality-definition/>. Published April 17, 2002. Revised September 8, 2020. Accessed September 27, 2021.
3. What does FDA regulate? U.S. Food and Drug Administration website. [www.fda.gov/about-fda/fda-basics/what-does-fda-regulate](http://www.fda.gov/about-fda/fda-basics/what-does-fda-regulate). Updated June 24, 2021. Accessed September 27, 2021.
4. When and why was FDA formed? U.S. Food and Drug Administration website. [www.fda.gov/AboutFDA/Transparency/Basics/ucm214403.htm](http://www.fda.gov/AboutFDA/Transparency/Basics/ucm214403.htm). Updated March 28, 2018. Accessed September 27, 2021.
5. Is it really 'FDA Approved'? U.S. Food and Drug Administration website. [www.fda.gov/consumers/consumer-updates/it-really-fda-approved](http://www.fda.gov/consumers/consumer-updates/it-really-fda-approved). Updated January 17, 2017. Accessed September 27, 2021.
6. Code of Federal Regulations (CFR), 1996 to present. Govinfo website. <https://www.govinfo.gov/help/cfr/about/>. Updated March 17, 2021. Accessed September 27, 2021.
7. Code of Federal Regulations: title 21—food and drugs. eCFR website. <https://www.ecfr.gov/current/title-21>. Updated September 21, 2021. Accessed September 27, 2021.
8. McKinney RJ. A research guide to the Federal Register and the Code of Federal Regulations. Law Librarians' Society of Washington, DC, website. <https://www.llsdc.org/fr-cfr-research-guide>. Published 2002. Updated September 16, 2019. Accessed September 27, 2021.
9. About NRC. United States Nuclear Regulatory Commission website. <https://www.nrc.gov/about-nrc.html>. Updated November 25, 2020. Accessed September 27, 2021.
10. History. United States Nuclear Regulatory Commission website. <https://www.nrc.gov/about-nrc/history.html>. Updated August 18, 2021. Accessed September 27, 2021.
11. NRC regulations title 10, Code of Federal Regulations. United States Nuclear Regulatory Commission website. <https://www.nrc.gov/reading-rm/doc-collections/cfr/index.html>. Updated September 14, 2021. Accessed October 5, 2021.
12. NRC: NMSS—state regulations and legislation. United States Nuclear Regulatory Commission website. <https://scp.nrc.gov/rulemaking.html>. Updated September 23, 2021. Accessed September 27, 2021.
13. History of The Joint Commission. The Joint Commission website. <https://www.jointcommission.org/about-us/facts-about-the-joint-commission/history-of-the-joint-commission/>. Accessed July 22, 2021.
14. About The Joint Commission. The Joint Commission website. <https://www.jointcommission.org/about-us/>. Accessed September 27, 2021.
15. Summary of the HIPAA security rule. U.S. Department of Health and Human Services website. <https://www.hhs.gov/hipaa/for-professionals/security/laws-regulations/index.html>. Reviewed July 26, 2013. Accessed September 27, 2021.
16. The history of HIPAA & the consequences of a HIPAA violation. Record Nations website. <https://www.recordnations.com/articles/history-hipaa/>. Accessed September 27, 2021.
17. Lutkevich B. HIPAA (Health Insurance Portability and Accountability Act). SearchHealthIT website. <https://searchhealthit.techtarget.com/definition/HIPAA/>. Updated August 2020. Accessed July 22, 2021.
18. HIPAA history. HIPAA Journal website. <https://www.hipaajournal.com/hipaa-history/>. Accessed September 27, 2021.

19. At-a-glance: OSHA. Occupational Safety and Health Administration website. <https://www.osha.gov/sites/default/files/publications/3439at-a-glance.pdf>. Accessed September 27, 2021.
20. About OHRP. U.S. Department of Health and Human Services website. <https://www.hhs.gov/ohrp/about-ohrp/index.html>. Reviewed February 12, 2016. Accessed September 27, 2021.
21. The U.S. Government and the World Health Organization. KFF website. <https://www.kff.org/coronavirus-covid-19/fact-sheet/the-u-s-government-and-the-world-health-organization/>. Published January 25, 2021. Accessed September 27, 2021.
22. Overview of ICH. ICH website. [https://admin.ich.org/sites/default/files/2021-06/OverviewOfICH\\_2021\\_0614.pdf](https://admin.ich.org/sites/default/files/2021-06/OverviewOfICH_2021_0614.pdf) Published June 2021. Accessed August 23, 2021.
23. Mission: harmonisation for better health. ICH website. <https://www.ich.org/page/mission/>. Accessed September 27, 2021.
24. ICH Association: 2021 annual work plan. ICH website. [https://admin.ich.org/sites/default/files/inline-files/ICHAssociation\\_WorkPlan\\_2021\\_Approved\\_2020\\_1118.pdf](https://admin.ich.org/sites/default/files/inline-files/ICHAssociation_WorkPlan_2021_Approved_2020_1118.pdf). Published October 6, 2020. Accessed September 27, 2021.
25. The Tuskegee timeline. Centers for Disease Control and Prevention website. <https://www.cdc.gov/tuskegee/timeline.htm/>. Reviewed April 22, 2021. Accessed September 27, 2021.
26. Pecorino PA. Chapter 7: human experimentation. Queensborough Community College website. [https://www.qcc.cuny.edu/socialsciences/ppecorino/medical\\_ethics\\_text/Chapter\\_7\\_Human\\_Experimentation/CONTENTS.htm](https://www.qcc.cuny.edu/socialsciences/ppecorino/medical_ethics_text/Chapter_7_Human_Experimentation/CONTENTS.htm). Published 2002. Accessed September 27, 2021.
27. 1962: Dr. Chester Southam injected live cancer cells into 22 elderly patients. Alliance for Human Research Protection website. <https://ahrp.org/1962-dr-chester-southam-injected-live-cancer-cells-into-22-elderly-patients-at-jewish-chronic-disease-hospital-in-brooklyn/>. Published December 28, 2014. Accessed September 27, 2021.
28. Pacchioli D. Subjected to science. Penn State University website. <https://news.psu.edu/story/141518/1996/03/01/research/subjected-science/>. Published March 1, 1996. Accessed September 27, 2021.
29. 1945–1947: Vanderbilt “nutrition study” exposed 820 pregnant women to radioactive iron. Alliance for Human Research Protection website. <https://ahrp.org/1945-1947-vanderbilt-university-nutrition-study-exposed-820-pregnant-women-to-tracer-doses-of-radioactive-iron/>. Published December 29, 2014. Accessed September 27, 2021.
30. 1945–1947: eighteen patients were injected with plutonium in AEC experiments. Alliance for Human Research Protection website. <https://ahrp.org/1945-1947-eighteen-patients-were-injected-with-plutonium-in-aec-experiments/>. Published December 29, 2014. Accessed September 27, 2021.
31. Advisory Committee on Human Radiation Experiments: final report. Office of Environment, Health, Safety and Security website. <https://ehss.energy.gov/ohre/roadmap/achre/report.html>. Accessed September 27, 2021.
32. Moreno JD, Schmidt U, Joffe S. The Nuremberg Code 70 years later. *JAMA*. 2017; 318:795–796. 28817743
33. The Nuremberg code. National Institutes of Health website. <https://history.nih.gov/display/history/Nuremberg+Code/>. Published 1949. Accessed September 27, 2021.
34. Peters B. What is the Declaration of Helsinki? Verywell Health website. <https://www.verywellhealth.com/declaration-of-helsinki-4846525>. Updated October 27, 2020. Accessed September 27, 2021.
35. WMA Declaration of Helsinki: ethical principles for medical research involving human subjects. World Medical Association website. <https://www.wma.net/policies-post/wma-declaration-of-helsinki-ethical-principles-for-medical-research-involving-human-subjects/>. Published July 9, 2018. Accessed September 27, 2021.
36. The Belmont Report. U.S. Department of Health and Human Services website. <https://www.hhs.gov/ohrp/regulations-and-policy/belmont-report/index.html>. Reviewed March 15, 2016. Accessed September 27, 2021.
37. Sather S. Chapter three: regulations and good clinical practice. In: *The CRC’s Guide to Coordinating Clinical Research*. 4th ed. CenterWatch; 2019: 21–31.



# Technegas Lung Ventilation

Geoffrey M. Currie

*School of Dentistry and Medical Sciences, Charles Sturt University, Wagga Wagga, Australia*

## RATIONALE

Technegas (Cyclomedica Asia Pacific) is a versatile yet straightforward system for producing high-quality  $^{99m}\text{Tc}$ -based ventilation studies using a carbon-based nanoparticle. Because Technegas is neither a gas nor produces aerosolized particles, it optimizes patient outcomes while maintaining staff safety. Technegas allows the protocol to move to 3-dimensional SPECT imaging with improved sensitivity and specificity (1–3). The nature of Technegas allows optimal ventilation imaging with good peripheral penetration, simple operation, efficient delivery, low radiation dose, and slow washout.

## CLINICAL INDICATIONS

The primary clinical indication for Technegas ventilation is in conjunction with  $^{99m}\text{Tc}$ -macroaggregated albumin perfusion lung imaging to evaluate suspected pulmonary embolism. In addition, Technegas ventilation imaging is used in evaluating chronic thromboembolic pulmonary hypertension, asthma, chronic obstructive pulmonary disease, emphysema, and quantitation before lung volume reduction surgery.

## CONTRAINDICATIONS

Technegas has no known contraindications.

## PATIENT PREPARATION/EDUCATION

The key to successful Technegas delivery is patient compliance, achieved through patient education and practice, which should not be rushed. A detailed explanation of the ventilation process at a language level that the patient understands, with ample clarification and questions, is essential. The practice run should be done under the same conditions as the actual ventilation procedure, including position (upright or supine) and the nose peg. The practice session improves timing, ventilation, and patient compliance (especially with seals) and offers the opportunity to select the appropriate mouthpiece for that patient.

## TECHNEGAS PREPARATION (4)

### Prepare the system:

1. Connect and turn on the argon supply to a 15 L/min flow rate.

2. Connect to main power supply and switch on.
3. Press the open button to open the chamber.

### Prepare the crucible (Fig. 1):

1. Using gloves and forceps, clear debris from the chamber and ash tray.
2. Wet the well of a new crucible with ethanol and drain but do not allow it to dry.
3. Use forceps to place the crucible between the chamber contacts, and ensure good contact by rotating forward and backward. Take care not to twist or fracture the crucible.
4. Add 200–900 MBq of  $^{99m}\text{Tc}$  in 0.13–0.17 mL with the well vertical, but do not overfill the crucible.
5. Depress and hold the draw interlock and the close button until the chamber is completely closed.

### Simmer (Fig. 1):

1. Press start to initiate the 6-min simmer cycle.
2. Prepare the patient, and practice the breathing technique required during the simmer cycle.
3. If the concentration of  $^{99m}\text{Tc}$  is low and requires a top-up, press cancel twice at the end of the simmer process to allow the draw to be opened and additional  $^{99m}\text{Tc}$  added to the well. Do not wet with ethanol for the reload. Close the chamber and reinitiate the 6-min simmer cycle.

### Burn (Fig. 1):

1. Press the start button to initiate the 15-s burn.
2. Verify the burn and then disconnect the mains and argon.
3. Transport the Technegas generator to the patient.
4. Administer the Technegas within the 10-min window.

### Ventilate the patient (Fig. 1):

1. Attach the patient administration set to the Technegas generator.
2. Commence the practiced breathing strategy with the patient.
3. Press the start button.
4. On inspiration, depress the patient delivery knob.
5. Monitor the lung count rate.
6. When the required count rate is achieved, release the delivery knob and allow the patient to take 4–5 breaths through the tube to clear the residual.



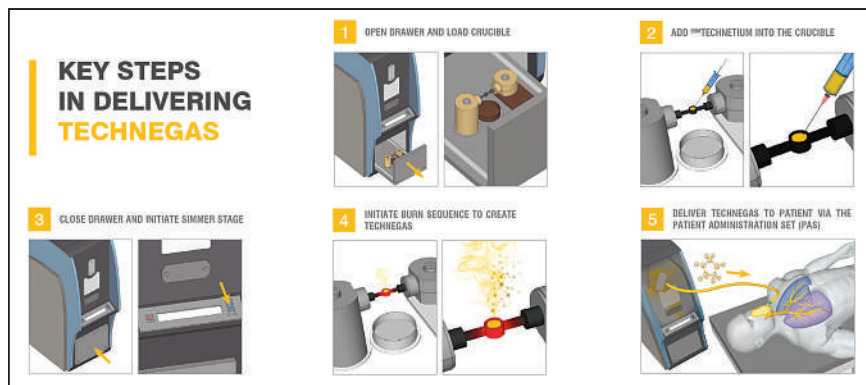


**FIGURE 1.** The 5 basic steps in delivering Technegas to patients. (Courtesy of Cyclomedica.)

7. Dispose of the patient administration set.
8. Return the Technegas generator to argon and main power supply, which will automatically commence a purge.
9. Commence the ventilation imaging protocol.

### ACQUISITION PARAMETERS

Ventilation acquisition protocols vary among departments. Planar-only supine protocols generally use a high-resolution collimator and a  $256 \times 256$  pixel matrix for 300,000–500,000 counts in 8 projections, listed here as dual-head projection pairs: anterior/posterior, left anterior oblique/right posterior oblique, right anterior oblique/left posterior oblique, and right lateral/left lateral. The corresponding perfusion study would adopt the same parameters with higher total counts of 800,000–1,000,000 per image. Alternative SPECT approaches are performed supine with the arms extended above the head. The venti-

lation time per projection is typically 12–15 s, whereas the perfusion is generally 8–10 s. Otherwise, ventilation and perfusion SPECT are usually performed with a  $128 \times 128$  matrix using high-resolution collimation and a noncircular (elliptic or contoured) orbit with projections every  $3^\circ$  (120 projections). CT may be performed with the SPECT and can be low-dose, nondiagnostic CT for attenuation correction, diagnostic CT, or a CT pulmonary angiogram.

### IMAGE PROCESSING

Planar data should be displayed, thresholded, and annotated with corresponding ventilation and perfusion images. SPECT data should undergo ordered-subset expectation maximization iterative reconstruction with a 3-dimensional Butterworth filter. Coregistration with the CT scan should be performed for attenuation correction, anatomic localization, and, if appropriate, fusion of contrast angiographic data.

### REFERENCES

1. Reinartz P, Schirp U, Zimmy M, et al. Optimizing ventilation-perfusion lung scintigraphy: parting with planar imaging. *Nuklearmedizin*. 2001;40:38–43. 11354986
2. Bailey DL, Schembri GP, Cooper RA, Bailey EA, Roach PJ. Reprojection of reconstructed V/Q SPECT scans to provide high count planar images [abstract]. *J Nucl Med*. 2005;46(suppl):337P.
3. Roach PJ, Bailey DL, Schembri GP, Thomas P. Transition from planar to SPECT V/Q scintigraphy: rationale, practicalities and challenges. *Semin Nucl Med*. 2010;40:397–407. 20920630
4. Currie G, Bailey D. A technical overview of Technegas as a lung ventilation agent. *J Nucl Med Technol*. 2021;49:311–317.



# A Technical Overview of Technegas as a Lung Ventilation Agent

Geoffrey M. Currie<sup>1,2</sup> and Dale L. Bailey<sup>3,4</sup>

<sup>1</sup>Charles Sturt University, Wagga Wagga, Australia; <sup>2</sup>Baylor College of Medicine, Houston, Texas; <sup>3</sup>Royal North Shore Hospital, Sydney, Australia; and <sup>4</sup>University of Sydney, Sydney, Australia

**CE credit:** For CE credit, you can access the test for this article, as well as additional JNMT CE tests, online at <https://www.snmlearningcenter.org>. Complete the test online no later than December 2024. Your online test will be scored immediately. You may make 3 attempts to pass the test and must answer 80% of the questions correctly to receive 1.0 CEH (Continuing Education Hour) credit. SNMMI members will have their CEH credit added to their VOICE transcript automatically; nonmembers will be able to print out a CE certificate upon successfully completing the test. The online test is free to SNMMI members; nonmembers must pay \$15.00 by credit card when logging onto the website to take the test.

Technegas is a carbon-based nanoparticle developed in Australia in 1984 and has been in widespread clinical use, including SPECT imaging, since 1986. Although <sup>81m</sup>Kr offers the ideal ventilation properties of a true gas, Technegas is considered preferred in more than 60 countries for ventilation imaging yet has limited adoption in the United States. In March 2020, a new U.S. Food and Drug Administration application was lodged for Technegas, and the impending approval warrants a detailed discussion of the technical aspects of the technology for those for whom it is new. Technegas is a simple yet versatile system for producing high-quality <sup>99m</sup>Tc-based ventilation studies. The design affords safety to patients and staff, including consideration of radiation and biologic risks. Technegas is the gold standard for the ventilation portion of SPECT-based ventilation–perfusion studies in pulmonary embolism and several respiratory pathologies. When approved by the U.S. Food and Drug Administration, Technegas will extend advantages to workflow, safety, and study quality for departments that adopt the technology.

**Key Words:** lung imaging; ventilation; Technegas

**J Nucl Med Technol 2021; 49:313–319**

DOI: 10.2967/jnmt.121.262887

Ventilation and perfusion (V/Q) lung scintigraphy has been used in the evaluation of patients with suspected pulmonary embolism for more than half a century. Although the underlying principles have not changed during this period, there have been significant advances in technology. Imaging equipment has emerged with superior resolution and sensitivity, SPECT techniques have added advantages over planar imaging alone, hybrid systems have allowed SPECT and CT to produce physiologic information coregistered with morphology, and PET and PET/CT have become more widely available. Concurrently, developments in

radiotracers have seen improved microspheres for perfusion in macroaggregated albumin and replacement of <sup>133</sup>Xe ventilation with <sup>99m</sup>Tc aerosols, <sup>81m</sup>Kr, and Technegas (Cyclo-medica Pty Ltd.), although <sup>133</sup>Xe is still used at some sites. Technegas is a carbon-based nanoparticle that has a strongly bound <sup>99m</sup>Tc atom trapped in a cagelike structure. It was developed in Australia in 1984 (1) and began seeing widespread clinical use in Australia from 1986, and more recently including SPECT (2). Although <sup>81m</sup>Kr offers the ideal ventilation properties of a true gas, Technegas is considered preferred in more than 60 countries for ventilation imaging yet has limited adoption in the United States. Indeed, in 1991 a Newsline article in *The Journal of Nuclear Medicine* (3) posed the question, “When, if ever, will the device that has won near ubiquitous use in Australia gain approval for lung ventilation studies in the U.S.?” In March 2020, a new U.S. Food and Drug Administration application was lodged for Technegas, and early in 2021 both the Society of Nuclear Medicine and Molecular Imaging and its Technologist Section, concerned about the decline in ventilation studies in response to coronavirus disease 2019 risk, requested fast tracking of Food and Drug Administration approval of Technegas. Since Technegas does not produce aerosolized particles, nor is it a gas, it allows imaging of the ventilation to the lungs to optimize patient outcomes while maintaining staff safety. The impending approval of Technegas by the U.S. Food and Drug Administration warrants a detailed discussion of the technical aspects of the technology for those for whom it is new. This discussion will not examine the broader debate on the role and application of V/Q imaging, clinical applications, or the advances in imaging technology (SPECT, SPECT/CT, and PET/CT) and the associated image interpretation. It is, however, important to note that using Technegas for ventilation imaging allows the entire V/Q protocol to move to 3-dimensional SPECT imaging with the associated improved sensitivity and specificity (4–6). SPECT performance is further enhanced with the addition of a coacquired low-dose CT scan (4–6).

Received Jul. 9, 2021; revision accepted Aug. 23, 2021.

For correspondence or reprints, contact: Geoffrey M. Currie ([gcurrie@csu.edu.au](mailto:gcurrie@csu.edu.au)).

Published online September 28, 2021.

COPYRIGHT © 2021 by the Society of Nuclear Medicine and Molecular Imaging.

## LUNG VENTILATION

Several approaches to lung ventilation studies are available in nuclear medicine, with the predominant approaches being  $^{81\text{m}}\text{Kr}$  as an inert gas,  $^{99\text{m}}\text{Tc}$ -diethylenetriaminepentaacetic acid aerosol, and the ultrafine  $^{99\text{m}}\text{Tc}$ -carbon dispersion of Technegas.  $^{81\text{m}}\text{Kr}$  use is limited by availability, cost, the short half-life, and the less practical SPECT.  $^{99\text{m}}\text{Tc}$ -diethylenetriaminepentaacetic acid has aerosolized droplets with varying sizes ( $0.5\text{--}2\text{ }\mu\text{m}$ ), with distribution dependent on the aerodynamics of gas flow. As a result, aerosol ventilation studies can be confounded by deposition in large airways, and this issue is exacerbated in patients with respiratory symptoms. The ultrafine Technegas particles ( $<0.1\text{ }\mu\text{m}$ ), by contrast, have a gaslike distribution, particlelike retention, and the attractive properties of  $^{99\text{m}}\text{Tc}$  to allow high-quality imaging, including SPECT. Internationally, Technegas is considered the best alternative for the ventilation portion of the V/Q scan (7,8).

## TECHNEGAS PRODUCTION

Technegas is hexagonally shaped graphite capsule enclosing  $^{99\text{m}}\text{Tc}$  (1). The fact that these graphite particles are small ( $<0.1\text{ }\mu\text{m}$ ) and hydrophobic allows penetration deep into the airways and resists attachment to the airways, making them ideal for evaluation of deposition in the lungs (9). Technegas is distributed in the lung airways by diffusion and becomes fixed in the lumen of the airways sufficiently long to allow SPECT (10).

The commercially available Technegas generator operates with  $^{99\text{m}}\text{Tc}$ -sodium pertechnetate eluted from the  $^{99}\text{Mo}/^{99\text{m}}\text{Tc}$  generator. The graphite crucible accommodates 0.17 mL, and this volume should not be exceeded. Once the  $^{99\text{m}}\text{Tc}$  has been added to the crucible, the liquid is evaporated (simmered) at  $70^\circ\text{C}$  for 6 min in an ultrapure argon environment. On completion of the simmer cycle, the combustion cycle (burn) is initiated, in which an alternating-current arc is produced between the terminals holding the crucible to ablate the graphite and  $^{99\text{m}}\text{Tc}$  (11). Temperatures of  $2,750^\circ\text{C}$  are created for 15 s in an ultrapure argon environment to produce the carbon nanoparticles (11). Operation of the Technegas generator is simple when the stepwise process is followed. Specific steps in the process are detailed in the user guide and will not be repeated here, but outlined below are general comments associated with each step for consideration when using the Technegas generator (Fig. 1).

## OPERATION OF THE TECHNEGAS GENERATOR

The first step is to ensure that the Technegas generator is in good working order, is connected to an adequate supply of argon (or a change of argon gas bottles), is connected to the main power supply, and is powered on (Fig. 2). The delivery to the patient can occur at the patient's bedside using battery power. This option is useful because it allows the Technegas generator to be prepared in a radiation-safe location remote from patient, staff, and scanning areas (e.g.,

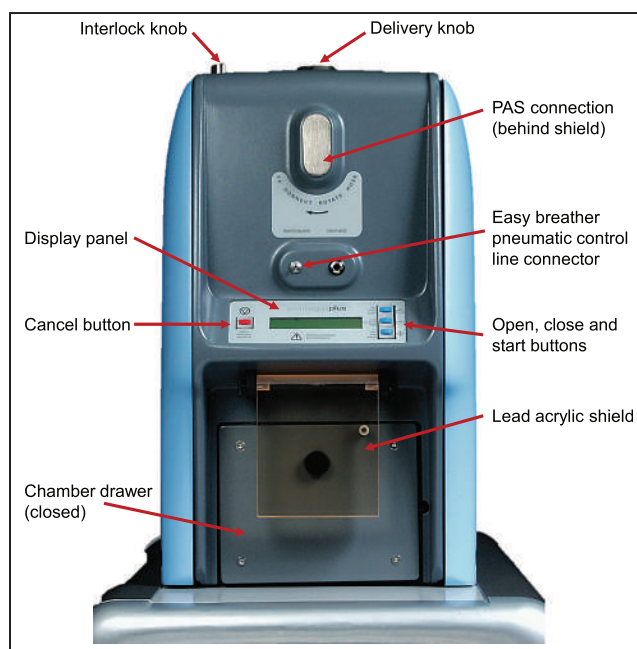


**FIGURE 1.** Annotated front view of Technegas generator. Chamber drawer is in closed position, and shield is closed down over administration set port. Not all models are fitted with easy-breather option. PAS = patient-administration set. (Courtesy of Cyclomedica.)

in or adjacent to the radiopharmacy) and delivered under battery power to patients in an inpatient trolley/gurney bay, in an outpatient consultation room, on the  $\gamma$ -camera, or in a remote ward. The burn must be performed while the generator is connected to the main power supply, after which there is a 7- to 10-min window to complete patient ventilation; thus, remote delivery requires careful planning.

The second step is the simmer phase, in which the  $^{99\text{m}}\text{Tc}$ -sodium pertechnetate is evaporated in the crucible well, usually 10–30 min before the patient arrives. Before loading the new crucible, one must ensure that the previous crucible has fractured and dropped into the collection tray, which should be emptied before a new crucible is loaded, usually

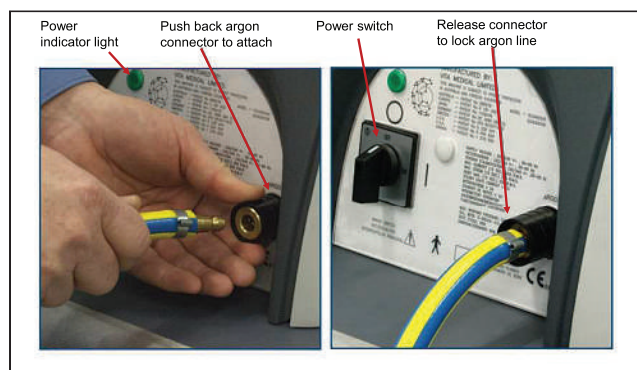


**FIGURE 2.** Annotated rear view of Technegas generator demonstrating connection of argon to system. (Courtesy of Cyclomedica.)



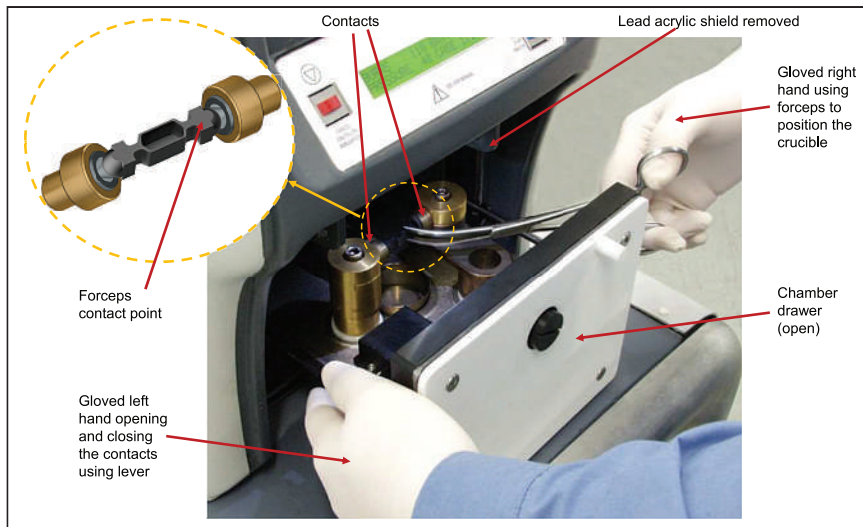


**FIGURE 3.** Use of gloves and good dexterity are required to place crucible between contacts, making good connection with fracturing crucible. For photography purposes, lead acrylic shield has been removed. (Courtesy of Cyclomedica.)

before arrival of the first lung scan patient of the day, to ensure that there is minimal radioactivity remaining. Visually inspecting the condition of the contacts and checking for any debris that might prevent the chamber from closing is also a useful step in preventative maintenance. The operator should avoid touching the parts of the crucible that will connect to the contacts because oil from the skin will reduce connection efficiency and Technegas yield. Loading the new crucible requires a degree of dexterity in manipulating it using forceps (Fig. 3). Because anything inside the chamber is potentially radioactive, gloves and standard radiation safety practices must be applied. The surfaces of the crucible well need to be wet with ethanol at the time the  $^{99m}\text{Tc}$  is added, or the  $^{99m}\text{Tc}$  volume may be displaced from the well during the simmer phase. The ethanol is generally applied before the crucible is loaded, but if the well is dry at the time the  $^{99m}\text{Tc}$  is added, the wetting can be repeated with the crucible in situ. The operator gently rotates the crucible back and forth between the contacts before adding the  $^{99m}\text{Tc}$  to ensure that a good connection is made to optimize Technegas yield. This rotation should not be a twisting motion, to avoid fracturing the fairly fragile crucible. The operator then adds 0.14–0.17 mL of  $^{99m}\text{Tc}$ -sodium pertechnetate containing 400–900 MBq. The meniscus should be flat or concave and not overflow the well (Fig. 4; top), as the  $^{99m}\text{Tc}$  would then simply be blown off the top of the crucible and a wet aerosol of free pertechnetate produced for inhalation, deteriorating image quality. If the total activity in 0.17 mL is lower than 400 MBq, multiple 6-min simmers can be performed to increase activity and avoid overloading the crucible volume. After ensuring that the argon pressure is optimized in the green zone of the regulator, the operator closes the drawer and commences the simmer.

The third step is preparing the patient with a practice run. This step is no doubt among the most important in optimizing Technegas performance. The key to successful Technegas delivery is patient compliance, which is achieved through good patient education and practice, and should not be rushed. A detailed explanation of the ventilation process in language that the patient understands, with ample opportunity for clarification and questions, is essential. The process will be foreign to many patients, although those who are familiar with snorkeling may be more comfortable with it. The difficulty is compounded by patients' different levels of respiratory distress, which can produce a large variation in patient performance and thus affect ventilation image quality. The practice

run should be done under the same conditions as the actual ventilation procedure in order to forestall any surprises. For example, if the patient practices while sitting but is lying down for the actual procedure, one can expect a difference in performance. Likewise, if the patient practices in a waiting area but undergoes the actual procedure on a

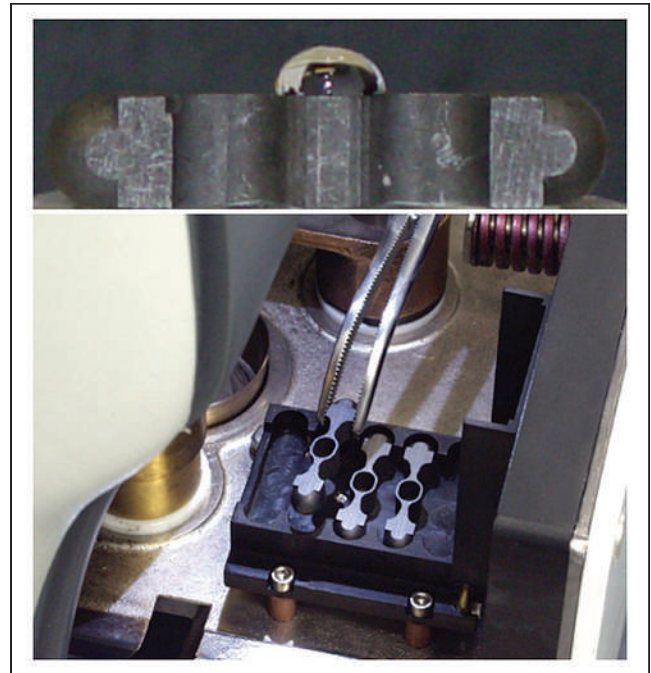


**FIGURE 4.** (Top) Excess  $^{99m}\text{Tc}$  added to crucible well will be blown off during simmer and wasted. (Reprinted with permission of 18). (Bottom) Built-in simmer oven for crucibles in chamber to allow multiple simmer cycles for low-concentration  $^{99m}\text{Tc}$ . (Courtesy of Cyclomedica.)



**TABLE 1**  
Technegas Tips

1	Performing ventilation upright produces distribution different from that when performed supine. $^{99m}\text{Tc}$ -macroaggregated albumin should be administered for perfusion in same position as that in which ventilation was performed.
2	Gloves and gown should be worn when performing the ventilation stage as this is biggest risk for contamination. This stage also requires face masks to be worn for coronavirus disease 2019 compliance.
3	For days on which eluate has high specific concentration, eluate should be diluted so that no more than 900 MBq are contained in 0.15-mL volume.
4	When used as per instruction, Technegas produces minimal contamination risk to staff and no risk of cross contamination between patients, a very important advantage with coronavirus disease 2019 (16).
5	Any unused crucibles in simmer oven at end of day can be cleansed with ethanol the next day and reloaded for simmer.
6	Since Technegas does not clear through kidneys, compared with $^{99m}\text{Tc}$ -diethylenetriaminepentaacetic acid aerosol studies, radiation dose to kidneys, bladder, and fetus is lower (17).

$\gamma$ -camera, one might expect a difference in response, especially if the  $\gamma$ -camera makes the patient feel anxious. A common error is to have the patient practice without the nose peg, which creates an environment and level of compliance completely different from when the nose is blocked. The practice session improves timing, the ventilation process, patient compliance (especially with seals), and optimization of the appropriate mouthpiece for that patient (Fig. 5). Practicing the

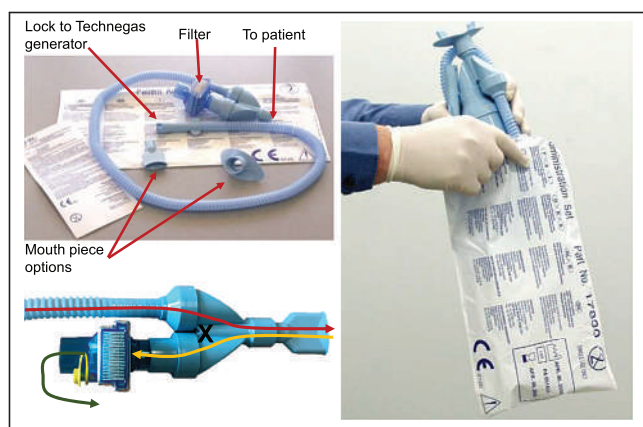


**FIGURE 5.** (Top left) Disposable administration set with multiple mouthpiece options to suit patient. (Bottom left) Administration set delivers Technegas to patient (red line) and returns patient breath through filter (yellow line) using 1-way valve to prevent communication between the 2 airflows (cross) and filtering both radioactive and biologic content of patient expiration to produce uncontaminated output into room air (green line). (Right) Entire administration set is disposed of in its original plastic bag. (Courtesy of Cyclomedica.)

process is as much about preparing the patient as it is about making the administering staff aware of any compliance issues and the projected number of inspirations required.

The fourth step is to initiate the burn phase, which produces the combination of  $^{99m}\text{Tc}$  and carbon as nanoparticles under high temperatures in just 15 s. This step should not be commenced until the patient is ready to be ventilated. As soon as the burn phase is completed, the Technegas should be delivered to the patient. The message “burn complete” is displayed, followed by an instruction to disconnect the generator from the main power supply. If the delivery is to take place at the production location, it is accomplished simply by switching the power button to off (Fig. 2). If the delivery is to be remote from the production location, the generator is disconnected from the main power supply and argon and transported to the patient.

The important fifth step is patient ventilation. The single most important inspiration is the first one, and this requires careful timing. The first release of Technegas (delivery knob) occurs under a small amount of pressure. The results are best when the release is timed during inspiration. If the release occurs during expiration or during the dead space at the end of inspiration or expiration, the high concentration Technegas in the first release is directed to the filter and wasted. The release should be timed to occur in the second quarter of the inspiration, and if practiced correctly, that inspiration will be a deep one. For that first inspiration, the patient will have been instructed to first breath out and then take a deep breath, hold for a second, and breath out. The operator should be providing these instructions during the delivery and should time the release with the first inspiration. The patient should return to normal-volume breaths after the initial inspiration, but care should be taken not to instruct the patient to “breath normally now,” as patients have a tendency to do exactly that and break the seal or remove the apparatus from their mouth. The biggest risk of contamination comes when patients try to breath in or out around rather than through the mouthpiece. Perhaps “continue to breathe through the tube with normal-size breaths” is a better instruction. Once the ventilation portion of the test is completed, the patient should continue to breathe through the administration set to remove any remaining airborne Technegas residue for 4–5 breaths. If the delivery knob is not depressed, the system is diverted to breathing room air. After the ventilation portion of the test has deposited the desired amount of Technegas, the entire administration set is stored in its original plastic bag (Fig. 5) and disposed of as biologic waste after 10 half-lives.

The count rate from the lungs in a posterior orientation on the  $\gamma$ -camera should be about 1,000–1,500 counts per second, which equates to between 20 and 50 MBq delivered to the lungs. This allows a standard  $^{99m}\text{Tc}$ -macroaggregated albumin administered dose to produce counts 4–7 times higher than the ventilation count. A perfusion count 4 times higher is the minimum to provide sufficient contrast to identify perfusion defects without being filled in by ventilation

counts, whereas 7 times higher is optimal. Consequently, an over-efficient ventilation delivery could undermine diagnostic integrity. This situation might occur when a patient is highly compliant, with excellent inspiration, or when the  $^{99m}\text{Tc}$  is in high specific concentration. For example, fresh eluate from a  $^{99}\text{Mo}/^{99m}\text{Tc}$  generator early in the generator life cycle can have substantially more than 900 MBq in 0.15 mL and, even in a suboptimal ventilation process, result in count rates in the lungs well in excess of 3,000 per second with 1 or 2 breaths. The long residence time of Technegas in the lungs means that radioactive decay is the only option to manage the count differential. A level of 3,000 counts per pixel would need to be delayed by a full half-life (6 h) before the perfusion is performed, for example. If the ventilation process is performed away from the  $\gamma$ -camera—with its instantaneous feedback on the amount deposited—then a radiation detector can be used to monitor the count rate in the lungs. In this case, the device should be calibrated against the  $\gamma$ -camera count rate so that specific readings on the radiation detector are known to equate to specific count rates on the  $\gamma$ -camera. Although it is common for the ventilation process to occur on the  $\gamma$ -camera itself, noncompliance during ventilation can contaminate the detector, increase the background count, and impact scanning for the remainder of the day.

The final step is the system purge, which takes a further 6 min and requires the Technegas generator to be reconnected to the argon and the main power supply. Residual Technegas in the chamber is purged through the system filter, after which the system is ready for the next simmer cycle. The purge—although occurring well within the acquisition window of the ventilation scan, let alone the entire V/Q study—is the rate-limiting step for a busy department. The patient-administration sets are single-use disposables and must be discarded between patients; however, on busy days with multiple ventilation scans scheduled, it is possible to use a single simmer phase and burn phase to ventilate more than 1 patient. Careful planning and timing are required, with each patient having an individual administration set. Because there is no biologic contamination from the patient into the Technegas system itself, changing administration sets between patients eliminates the risk of contamination between patients. The first patient ventilated should be the patient with the least compliance or greatest difficulties, to capitalize on the higher activity available for the first release. The residual can then be used for the second patient, who has a more optimal breathing status.

### LOW SPECIFIC CONCENTRATION OF $^{99m}\text{Tc}$

There are many situations in which the  $^{99m}\text{Tc}$  eluate concentration may produce less than 400 MBq in the 0.17-mL crucible well volume. Some clinical departments do not have an on-site  $^{99}\text{Mo}/^{99m}\text{Tc}$  generator, and unit doses or bulk  $^{99m}\text{Tc}$  may have a low specific concentration, especially at the end of the day. Clinical sites operating with

smaller generators may not produce a concentration sufficient to add 400 MBq to the crucible in 0.17 mL. For example, a generator eluted with 40 GBq in 20 mL will, even at the time of elution, have only 300 MBq in 0.15 mL, which obviously decreases to 150 MBq in the afternoon at 6 h after elution. Even departments with large generators can have low specific concentrations of  $^{99m}\text{Tc}$  toward the end of the weekly generator cycle. For example, a  $^{99}\text{Mo}/^{99m}\text{Tc}$  generator calibrated Monday with 120 GBq might, by the end of the week, be expected to have a yield only on the order of 50 GBq (accommodating elution efficiency) and, if eluted in 20 mL, would produce less than 400 MBq in 0.15 mL at elution time and less than 200 MBq at 6 h after elution.

This problem has several possible solutions, with the best approach being dependent on the specific circumstances. The first option is to simply perform multiple simmers, adding  $^{99m}\text{Tc}$  to the crucible well between simmers. At the end of the simmer cycle, cancelling the process and opening the chamber drawer allows  $^{99m}\text{Tc}$  to be added because the volume has been reduced by evaporation, effectively doubling the total activity. This approach is perhaps the best for low-volume departments (in which a low specific concentration may impact only 1 or 2 patients per day) at the end of the day or toward the end of the generator week. It may also occasionally be necessary to do 3 or more simmer cycles (e.g., when the  $^{99}\text{Mo}/^{99m}\text{Tc}$  generator has a low yield at the end of the day or after hours). For those departments receiving bulk  $^{99m}\text{Tc}$  or unit doses from centralized radiopharmacies, a more efficient approach would be to purchase larger-volume crucibles. The standard crucible has a 0.15-mL well that accommodates up to 0.17 mL, whereas the larger crucibles have a volume of 0.3 mL, accommodating enough  $^{99m}\text{Tc}$  to be equivalent to a double simmer cycle.

Some models of the Technegas generator have a built-in simmer oven that allows up to 5 crucibles to be mounted and loaded with  $^{99m}\text{Tc}$  and evaporated during each simmer cycle (Fig. 4, bottom). The crucible can have an additional 0.15 mL added to the first dose between simmer cycles or between full cycles of patient delivery. Because the crucibles are not in connection with the contacts, no arc is formed and no Technegas is produced during a burn cycle. An alternative approach that predates the built-in crucible ovens is an external crucible oven. These are simple hot plates, enclosed and shielded for radiation safety, in which up to 10 crucibles can be loaded with  $^{99m}\text{Tc}$  and evaporated multiple times. These are no longer commercially available but can be manufactured locally when a built-in oven is not available (the model for the U.S. market will not include the built-in crucible oven). In either case, the preloaded and preevaporated crucible is required to undergo a full simmer-and-burn cycle when placed between the contacts.

### TECHNEGAS VENTILATION IMAGING PROTOCOL

After the patient has inhaled the Technegas to a rate of 1,000–1,500 counts per second, imaging begins

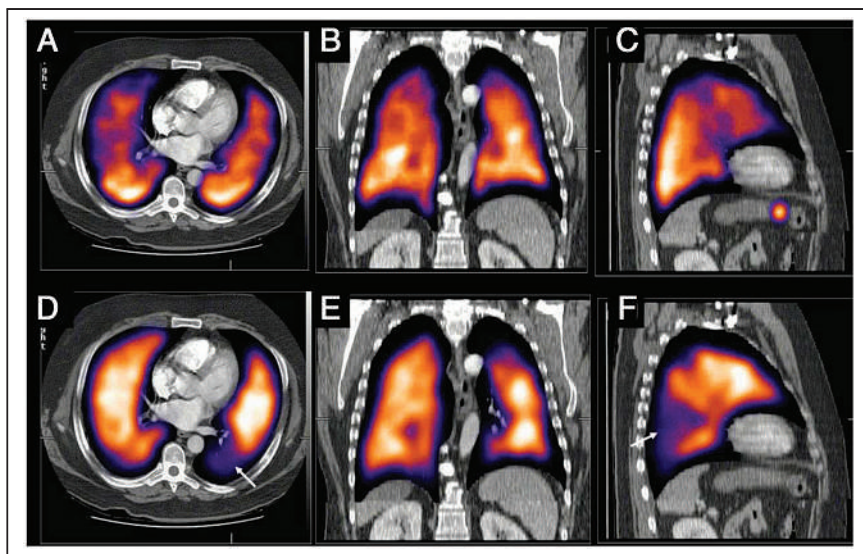


**FIGURE 6.** State-of-art contemporary SPECT/CT imaging of lung ventilation (top row) and perfusion (bottom row) in 3 orthogonal planes. SPECT/CT images demonstrate segmental perfusion defect (arrow in D and F) in left lower lobe. This appears mismatched when compared with corresponding ventilation images. Notch at apex of left lung seen in sagittal views (C and F) is matched on ventilation and perfusion and therefore is unlikely to be due to embolus.

immediately. Planar protocols (which are not recommended today, SPECT/CT being preferred) would involve 8 projections for 500,000–1,000,000 counts, or 5 min per image (anterior/posterior; 45° right anterior oblique/45° left posterior oblique; 45° left anterior oblique/45° right posterior oblique; and left lateral/right lateral). The advised SPECT approaches include a minimum of 120 projections at 10–12 s per projection with a  $128 \times 128$  matrix, using a high-resolution collimator despite the respiratory motion limits on spatial resolution. After iterative reconstruction, some sites produce planar-equivalent images from the dataset. One approach is to sum several projections on either side of the required view (anterior, for example, would be projection 1 summed with projections 2, 3, 119, and 120) (4). A better approach is to reproject the SPECT data with an associated attenuation map (5). More commonly, however, the SPECT data provide the insights (Fig. 6) required and the planar extracted data are not required or produced. Although the principal application of the V/Q study is in the evaluation of known or suspect pulmonary embolism (12), Technegas ventilation studies are also useful in the evaluation of chronic obstructive pulmonary disease, chronic thromboembolic pulmonary hypertension, silicosis, cystic fibrosis, asthma, and emphysema, and in presurgical evaluation of regional variability in lung function, although a discussion of the clinical applications is beyond the scope of this article and can be found elsewhere (6).

### PERTECHNEGAS

If the ultra-pure argon (>99.99%) is adjusted with the addition of 2%–3% oxygen during the burn phase, the

resulting carbon-bound  $^{99m}\text{Tc}$  produces the same gaslike distribution in the lungs but with rapid clearance from the lungs (7- to 10-min half-clearance time) (1,13), referred to as pertechne-gas. Because the standard Technegas has no effective clearance, it cannot be used for lung clearance studies. The oxygen-containing variant pertechne-gas allows functional dynamic studies for lung clearance (13).

### GALLIGAS

$^{68}\text{Ga}$ -chloride from a  $^{68}\text{Ge}/^{68}\text{Ga}$  generator can be added to the Technegas generator in the same way as  $^{99m}\text{Tc}$  is used (no modifications) for ventilation PET imaging. This substance is commonly referred to as galligas. One important consideration for galligas is that the standard Technegas generator is designed to shield the 140-keV  $\gamma$ -emissions of  $^{99m}\text{Tc}$  and is therefore inadequate, from a radiation

safety perspective, for shielding the 511-keV  $\gamma$ -emissions of  $^{68}\text{Ga}$  (14).  $^{68}\text{Ga}$ -galligas can be used in combination with  $^{68}\text{Ga}$ -labeled microspheres to perform PET-based V/Q (15). This use exploits the advantages of PET/CT in terms of superior resolution; superior sensitivity; the capacity for respiratory gating, dynamic imaging, and quantification; decreased imaging time; and potentially decreased patient-absorbed radiation dose from the V/Q study (14), compared with SPECT imaging. Conversely,  $^{68}\text{Ga}$  is more expensive and less readily available than  $^{99m}\text{Tc}$ , even for those sites with a  $^{68}\text{Ge}/^{68}\text{Ga}$  generator, and PET/CT is not as widely available as SPECT/CT and generally has a demanding oncology case load. However, galligas is an excellent tool for studying regional ventilation in respiratory physiology and research.

An alternative to galligas that emerged in conference abstracts in 2011 and 2012 was the potential for  $^{18}\text{F}$ -fluorogas ventilation in combination with  $^{64}\text{Cu}$ -macroaggregated albumin. Details are scarce in the mainstream literature, and clinical use has not emerged. The obvious barrier to both  $^{68}\text{Ga}$  and  $^{18}\text{F}$  PET imaging of the lungs is that the lungs are of low density, producing less attenuation of the 511-keV photon emissions of  $^{68}\text{Ga}$ . In addition, the positron is of high energy (especially for  $^{68}\text{Ga}$ ) and therefore travels some distance before annihilation, thus reducing spatial resolution (14).

### PRACTICAL PROTOCOL

Operation of the Technegas system uses a stepwise procedure that is simple, safe, and effective (Fig. 7).

Step 1 is to check and load the generator: check that the main power supply and argon are connected, switch the power on, ensure that the argon regulator is in the green



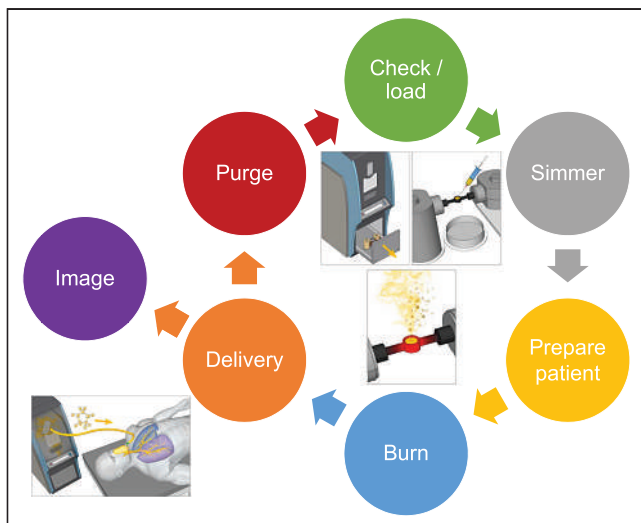


**FIGURE 7.** Technegas production cycle, beginning with checking and loading chamber. (Inset courtesy of Cyclomedica.)

zone, open the chamber drawer (“open” button), check for debris and whether the ash tray needs emptying, wet and drain the well of the crucible with ethanol, load the crucible between the contacts, add the  $^{99m}\text{Tc}$ -pertechnetate to the crucible well, and close the drawer by simultaneously holding down the interlock knob and the “close” button until the chamber is fully closed.

Step 2 is to perform the simmer: press the start button to initiate the 6-min simmer cycle, and recheck the argon regulator to ensure that the pressure stays in the green zone as the argon purge is initiated.

Step 3 is to prepare the patient: identify the correct patient, explain the procedure, obtain informed consent, open a new administration set, have the patient practice breathing through the apparatus with specific attention to keeping an airtight seal, change the mouth piece if necessary, and identify and resolve any compliance issues.

Step 4 is to perform the burn: position and prepare the patient for Technegas delivery before initiating the burn, and press the “start” button to initiate the 15-s burn.

Step 5 is to deliver the Technegas: verify the burn, disconnect the main power supply and argon, transport the entire Technegas generator to the patient and connect the administration set to the system, ensure that the patient has the appropriate seal and press the “start” button to commence Technegas delivery, release the Technegas for patient ventilation by depressing the delivery knob during patient inspiration, and monitor the activity delivered with a target of 1,000–1,500 counts per second on the  $\gamma$ -camera or equivalent using a radiation detector.

Step 6 is to purge the system: confirm successful patient ventilation, return the Technegas generator to the main power supply and the argon supply and connect both, adjust the argon regulator to the green zone, and turn on the power switch so that the system cycles through a 6-min purge. At the end of the purge, the system is ready for the next patient cycle.

Step 7 is to obtain the images: on successful patient ventilation, commence the ventilation phase of the lung scan immediately, and dispose of the administration set.

## CONCLUSION

Technegas is a simple yet versatile system for producing high-quality  $^{99m}\text{Tc}$ -based ventilation studies. The design affords safety to patients and staff, including consideration of radiation and biologic risks. Technegas is the gold standard for ventilation studies for performing SPECT-based V/Q studies in pulmonary embolism and several respiratory pathologies. When approved by the U.S. Food and Drug Administration, Technegas will extend advantages to workflow, safety, and study quality for departments that adopt the technology.

## DISCLOSURE

No potential conflict of interest relevant to this article was reported.

## REFERENCES

- Burch WM, Sullivan PJ, McLaren C. Technegas: a new ventilation agent for lung scanning. *Nucl Med Commun*. 1986;7:865–871.
- McLaren CJ. Ventilation and perfusion lung tomography [abstract]. *Aust N Z J Med*. 1987;17(suppl 2):459.
- Rojas-Burke J. High hopes for Technegas. *J Nucl Med*. 1991;32(11):24N–25N, 29N–30N.
- Reinartz P, Schirp U, Zimmy M, et al. Optimizing ventilation-perfusion lung scintigraphy: parting with planar imaging. *Nuklearmedizin*. 2001;40:38–43.
- Bailey DL, Schembri GP, Cooper RA, Bailey EA, Roach PJ. Reprojection of reconstructed V/Q SPECT scans to provide high count planar images [abstract]. *J Nucl Med*. 2005;46(suppl):337P.
- Roach PJ, Bailey DL, Schembri GP, Thomas P. Transition from planar to SPECT V/Q scintigraphy: rationale, practicalities and challenges. *Semin Nucl Med*. 2010;40:397–407.
- Leblanc M, Tessier M, Ollenberger G, O'Brien C. CANM guidelines for ventilation/perfusion (V/P SPECT) in pulmonary embolism. Canadian Association of Nuclear Medicine website. [https://canm-acmn.ca/resources/Documents/Guidelines\\_Resources/MasterDocument\\_Final\\_Nov\\_21\\_incl-Exec-Sum\\_ver3\\_Dec.%2012\\_.pdf](https://canm-acmn.ca/resources/Documents/Guidelines_Resources/MasterDocument_Final_Nov_21_incl-Exec-Sum_ver3_Dec.%2012_.pdf) Published November 2018. Accessed September 8, 2021.
- Roach PJ, Schembri G, Bailey DL. V/Q scanning using SPECT and SPECT/CT. *J Nucl Med*. 2013;54:1588–1596.
- Roach PJ, Bailey DL, Harris BE. Enhancing lung scintigraphy with single photon emission computed tomography. *Semin Nucl Med*. 2008;38:441–449.
- Roach PJ, Bailey DL, Schembri GP. Reinventing ventilation/perfusion lung scanning with SPECT. *Nucl Med Commun*. 2008;29:1023–1025.
- Weibe L, Burch W, Abrams D. Technegas:  $^{99m}\text{Tc}$ -metal core graphite nanoparticles for pulmonary ventilation imaging. *Curr Radiopharm*. 2010;3:49–59.
- Bajc M, Olsson B, Gottsäter A, Hindorf C, Jögi J. V/P SPECT as a diagnostic tool for pregnant women with suspected pulmonary embolism. *Eur J Nucl Med Mol Imaging*. 2015;42:1325–1330.
- Mackey DWJ, Jackson P, Baker RJ, et al. Physical properties and use of pertechnetate as a ventilation agent. *J Nucl Med*. 1997;38:163–167.
- Bailey DL, Eslick EM, Schembri GP, Roach PJ.  $^{68}\text{Ga}$  PET ventilation and perfusion lung imaging: current status and future challenges. *Semin Nucl Med*. 2016;46:428–435.
- Hofman MS, Beauregard JM, Barber TW, Neels OC, Eu P, Hicks RJ.  $^{68}\text{Ga}$  PET/CT ventilation-perfusion imaging for pulmonary embolism: a pilot study with comparison to conventional scintigraphy. *J Nucl Med*. 2011;52:1513–1519.
- Currie G. 2020, Post-COVID19 “new normal” for nuclear medicine practice: an Australasian perspective. *J Nucl Med Technol*. 2020;48:234–240.
- Schembri GP, Miller A, Smart RC. Radiation dosimetry and safety issues in the investigation of pulmonary embolism. *Semin Nucl Med*. 2010;40:442–454.
- Currie G, Wheat J, Traviss ZB. The impact of exceeding recommended crucible volumes in the Technegas generator. *Internet J Nucl Med*. 2006;3.

# Lung Perfusion Scintigraphy Early After COVID-19: A Single-Center Retrospective Study

Sajal De<sup>1</sup>, Mudalsha Ravina<sup>2</sup>, Tinu Lukose<sup>2</sup>, Ranganath T. Ganga<sup>1</sup>, and Dibakar Sahu<sup>1</sup>

<sup>1</sup>Department of Pulmonary Medicine, All India Institute of Medical Sciences, Raipur, India; and <sup>2</sup>Department of Nuclear Medicine, All India Institute of Medical Sciences, Raipur, India

The incidence of thromboembolic complications in coronavirus disease 2019 (COVID-19) infection is well recognized. The present study retrospectively evaluated the type and prevalence of lung perfusion defects in early-post-COVID-19 patients with hypoxia and was aimed to identify the risk factors for mismatched perfusion defects. **Methods:** We analyzed SPECT/CT images of 54 early-post-COVID-19 patients (44 men and 10 women). Logistic regression analysis was used to examine the risk. **Results:** The mean age of the study population was 55.4 y (range, 34–76 y). All received prophylactic anticoagulation from the day of hospitalization to the date of perfusion scanning. The median interval between COVID-19-positive reports and lung perfusion scanning was 22 d. Lung perfusion defects (of any type) were observed in most (87%). Twenty-three subjects (42.6%) had mismatched perfusion defects. Mismatched perfusion defects were segmental in 14 subjects (25.9%) and subsegmental in 11 (20.4%). Higher age was a risk factor for mismatched perfusion defects (odds ratio, 1.06; 95% CI, 0.99–1.13;  $P = 0.06$ ). Subjects with a serum D-dimer level of at least 2,500 ng/mL on the day before the scan were not at higher risk for having mismatched perfusion defects (odds ratio, 1.14; 95% CI, 0.34–3.9;  $P = 0.83$ ). **Conclusion:** Despite prophylactic anticoagulation, mismatched perfusion defects suggestive of pulmonary thromboembolism were observed. Serum D-dimer level in patients early after COVID-19 is a poor predictor of mismatched perfusion defects. Confirmed evidence of pulmonary embolism by imaging studies should support the decision to extend anticoagulant prophylaxis in post-COVID-19 patients.

**Key Words:** early-post-COVID-19 patients; D-dimer; lung perfusion scan; novel coronavirus disease 2019

**J Nucl Med Technol 2021; 49:320–323**  
DOI: 10.2967/jnmt.121.262440

Severe acute respiratory syndrome coronavirus 2 (SARS-CoV-2), a novel member of the enveloped RNA  $\beta$ -coronavirus family, causes coronavirus disease 2019

(COVID-19). Most COVID-19 patients are either asymptomatic or mildly symptomatic.

The thrombogenic potential of SARS-CoV-2 infection is well recognized (1). The coagulation abnormalities, along with prolonged bed rest due to hospitalization, lead to high incidences of venous thromboembolism and thromboembolic complications, mostly pulmonary embolism (PE). Thromboprophylaxis with low-molecular-weight heparin is currently recommended for the treatment of hospitalized COVID-19 patients. Despite adequate anticoagulant therapy, both venous thromboembolism and PE, especially in severe and critically ill COVID-19 patients, have been reported (1). An observational study of over 500 COVID-19 patients admitted to 8 intensive care units in France reported 22.7% thrombotic complications, mostly PE (2). A metaanalysis of over 7,000 COVID-19 patients showed that the pooled in-hospital incidence of PE in the general ward and intensive care unit was 14.7% and 23.4%, respectively (3). Currently, there is no recommendation on whether prophylactic anticoagulation should be used for COVID-19 patients with a raised level of serum D-dimer at the time of discharge.

Multidetector CT pulmonary angiography (CTPA) is the gold standard for diagnosing PE. A ventilation-perfusion scan is an alternative to CTPA for diagnosing PE. However, there is a potential risk of infection transmission during ventilation-perfusion scanning (4). Lung perfusion scintigraphy by SPECT/CT is a safe alternative for diagnosing PE, especially for COVID-19 patients. The role of SPECT/CT in diagnosing PE in COVID-19 patients has been established (4). A perfusion scan of the COVID-19 patient is useful for evaluating residual-clot burden and small-vessel injuries (5). The presence of at least 1 wedge-shaped peripheral perfusion defect estimated as at least 50% involvement of a pulmonary segment without a corresponding CT image abnormality is indicative of PE in COVID-19 (4).

After recovery from active infection, a few COVID-19 patients, especially those who were severely or critically ill, continue to have hypoxia. The causes of persistent hypoxia in early-post-COVID-19 patients are not fully understood. Impaired lung perfusion is considered one of the underlying pathophysiologic mechanisms. The presence of perfusion defects in early-post-COVID-19 patients with persistent hypoxia has not, to our knowledge, been previously

Received Apr. 15, 2021; revision accepted May 21, 2021.  
For correspondence or reprints, contact Sajal De (sajalde@yahoo.com).  
Published online July 30, 2021.

Immediate Open Access: Creative Commons Attribution 4.0 International License (CC BY) allows users to share and adapt with attribution, excluding materials credited to previous publications. License: <https://creativecommons.org/licenses/by/4.0/>. Details: <http://jnmt.snmjournals.org/site/misc/permission.xhtml>.

COPYRIGHT © 2021 by the Society of Nuclear Medicine and Molecular Imaging.



investigated. The present study retrospectively evaluated the type and prevalence of lung perfusion defects in early–post-COVID-19 patients with hypoxia and was aimed to identify the risk factors for mismatched perfusion defects.

## MATERIALS AND METHODS

### Study Design and Participants

We conducted a retrospective analysis of 54 early–post-COVID-19 patients admitted to the pulmonary medicine department of our institute between August 2020 and March 2021. The Institutional Ethics Committee approved this retrospective study, and the requirement to obtain informed consent was waived. All subjects had microbiologically confirmed SARS-CoV-2 infection (either by reverse-transcription polymerase chain reaction or rapid antigen testing). After 2 consecutively negative reverse-transcription polymerase chain reaction results for SARS-CoV-2, these patients were shifted from the COVID-19 wards to the pulmonary ward for ongoing treatment of hypoxia. The study subjects were stratified into 2 categories: moderate COVID-19 (i.e., those who received low-flow [e.g., nasal cannula] or high-flow [e.g., face mask, nonrebreathing mask, and high-flow nasal cannula] oxygen therapy) and severe COVID-19 (i.e., those who received invasive or noninvasive ventilator support during active COVID-19 infection).

### Data Collection

The demographic characteristics, comorbidities, clinical profile, laboratory reports, and treatment received were extracted from the medical records.

### Imaging Protocol

After intravenous injection of 148–222 MBq (4–6 mCi) of  $^{99m}\text{Tc}$ -macroaggregated albumin containing  $4\text{--}6 \times 10^5$  particles, SPECT imaging with low-dose CT was performed with the patient supine. Planar imaging was done in multiple projections (anterior and posterior; right and left lateral; right anterior and posterior oblique; and left anterior and posterior oblique). The images were reconstructed in the transaxial, coronal, and sagittal views and were reviewed for perfusion defects. The mismatched perfusion defects in this study were based on a mismatch between CT and scintigraphy images. The perfusion defects were further categorized as mismatched segmental perfusion defects (a wedge-shaped peripheral defect involving  $\geq 50\%$  of a pulmonary segment in all 3 orthogonal planes and without corresponding parenchymal abnormalities in the CT images), mismatched subsegmental perfusion defects (at least 1 wedge-shaped peripheral defect involving  $< 50\%$  of a pulmonary segment in all 3 orthogonal planes and without corresponding parenchymal abnormalities in the CT images), matched segmental perfusion defects (any perfusion defect involving  $\geq 50\%$  of a pulmonary segment in all 3 orthogonal planes with corresponding parenchymal abnormalities [e.g., consolidation, ground-glass opacities, or fibrosis] in the CT images), or matched subsegmental perfusion defects (any perfusion defect involving  $< 50\%$  of a pulmonary segment in all 3 orthogonal planes with corresponding parenchymal abnormalities [e.g., consolidation, ground-glass opacities, or fibrosis] in the CT images).

### Statistical Analysis

The study variables were expressed as mean  $\pm$  SD, median with interquartile range, and proportion. The odds ratio with 95% CIs

was calculated using logistic regression analysis to examine the association of risk factors with mismatched perfusion defects (segmental, subsegmental, or both). The risk factors assessed in this study were age, sex, serum D-dimer level on the day before the perfusion study, interval (in days) between lung scintigraphy and positive COVID-19 reports, and severity of disease (categorical variables). The statistical analysis was performed with SPSS, version 20.0 (IBM). A *P* value of less than 0.05 was taken as statistically significant.

## RESULTS

### Demographic Profile

The total study population was 54, and most were men ( $n = 44$ , 81.5%). The mean age was 55.4 y (median, 56 y; range, 34–76 y). A history of diabetes mellitus, hypertension, and coronary artery disease was present in 19 (35.2%), 24 (44.4%), and 3 (5.6%) subjects, respectively. Fourteen subjects had moderate COVID-19 infections (25.9%), and 40 had severe COVID-19 infections (74.1%). All patients received low-molecular-weight heparin prophylaxis from the day of hospitalization to the date of the perfusion scan. The serum D-dimer level on the day before perfusion scanning was available for 44 subjects. The median serum D-dimer level was 3,540 ng/mL (interquartile range, 1,457–6,549 ng/mL, range, 500–15,000 ng/mL). The median interval between COVID-19–positive reports and lung perfusion scanning was 22 d (interquartile range, 15–33 d; range, 8–107 d). The single person with the highest interval was taking an oral apixaban tablet.

### Perfusion Scintigraphy

Lung perfusion defects (of any type) were observed in 47 subjects (87%). Matched perfusion defects were the commonest and were observed in 39 subjects (72.2%). The type and prevalence of perfusion defects are presented in Table 1. Perfusion defects did not differ between moderate and severe COVID-19. Mismatched perfusion defects were observed in 23 subjects (42.6%). Most cases (61%) of mismatched perfusion were segmental. Six subjects had both matched and mismatched segmental perfusion defects. More cases of mismatched segmental perfusion defects were in the right lung than in the left (8 vs. 4,  $P < 0.01$ ).

There was no significant difference in serum D-dimer level between subjects with only mismatched segmental perfusion defects and subjects with only matched segmental perfusion defects (median, 3,700 vs. 3,804 ng/mL;  $P > 0.05$ ). Logistic regression analysis showed that the risk of mismatched perfusion defects increased as age increased (odds ratio, 1.06; 95% CI, 0.99–1.13;  $P = 0.06$ ). A longer interval between positive COVID-19 results and the scintigraphy study did not create a lower risk of mismatched perfusion defects (odds ratio, 0.66; 95% CI, 0.22–1.96;  $P = 0.5$ ). The risk for mismatched perfusion defects in men was not higher compared than that in women (odds ratio, 1.14; 95% CI, 0.28–4.62;  $P = 0.9$ ). Patients with severe COVID-19 were not at higher risk of having mismatched perfusion defects than were patients with moderate COVID-19

**TABLE 1**  
Distribution of Various Types of Lung Perfusion Abnormalities

Type of abnormality	Moderate COVID-19 ( <i>n</i> = 14)	Severe COVID-19 ( <i>n</i> = 40)	Total ( <i>n</i> = 54)
Perfusion defects (any)	14 (100)	33 (82.6)	47 (87)
Mismatched perfusion defects	7 (50)	16 (40)	23 (42.6)
Segmental	3 (21.4)	11 (27.5)	14 (25.9)
Subsegmental	4 (28.6)	7 (17.5)	11 (20.4)
Both segmental and subsegmental	0	2 (5)	2 (3.7)
Matched perfusion defects	11 (78.6)	28 (70)	39 (72.2)
Segmental	6 (42.9)	13 (32.5)	19 (35.2)
Subsegmental	7 (50)	23 (57.5)	30 (55.6)
Both segmental and subsegmental	2 (14.3)	8 (20)	10 (18.5)
Both matched and mismatched perfusion defects	4 (28.6)	11 (27.5)	15 (27.8)

Data are number followed by percentage in parentheses.

(OR, 0.67; 95% CI, 0.19–2.27; *P* = 0.5). Patients with a serum D-dimer level of at least 2,500 ng/mL before the day of the scan were not at higher risk of having mismatched perfusion defects (odds ratio, 1.14; 95% CI, 0.34–3.9; *P* = 0.83).

## DISCUSSION

The present study showed mismatched perfusion defects suggestive of PE in early–post-COVID-19 patients, despite receiving anticoagulation prophylaxis from the first day of hospitalization. Lung perfusion defects in COVID-19 were matched or mismatched, and the distribution was segmental or subsegmental. A higher age carried a higher risk for having mismatched perfusion defects.

SARS-CoV-2 binds with the angiotensin-converting enzyme 2 receptor present on the cell surface. Binding of the virus on angiotensin-converting enzyme 2 receptors leads to upregulation of angiotensin II and activation of the renin-angiotensin-aldosterone system. Both this system and angiotensin II enhance platelet activity and activate the coagulation cascade, as well as increasing the expression of interleukin 6 and other inflammatory markers, which further amplifies the coagulation cascade (6). Increased levels of clotting factors, with disruption of the normal homeostasis of vascular endothelial cells in COVID-19, lead to microangiopathy and thrombus formation. Lung autopsies of COVID-19 patients have demonstrated endothelial injury, with intracellular virus in the pulmonary vasculature, microangiopathy, and widespread thrombosis with occlusion of alveolar capillaries (7). Deposition of fibrin and thrombin in the pulmonary microvasculature leads to impaired lung perfusion. The subsegmental mismatched perfusion defects in our study confirm the small-vessel injuries.

CTPA helps to visualize clots within the pulmonary vasculature, and most investigators have used CTPA for diagnosing PE in COVID-19. A Dutch study observed that most PE diagnosed by CTPA in COVID-19 patients was in segmental or more proximal arteries (8). Another study found that most PE diagnosed by CTPA was subsegmental (93%)

(9). Therefore, PE in COVID-19 involves both segmental and subsegmental pulmonary arteries. CTPA can miss the thrombus in distal subsegmental small vessels and be unable to assess tissue perfusion. Thus, there is a risk of underestimation of PE in COVID-19 by CTPA (5). Idilman et al. identified 25.8% perfusion defects on the dual-energy CT scans of 31 patients with mild to moderate COVID-19 (10). Most PE (75%) in their study was without macroscopic thromboembolism on CTPA. Except for a few case reports and small case series, lung perfusion defects, especially in early–post-COVID-19 patients, have not been much investigated (11–13). The prevalence of segmental mismatched perfusion defects—that is, PE—in our study was similar to that in a previous study (3). The longer interval between COVID-19–positive reports and scanning did not reduce the risk for mismatched perfusion defects. Therefore, despite anticoagulant prophylaxis, PE of COVID-19 takes longer to resolve. Mismatched perfusion defects in our study were more on the right side, similar to the observation by Mueller-Peltzer et al. (14).

Serum D-dimer is considered a sensitive test to diagnose thrombotic states, including PE. A systematic review and metaanalysis showed that serum D-dimer in severe COVID-19 was significantly higher than non-severe forms and correlated with the disease severity (15). In COVID-19 patients, the rise in serum D-dimer is due to activation of the blood coagulation cascade secondary to a systemic inflammatory response or as a direct consequence of the virus itself. Serum D-dimer in COVID-19 patients correlates poorly with the venous thromboembolism score (16). Several investigators tried to find the D-dimer cutoff that identifies the risk of PE in active COVID-19 infection. Cui et al. found that a serum D-dimer level of 1,500 ng/mL has 85.0% sensitivity and 88.5% specificity for predicting venous thromboembolism (17). Léonard-Lorant et al. observed that a serum D-dimer threshold of 2,660 µg/L detected all cases of PE by CTPA in COVID-19 patients (18). We observed that subjects with a serum D-dimer level of at least 2,500 ng/mL were not at higher risk of having mismatched perfusion defects. Therefore, an elevated level

of serum D-dimer in early-post-COVID-19 patients is not necessarily attributable to underlying PE.

This study had several limitations. It was a single-center retrospective study, and not all early-post-COVID-19 patients with hypoxia were investigated. Serial serum D-dimer levels were not available for all patients. The number of subjects was small, and no patients with mild COVID-19 were enrolled.

## CONCLUSION

The present study showed that SPECT/CT images suggestive of PE were independent of serum D-dimer level before the day of scanning. An elevated level of serum D-dimer in early-post-COVID-19 patients should not be a criterion for posthospitalization anticoagulant therapy unless imaging studies confirm the PE. Carefully designed prospective studies are necessary to identify the post-COVID-19 patients who will require extended thromboprophylaxis.

## DISCLOSURE

No potential conflict of interest relevant to this article was reported.

## REFERENCES

- Helms J, Tacquard C, Severac F, et al. High risk of thrombosis in patients with severe SARS-CoV-2 infection: a multicenter prospective cohort study. *Intensive Care Med.* 2020;46:1089–1098.
- Tacquard C, Mansour A, Godon A, et al.; French Working Group on Perioperative Hemostasis. Impact of high-dose prophylactic anticoagulation in critically ill patients with coronavirus disease 2019 pneumonia. *Chest.* 2021;159:2417–2427.
- Roncon L, Zuin M, Barco S, et al. Incidence of acute pulmonary embolism in COVID-19 patients: systematic review and meta-analysis. *Eur J Intern Med.* 2020; 82:29–37.
- Lu Y, Macapinlac HA. Perfusion SPECT/CT to diagnose pulmonary embolism during COVID-19 pandemic. *Eur J Nucl Med Mol Imaging.* 2020;47:2064–2065.
- Dhawan RT, Gopalan D, Howard L, et al. Beyond the clot: perfusion imaging of the pulmonary vasculature after COVID-19. *Lancet Respir Med.* 2021;9:107–116.
- Potus F, Mai V, Lebreton M, et al. Novel insights on the pulmonary vascular consequences of COVID-19. *Am J Physiol Lung Cell Mol Physiol.* 2020;319: L277–L288.
- Ackermann M, Verleden SE, Kuehnel M, et al. Pulmonary vascular endothelialitis, thrombosis, and angiogenesis in Covid-19. *N Engl J Med.* 2020;383:120–128.
- Klok FA, Kruip MJHA, van der Meer NJM, et al. Confirmation of the high cumulative incidence of thrombotic complications in critically ill ICU patients with COVID-19: an updated analysis. *Thromb Res.* 2020;191:148–150.
- Mandal AKJ, Kho J, Ioannou A, Van den Abbeele K, Missouri CG. Covid-19 and in situ pulmonary artery thrombosis. *Respir Med.* 2021;176:106176.
- Idilman IS, TelliDizman G, ArdaliDuzgun S, et al. Lung and kidney perfusion deficits diagnosed by dual-energy computed tomography in patients with COVID-19-related systemic microangiopathy. *Eur Radiol.* 2021;31:1090–1099.
- Kobes N, Guernou M, Lussato D, et al. Ventilation/perfusion SPECT/CT findings in different lung lesions associated with COVID-19: a case series. *Eur J Nucl Med Mol Imaging.* 2020;47:2453–2460.
- Das JP, Yeh R, Schöder H. Clinical utility of perfusion (Q)-single-photon emission computed tomography (SPECT)/CT for diagnosing pulmonary embolus (PE) in COVID-19 patients with a moderate to high pre-test probability of PE. *Eur J Nucl Med Mol Imaging.* 2021;48:794–799.
- Kurkowska S, Piwowarska-Bilska H, Iwanowski J, et al. Lung perfusion SPECT/CT images associated with COVID-19: a case series. *Nucl Med Rev Cent East Eur.* 2021;24:35–36.
- Mueller-Peltzer K, Krauss T, Benndorf M, et al. Pulmonary artery thrombi are co-located with opacifications in SARS-CoV2 induced ARDS. *Respir Med.* 2020; 172:106135.
- Paliogiannis P, Mangoni AA, Dettori P, Nasrallah GK, Pintus G, Zinellu A. D-Dimer concentrations and COVID-19 severity: a systematic review and meta-analysis. *Front Public Health.* 2020;8:432.
- Yu B, Li X, Chen J, et al. Evaluation of variation in D-dimer levels among COVID-19 and bacterial pneumonia: a retrospective analysis. *J Thromb Thrombolysis.* 2020;50:548–557.
- Cui S, Chen S, Li X, Liu S, Wang F. Prevalence of venous thromboembolism in patients with severe novel coronavirus pneumonia. *J Thromb Haemost.* 2020;18: 1421–1424.
- Léonard-Lorant I, Delabranche X, Séverac F, et al. Acute pulmonary embolism in patients with COVID-19 at CT angiography and relationship to d-dimer levels. *Radiology.* 2020;296:E189–E191.

---

---

# Immune Checkpoint Inhibitor–Related Adverse Effects and $^{18}\text{F}$ -FDG PET/CT Findings

Jan-Henning Schierz<sup>1</sup>, Ismet Sarikaya<sup>2</sup>, Uwe Wollina<sup>3</sup>, Leonore Unger<sup>4</sup>, and Ali Sarikaya<sup>5</sup>

<sup>1</sup>Department of Radiology, Municipal Hospital Dresden, Dresden, Germany; <sup>2</sup>Department of Nuclear Medicine, Kuwait University Faculty of Medicine, Kuwait; <sup>3</sup>Department of Dermatology, Municipal Hospital Dresden, Dresden, Germany; <sup>4</sup>Department of Rheumatology, Municipal Hospital Dresden, Dresden, Germany; and <sup>5</sup>Department of Nuclear Medicine, Trakya University Faculty of Medicine, Edirne, Turkey

Immune checkpoint inhibitor (ICI) treatments activate T cells against tumors. Activated T cells attack not only the tumor but also healthy cells, causing an autoimmune reaction in various tissues. These immune-related adverse effects (IRAEs) cause  $^{18}\text{F}$ -FDG uptake in various tissues due to inflammation. It is important to recognize and report these findings on  $^{18}\text{F}$ -FDG PET/CT studies.  $^{18}\text{F}$ -FDG PET helps to determine the presence, location, and severity of IRAEs. In severe cases, ICI treatments are interrupted or suspended and antiinflammatory treatments are started.  $^{18}\text{F}$ -FDG uptake due to IRAEs may mimic metastases or disease progression. Their presence may also help in predicting response to treatment and have prognostic implications. In this review article, we provide basic information about ICI treatments, IRAEs, and  $^{18}\text{F}$ -FDG PET/CT findings.

**Key Words:** immune checkpoint inhibitor;  $^{18}\text{F}$ -FDG PET/CT; adverse effect; autoimmune

**J Nucl Med Technol 2021; 49:324–329**

DOI: 10.2967/jnmt.121.262151

Immune checkpoint inhibitor (ICI) treatments have been increasingly used in oncology in the last 10 years. ICI treatments activate T cells against tumors by blocking inhibitory ICI immunoreceptors or their ligands. Activated T cells attack not only the tumor but also healthy and normal cells, causing an autoimmune reaction in various tissues. These immune-related adverse effects (IRAEs) cause increased uptake on  $^{18}\text{F}$ -FDG PET/CT studies due to inflammation in various tissues.  $^{18}\text{F}$ -FDG PET has high sensitivity in detecting inflammation and determining its severity and extent. It is important to recognize and report IRAE-related findings on PET images. On the basis of the severity and extent of IRAEs, physicians interrupt or suspend ICI treatment and start steroid or immunosuppressive treatments. The presence and severity of IRAEs may help to predict response to ICI treatment and may have prognostic value, indicating a more favorable prognosis (1–3). Depending on the location,

particularly in lymph nodes, IRAE-related uptake may mimic metastases or disease progression, and therefore it is important to be aware of these immune-related side effects. In this review article, we will describe first the ICIs, then the mechanism of autoimmune reactions in patients receiving ICI treatment, and finally the  $^{18}\text{F}$ -FDG PET/CT findings.

## IMMUNE CHECKPOINT INHIBITORS

Immune checkpoints play an important role in immune regulation. There are various checkpoint molecules (immunoreceptors) on T cells, some of them being inhibitory (suppressing the T cells) and some stimulatory (activating the T cells) (4,5). Tumors or antigen-presenting cells (e.g., macrophages or dendritic cells) have various ligands on their surfaces that bind to inhibitory or stimulatory checkpoint receptors on T cells, resulting in activation or suppression of T cells (5). Activated T cells subsequently kill the microorganisms (viruses, bacteria, fungi, and parasites) and tumors but then can also attack healthy cells, resulting in autoimmune diseases. Suppression of T cells prevents autoimmune diseases but results in reduced protection against microorganisms. The tumor microenvironment can also suppress T cells. In normal conditions, inhibitory immune checkpoint immunoreceptors are activated to prevent T cells from attacking normal tissues.

In the last 10 years, various medications (antibodies) have been developed to block (inhibit) inhibitory checkpoint molecules (immunoreceptors or their ligands) in the treatment of tumors and infection. These medications are called immune checkpoint inhibitors (ICIs). Currently approved ICI medications block cytotoxic T-lymphocyte–associated protein 4 (ipilimumab), programmed death receptor 1 (pembrolizumab, nivolumab), or its ligand (atezolizumab, avelumab, durvalumab, and cemiplimab) (4,6). These medications are approved to be used in the treatment of various cancers such as melanoma (ipilimumab, nivolumab, pembrolizumab), non-small cell lung cancer (pembrolizumab, nivolumab), renal cancer (nivolumab, ipilimumab), and bladder cancer (atezolizumab) (4,6).

Inhibition of cytotoxic T-lymphocyte–associated protein 4 and programmed death receptor 1 or its ligand through

---

Received Feb. 17, 2021; revision accepted May 20, 2021.  
For correspondence or reprints, contact Ismet Sarikaya (isarikaya99@yahoo.com).

Published online July 30, 2021.

COPYRIGHT © 2021 by the Society of Nuclear Medicine and Molecular Imaging.

ICI treatment activates T cells to kill tumor cells but also causes T cells to target healthy tissues, resulting in IRAEs (autoimmune manifestations). They can also cause a flare of prior autoimmune disease. IRAEs are commonly seen in patients receiving ICI treatments and are dependent on dose and type of ICI treatment and various other factors. IRAEs can be clinically evident or silent and can involve any tissues, resulting in such conditions as encephalitis, hypophysitis, thyroiditis, sarcoidlike reactions, pneumonitis, hepatitis, pancreatitis, adrenalitis, colitis, nephritis, arthritis, and skin manifestations. Most fatalities are seen in cases of encephalitis, myocarditis, pneumonitis, and hepatitis (7). IRAEs can be seen a few weeks to months after starting ICI treatment. Clinical, laboratory, radiologic, and  $^{18}\text{F}$ -FDG PET/CT imaging findings can help to diagnose IRAEs. Optimal management of IRAEs varies according to the organ involved and the severity or grade of involvement and includes close monitoring, treatment interruption or suspension, and corticosteroid administration (prednisone or methylprednisolone) (8).

### $^{18}\text{F}$ -FDG PET/CT IMAGING

$^{18}\text{F}$ -FDG PET/CT imaging is used to assess the response to ICI treatment in various tumors, particularly melanoma and non-small cell lung cancer.  $^{18}\text{F}$ -FDG PET response patterns in ICI treatment show some atypical patterns different from those seen with other treatments, such as chemotherapy or radiotherapy. This difference occurs because ICI treatments induce an influx of T lymphocytes into the tumor, and these T lymphocytes take up  $^{18}\text{F}$ -FDG and subsequently further increase the metabolic activity of the tumor environment (9,10). Immune-related response criteria such as PERCIST or immune RECIST have been established to better assess the response in patients receiving ICI treatments (11,12).

$^{18}\text{F}$ -FDG PET-positive IRAEs, such as sarcoidlike syndrome, thyroiditis, hypophysitis, enterocolitis, pancreatitis, hepatitis, pneumonitis, arthritis, enthesitis, and myositis, have been reported in various articles (13,14).

$^{18}\text{F}$ -FDG PET is sensitive in detecting early inflammation even before clinical symptoms start and radiologic changes develop (15,16). Cells involved in inflammation actively use glucose, which is the main reason for increased  $^{18}\text{F}$ -FDG uptake at inflammatory sites. In addition, increased blood flow and capillary permeability also contribute to increased  $^{18}\text{F}$ -FDG activity at inflammation sites; this activity is non-specific and can be seen with any kind of radiotracer. It has been reported that a significant number of patients with PET-detectable IRAEs are asymptomatic (1,17). Early detection of IRAEs allows early management. Their presence may help predict the response to treatment and indicate a more favorable prognosis (1–3). In a study by Sachpekidis et al., in 10% of patients PET/CT showed sarcoidlike lymphadenopathy as a response to treatment, and these patients showed disease control (2). In another study, 9

patients with IRAE findings on PET had a complete response at the final evaluation (1). Patients with PET-detectable IRAEs had a significantly longer progression-free survival than did those without IRAEs on PET (3).

Colitis is one of the most common manifestations of IRAEs. On unenhanced CT as a part of PET/CT, colonic wall thickening and pericolic fat stranding may be seen in association with diffuse or segmental increased  $^{18}\text{F}$ -FDG uptake.  $^{18}\text{F}$ -FDG PET/CT imaging was reported to be more sensitive than CT in the early detection of colitis as a result of ICI treatment (6,17,18). However,  $^{18}\text{F}$ -FDG PET has a low specificity for colitis due to physiologic mucosal, muscular, and luminal activity. In addition, metformin use can induce high bowel activity, and it is recommended that metformin be stopped for 48 h before the  $^{18}\text{F}$ -FDG PET study. Figure 1 shows sagittal  $^{18}\text{F}$ -FDG PET/CT images of a 71-y-old patient with a history of melanoma. PET/CT before treatment did not show abnormal findings in the sigmoid colon, but PET/CT 4 mo after nivolumab treatment

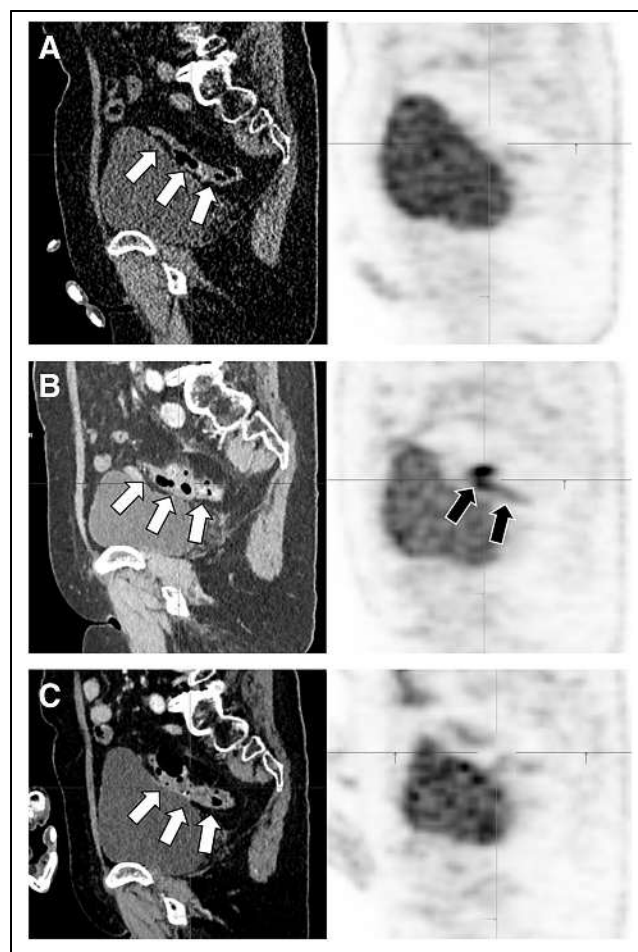


**FIGURE 1.** Selected sagittal  $^{18}\text{F}$ -FDG PET/CT images of pelvis. Initial scan before treatment shows normal findings in colon (arrows, A), PET/CT scan 4 mo after nivolumab treatment shows colitis in sigmoid colon (arrows, B), and PET/CT scan 6 mo after discontinuation of nivolumab shows significant reduction in sigmoid activity (arrows, C).

showed thickening in the sigmoid wall, with inflamed diverticula and increased uptake without clinical symptoms. PET 6 mo after discontinuation of nivolumab (treatment change to dabrafenib and trametinib because of disease progression) showed only mild thickening in the sigmoid wall as a late inflammatory residue (fatty infiltration) and only mild uptake.

$^{18}\text{F}$ -FDG PET has high sensitivity in detecting rheumatologic manifestations of IRAEs such as arthritis, myositis, tenosynovitis, and polymyalgia rheumatica and in determining their extent and severity. Figure 2 shows serial  $^{18}\text{F}$ -FDG PET total-body images of a 48-y-old patient with a history of melanoma who received various ICI treatments. A PET image after 22 mo of nivolumab treatment showed mildly increased uptake in the left knee and, bilaterally, in the mediastinal and hilar lymph nodes (sarcoidlike). The patient had no clinical symptoms related to these findings. A PET image after 3 mo of treatment with pembrolizumab (change in therapy due to persistent metastasis in the 12th rib) showed diffusely increased metabolic activity in the muscles of the upper and lower extremities, a finding that indicated myositis because it correlated with clinical findings of swollen arms and legs. The PET image also showed interval slight progression in left knee uptake, mildly increased uptake in the right knee and left ankle, and bowel activity, without clinical signs. A PET image after 2 mo of nivolumab treatment showed markedly and diffusely increased bilateral uptake in all joints of upper and lower extremities. Antibody treatment was stopped, and prednisolone treatment was started by the clinician because of the

PET image findings and laboratory and clinical correlation. A PET image 12 mo after stopping nivolumab treatment (steroid treatment stopped 6 mo before PET) showed complete resolution of inflammatory uptake in the joints. No evidence of tumor was seen (complete metabolic response), and the mild sarcoidlike uptake was stable. Figure 3 shows  $^{18}\text{F}$ -FDG PET images after 1 mo and 1 y of nivolumab treatment in a 40-y-old patient with a history of melanoma. Before treatment, there was increased uptake in the bone marrow and mild, diffusely increased uptake in the knees. After treatment, there was increased uptake in the interspinous bursae of the lumbar spine, which was highly suggestive of polymyalgia rheumatica, and there was a further increase in uptake in the knees.

IRAE-related focal areas of uptake or uptake in lymph nodes can mimic metastatic disease or disease progression (19,20). Sarcoidlike reactions may mimic lymph node, lung, and skin metastases. Sarcoidlike reactions are characterized by the presence of noncaseating granulomas. In sarcoidlike reactions,  $^{18}\text{F}$ -FDG PET/CT usually shows bilateral symmetric hypermetabolic mediastinal and hilar lymphadenopathy with or without hypermetabolic focal nodular opacities or consolidations in the lungs. Uptake in the portocaval lymph nodes and subcutaneous hypermetabolic nodules due to noncaseating granulomas may also be seen in sarcoidlike reactions (10,21). Figure 4 shows  $^{18}\text{F}$ -FDG PET images of a 60-y-old patient with melanoma. A PET image for initial staging showed metastatic disease in the lungs, liver, left adrenal, and mesenteric lymph nodes and diffuse uptake in the stomach due to gastritis from *Helicobacter pylori*. A PET scan 6 mo after nivolumab treatment showed complete metabolic resolution of most lesions, with some residual tumor in the liver and progression of a left adrenal metastasis. New symmetric hypermetabolic lymph nodes in both hila and mediastinum were likely due to a sarcoidlike reaction. A nivolumab-induced flare in gastric uptake was also seen.

IRAE-related thyroiditis might be acute and transient, with biochemically and clinically accompanying thyrotoxicosis, or progressing to hypothyroidism (22). Selected CT images of a 61-y-old patient with melanoma showed reduction in thyroid size 1 y after treatment with nivolumab, as compared with baseline image (Figs. 5A and 5C). A PET image after the start of nivolumab showed diffusely increased uptake in the thyroid gland, with a cold defect in the lower pole of the right lobe corresponding to a nodule seen on CT. The thyroid-stimulating hormone level was

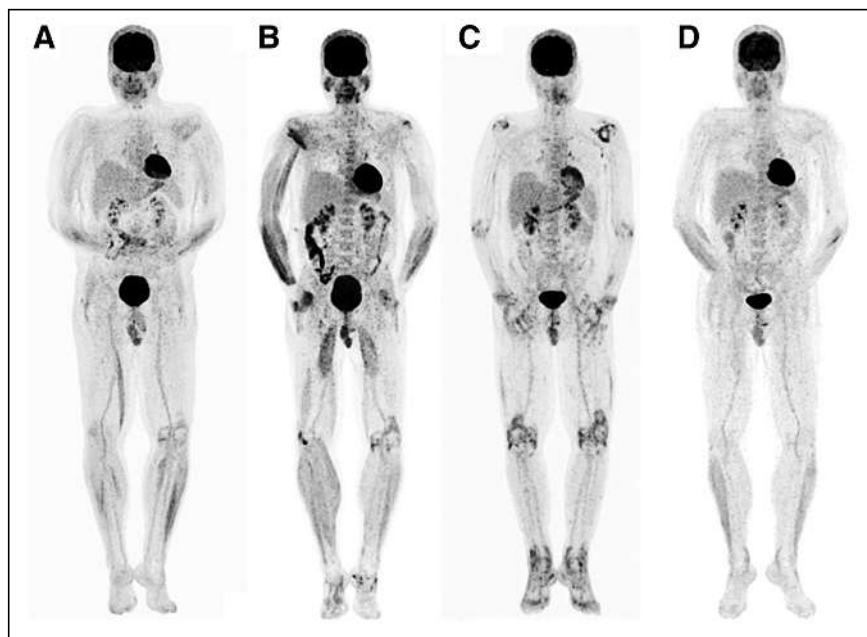


**FIGURE 2.** Serial total-body  $^{18}\text{F}$ -FDG PET maximum-intensity projections of patient with history of melanoma after treatment with nivolumab (A), pembrolizumab (B), nivolumab (C), and steroids (D). Development, progression, and regression of arthritis are seen, as well as mild sarcoidlike uptake in chest and myositis.





**FIGURE 3.** Sagittal total-body maximum-intensity-projection  $^{18}\text{F}$ -FDG PET images before (A) and after (B) nivolumab treatment. Increased uptake in lumbar spine is due to bursitis (arrows).

43 mU/L. Figure 6 shows diffusely increased uptake in the thyroid gland in a 65-y-old patient with a history of melanoma who was treated with nivolumab for 20 mo (whole body). Thyroiditis and hypothyroidism were confirmed by laboratory findings, and patient began taking thyroxine. There was also mild diffusely increased uptake in the liver ( $\text{SUV}_{\text{mean}}$ , 3;  $\text{SUV}_{\text{max}}$ , 5.2; liver-to-blood-pool  $\text{SUV}_{\text{mean}}$  ratio, 1.6) and elevated glutamate dehydrogenase and  $\gamma$ -glutamyl transferase levels, indicating hepatitis. Colonic uptake was due to

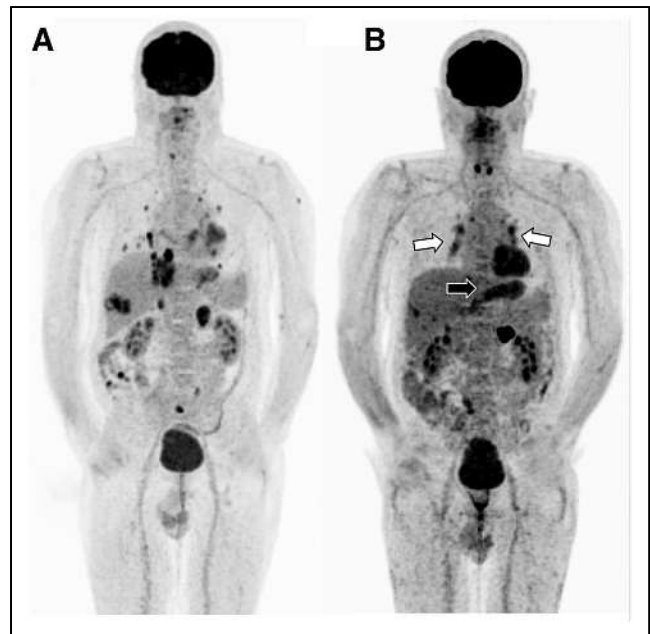


**FIGURE 4.** Total-body  $^{18}\text{F}$ -FDG PET maximum-intensity-projection images before (A) and after (B) nivolumab treatment in a melanoma case with multiple metastases. Increased bilateral uptake in hilar and mediastinal lymph nodes is due to sarcoidlike reaction (white arrows) and diffuse uptake in the stomach is due to gastritis (black arrow).

metformin use. Because of physiologic uptake in the liver,  $^{18}\text{F}$ -FDG PET may not show early hepatitis; however, in more severe cases it is possible to see diffusely increased hepatic uptake. ICI treatment-related T-cell activation can induce increased uptake in the spleen (reversal in liver-to-spleen uptake ratio), which may interfere with detection of hepatitis on PET images (10). However, careful visual assessment and obtaining a liver-to-blood-pool  $\text{SUV}_{\text{mean}}$  ratio can help detect hepatitis in such cases. A normal liver-to-blood-pool  $\text{SUV}_{\text{mean}}$  ratio ranges from 1.3 to 1.4 in various reports (23–25). Because the SUVs are affected by body weight and various other factors, the liver-to-blood-pool  $\text{SUV}_{\text{mean}}$  ratio is more accurate than  $\text{SUV}_{\text{mean}}$  alone when assessing the metabolic activity of the liver (25).

On  $^{18}\text{F}$ -FDG PET scans, the normal pituitary gland may show mild uptake. Prominent uptake in the pituitary gland could be from hypophysitis, but pituitary adenomas or metastasis should be ruled out by a clinical, laboratory, and radiologic assessment. Figure 7 shows increased uptake in the pituitary gland in a 61-y-old patient with a history of melanoma who was treated with nivolumab (pituitary-to-frontal  $\text{SUV}_{\text{max}}$  ratio was 1, as compared with 0.3 in a patient with normal uptake in the pituitary gland). Laboratory values did not show pituitary insufficiency, but MRI after 3 mo of therapy showed a swollen, inhomogeneously enhancing hypophysis with a thickened hypophyseal stalk, indicative of hypophysitis, as compared with pretreatment MRI, which showed a typical flat, homogeneously enhancing hypophysis after contrast administration (26).

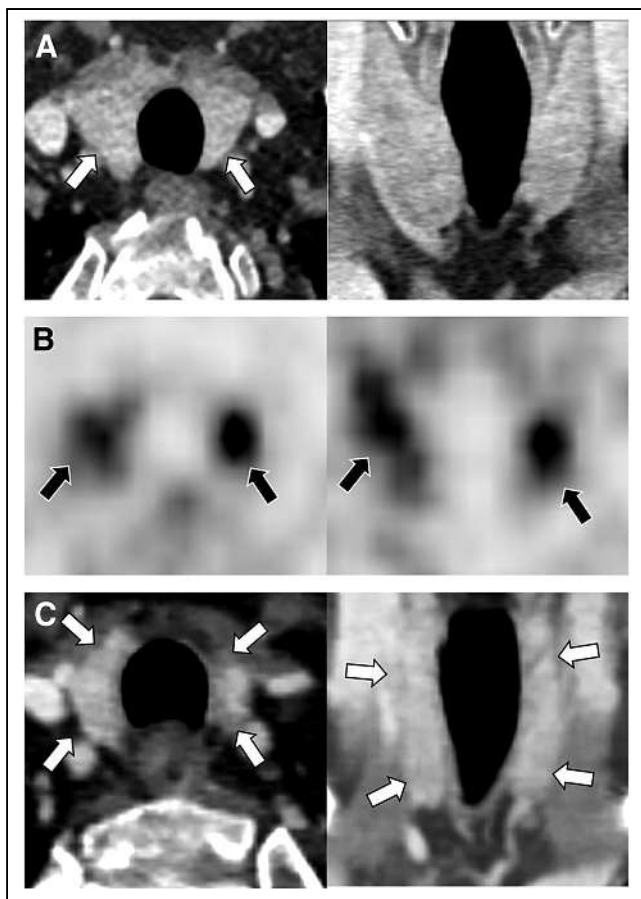


**FIGURE 5.** Selected transaxial and coronal contrast-enhanced CT images (A and C, before and 1 year after nivolumab treatment, respectively) and PET images (B, with start of nivolumab) in a case with history of melanoma. PET shows diffusely increased uptake in the thyroid due to thyroiditis (arrows), CT shows decrease in thyroid size 1 year after treatment as compared with pretreatment size (arrows pointing to the thyroid gland). Nodule in the right lower lobe is causing cold area on PET.

$^{18}\text{F}$ -FDG PET/CT has a high sensitivity in determining the severity (grade) and extent of inflammation in certain tissues such as joints and colon—information that is important in the management of patients starting steroid treatment and interrupting or suspending ICI treatment. However, care should be taken when assessing inflammation or tumors in patients who are receiving or recently received high-dose steroid treatment, as such treatment may cause a false-negative  $^{18}\text{F}$ -FDG PET result or may underestimate the metabolic activity of inflammation or tumors (27,28).

In routine oncologic studies,  $^{18}\text{F}$ -FDG PET imaging cannot accurately assess myocardial inflammation because of various degrees of physiologic myocardial uptake. If there is clinical concern about myocarditis, a cardiac  $^{18}\text{F}$ -FDG PET imaging protocol or cardiac MRI is used to demonstrate myocardial involvement (29,30).

Pelvic/urinary excreted activity may limit evaluation of the kidneys, but in renal involvement, focal or diffuse renal parenchymal  $^{18}\text{F}$ -FDG uptake may be seen in a careful



**FIGURE 6.** Total-body  $^{18}\text{F}$ -FDG PET image after nivolumab treatment shows diffuse uptake in thyroid gland due to thyroiditis (arrows), mild diffuse uptake in liver due to hepatitis (arrow), and diffuse colonic uptake due to metformin use (arrows) in a case with history of melanoma.

assessment of images (31). In addition, delayed PET imaging can help to better assess renal parenchymal involvement.

$^{18}\text{F}$ -FDG PET is also limited in assessing the brain because of physiologic high uptake in the gray matter. In encephalitis,

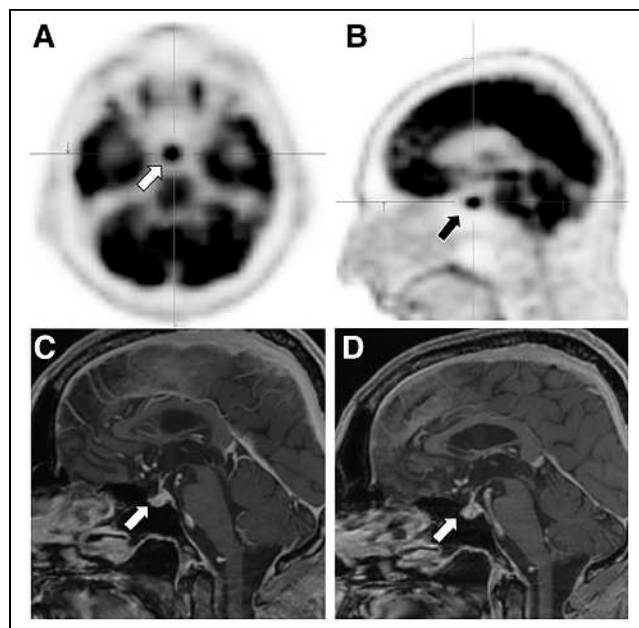


**FIGURE 7.** Selected transaxial and sagittal  $^{18}\text{F}$ -FDG PET images (A and B) and sagittal MR images (C and D, before and after treatment, respectively) show findings consistent with hypophysitis (arrows).

diffusely decreased and heterogeneous uptake may be seen. In limbic encephalitis, increased uptake may be seen in one or both mesial temporal lobes. PET/MRI or MRI of the brain can further help identify brain involvement; in particular, MRI T2-weighted fluid-attenuated inversion recovery sequences are very sensitive in inflammation (32,33).

Potential skeletal adverse effects related to immune checkpoint inhibitors have been reported as bone fractures and resorptive or destructive bone lesions due to localized inflammation, such as sterile osteitis, leading to osteoclast activation and bone resorption (34). These changes can cause increased uptake in the bones on <sup>18</sup>F-FDG PET, but no cases have yet been reported.

## CONCLUSION

ICI treatment-related autoimmune adverse effects are common. It is important to recognize and report findings of IRAE-related adverse effects on <sup>18</sup>F-FDG PET scans.

## DISCLOSURE

No potential conflict of interest relevant to this article was reported.

### KEY POINTS

**QUESTION:** What is the importance of recognizing findings of ICI treatment-related adverse effects on <sup>18</sup>F-FDG PET scans?

**PERTINENT FINDINGS:** IRAEs are commonly seen in patients receiving ICI treatments and cause increased uptake in various tissues on <sup>18</sup>F-FDG PET studies.

**IMPLICATIONS FOR PATIENT CARE:** Recognizing IRAEs on PET scan is important, as their presence and severity alert physicians to the need to interrupt or suspend ICI treatment and start antiinflammatory treatment. Their presence may also help in predicting the response to treatment. Being aware of IRAE-related uptake on <sup>18</sup>F-FDG PET scans also prevents false-positive results for metastasis or disease progression.

## REFERENCES

- Nobashi T, Baratto L, Reddy SA, et al. Predicting response to immunotherapy by evaluating tumors, lymphoid cell-rich organs, and immune-related adverse events using FDG-PET/CT. *Clin Nucl Med*. 2019;44:e272–e279.
- Sachpekidis C, Larrière L, Kopp-Schneider A, Hassel JC, Dimitrakopoulou-Strauss A. Can benign lymphoid tissue changes in <sup>18</sup>F-FDG PET/CT predict response to immunotherapy in metastatic melanoma? *Cancer Immunol Immunother*. 2019;68:297–303.
- Sachpekidis C, Kopp-Schneider A, Hakim-Meibodi L, Dimitrakopoulou-Strauss A, Hassel JC. <sup>18</sup>F-FDG PET/CT longitudinal studies in patients with advanced metastatic melanoma for response evaluation of combination treatment with vemurafenib and ipilimumab. *Melanoma Res*. 2019;29:178–186.
- Dyck L, Mills KHG. Immune checkpoints and their inhibition in cancer and infectious diseases. *Eur J Immunol*. 2017;47:765–779.
- He X, Xu C. Immune checkpoint signaling and cancer immunotherapy. *Cell Res*. 2020;30:660–669.
- Vani V, Regge D, Cappello G, Gabelloni M, Neri E. Imaging of adverse events related to checkpoint inhibitor therapy. *Diagnostics (Basel)*. 2020;10:216.
- Martins F, Sofiya L, Sykietis GP, et al. Adverse effects of immune-checkpoint inhibitors: epidemiology, management and surveillance. *Nat Rev Clin Oncol*. 2019;16:563–580.
- Rudzki JD. Management of adverse events related to checkpoint inhibition therapy. *Memo*. 2018;11:132–137.
- Decazes P, Bohn P. Immunotherapy by immune checkpoint inhibitors and nuclear medicine imaging: current and future applications. *Cancers (Basel)*. 2020;12:371.
- Prigent K, Aide N. <sup>18</sup>F-fluorodeoxyglucose PET/computed tomography for assessing tumor response to immunotherapy and detecting immune-related side effects: a checklist for the PET reader. *PET Clin*. 2020;15:1–10.
- Aide N, Hicks RJ, Le Tourneau C, Lheureux S, Fanti S, Lopci E. FDG PET/CT for assessing tumour response to immunotherapy: report on the EANM symposium on immune modulation and recent review of the literature. *Eur J Nucl Med Mol Imaging*. 2019;46:238–250.
- Dimitrakopoulou-Strauss A. Monitoring of patients with metastatic melanoma treated with immune checkpoint inhibitors using PET-CT. *Cancer Immunol Immunother*. 2019;68:813–822.
- Mekki A, Dercle L, Lichtenstein PH, et al. Detection of immune-related adverse events by medical imaging in patients treated with anti-programmed cell death 1. *Eur J Cancer*. 2018;96:91–104.
- Iravani A, Hicks RJ. Pitfalls and immune-related adverse events. In: Lopci E, Fanti S, eds. *Atlas of Response to Immunotherapy*. Springer; 2020:101–115.
- Signore A, Anzola KL, Auletta S, et al. Current status of molecular imaging in inflammatory and autoimmune disorders. *Curr Pharm Des*. 2018;24:743–753.
- Sollini M, Lauri C, Boni R, Lazzeri E, Erba PA, Signore A. Current status of molecular imaging in infections. *Curr Pharm Des*. 2018;24:754–771.
- Lang N, Dick J, Slynko A, et al. Clinical significance of signs of autoimmune colitis in <sup>18</sup>F-fluorodeoxyglucose positron emission tomography-computed tomography of 100 stage-IV melanoma patients. *Immunotherapy*. 2019;11:667–676.
- Bronstein Y, Ng CS, Hwu P, Hwu WJ. Radiologic manifestations of immune-related adverse events in patients with metastatic melanoma undergoing anti-CTLA-4 antibody therapy. *AJR*. 2011;197:W992–W1000.
- Das JP, Halpenny D, Do RK, Ulaner GA. Focal immunotherapy-induced pancreatitis mimicking metastasis on FDG PET/CT. *Clin Nucl Med*. 2019;44:836–837.
- Jespersen H, Bjursten S, Ny L, Levin M. Checkpoint inhibitor-induced sarcoid reaction mimicking bone metastases. *Lancet Oncol*. 2018;19:e327.
- Cheshire SC, Board RE, Lewis AR, Gudur LD, Dobson MJ. Pembrolizumab-induced sarcoid-like reactions during treatment of metastatic melanoma. *Radiology*. 2018;289:564–567.
- Delivanis DA, Gustafson MP, Bornschlegl S, et al. Pembrolizumab-induced thyroiditis: comprehensive clinical review and insights into underlying involved mechanisms. *J Clin Endocrinol Metab*. 2017;102:2770–2780.
- Chiaravalloti A, Danieli R, Abbatiello P, et al. Factors affecting intrapatient liver and mediastinal blood pool <sup>18</sup>F-FDG standardized uptake value changes during ABVD chemotherapy in Hodgkin's lymphoma. *Eur J Nucl Med Mol Imaging*. 2014;41:1123–1132.
- Boktor RR, Walker G, Stacey R, Gledhill S, Pitman AG. Reference range for intrapatient variability in blood-pool and liver SUV for <sup>18</sup>F-FDG PET. *J Nucl Med*. 2013;54:677–682.
- Sarikaya I, Albatineh AN, Sarikaya A. Revisiting weight-normalized SUV and lean-body-mass-normalized SUV in PET studies. *J Nucl Med Technol*. 2020;48:163–167.
- Caranci F, Leone G, Ponsiglione A, et al. Imaging findings in hypophysitis: a review. *Radiol Med (Torino)*. 2020;125:319–328.
- Delbeke D, Coleman RE, Guiberteau MJ, et al. Procedure guideline for tumor imaging with <sup>18</sup>F-FDG PET/CT 1.0. *J Nucl Med*. 2006;47:885–895.
- van der Geest KSM, Treglia G, Glaudemans AWJM, et al. Diagnostic value of (<sup>18</sup>F)FDG-PET/CT in polymyalgia rheumatica: a systematic review and meta-analysis. *Eur J Nucl Med Mol Imaging*. 2021;48:1876–1889.
- Dweck MR, Abgral R, Trivieri MG, et al. Hybrid magnetic resonance imaging and positron emission tomography with fluorodeoxyglucose to diagnose active cardiac sarcoidosis. *JACC Cardiovasc Imaging*. 2018;11:94–107.
- Chen W, Jeudy J. Assessment of myocarditis: cardiac MR, PET/CT, or PET/MR? *Curr Cardiol Rep*. 2019;21:76.
- Alessandrino F, Sahu S, Nishino M, et al. Frequency and imaging features of abdominal immune-related adverse events in metastatic lung cancer patients treated with PD-1 inhibitor. *Abdom Radiol (NY)*. 2019;44:1917–1927.
- Galmiche S, Lheure C, Kramkimel N, et al. Encephalitis induced by immune checkpoint inhibitors in metastatic melanoma: a monocentric retrospective study. *J Eur Acad Dermatol Venereol*. 2019;33:e440–e443.
- Larkin J, Chmielowski B, Lao CD, et al. Neurologic serious adverse events associated with nivolumab plus ipilimumab or nivolumab alone in advanced melanoma, including a case series of encephalitis. *Oncologist*. 2017;22:709–718.
- Moseley KF, Naidoo J, Bingham CO, et al. Immune-related adverse events with immune checkpoint inhibitors affecting the skeleton: a seminal case series. *J Immunother Cancer*. 2018;6:104.

---

# Can the Diagnostic Accuracy of Bone Scintigraphy Be Maintained with Half the Scanning Time?

Valeria M. Moncayo<sup>1</sup>, Sebastine Chimafor<sup>2</sup>, Elizabeth Lulaj<sup>3</sup>, John A. Malko<sup>1</sup>, and Raghuveer Halkar<sup>1</sup>

<sup>1</sup>Department of Radiology and Imaging Sciences, Emory University Hospital, Atlanta, Georgia; <sup>2</sup>Department of Radiology, Grady Health System, Atlanta, Georgia; and <sup>3</sup>Johns Hopkins Medical Institute, Johns Hopkins University, Baltimore, Maryland

We aimed to show that the acquisition time of a conventional bone scan could be reduced by half without losing the diagnostic value of the scan. **Methods:** Fifty adult patients (37 male and 13 female; mean age, 62.5 y; SD, 8.7 y) were enrolled. The patients were injected with 925–1,110 MBq (25–30 mCi) of <sup>99m</sup>Tc-methylene diphosphonate intravenously. The standard-protocol whole-body planar images were acquired first (scan speed, 10 cm/min; acquisition time, ~20 min) and were followed immediately by the half-time protocol whole-body planar images (scan speed, 20 cm/min; acquisition time, ~10 min). Both sets of images were interpreted by 2 nuclear medicine physicians. Each reviewer, when reviewing the standard-protocol images, was self-masked to the result he or she had obtained when reviewing the half-time images, and vice versa. This self-masking was accomplished by allowing a minimum of 2 wk to elapse between the 2 interpretations. We used the  $\kappa$ -coefficient to compare agreement between the standard-protocol results and the half-time results. **Results:** There was no difference in clinically significant diagnostic information between the half-time and standard protocols. The diagnostic quality of half-time and standard-protocol images did not significantly differ ( $0.86 < \kappa < 1.0$ ). **Conclusion:** Our data suggest that if we reduce the <sup>99m</sup>Tc-methylene diphosphonate dose by half and keep the acquisition time at its standard value, we gain the benefit of reduced dose without loss of diagnostic value.

**Key Words:** Image Wisely; half-time acquisition; <sup>99m</sup>Tc-MDP bone scan

**J Nucl Med Technol 2021; 49:330–333**  
DOI: 10.2967/jnmt.121.262163

Medical imaging is a major source of the radiation dose to humans (1). The dose delivered by the injected radiopharmaceuticals used in medical imaging is second only to the dose given by CT. Many of the radiopharmaceutical dose recommendations were formulated in the 1970s and early 1980s, and although there has been a significant improvement in  $\gamma$ -camera technology since then, many of those recommended radiopharmaceutical doses have remained unchanged. With the increase in the use of medical imaging that applies ionizing radiation, the dose

delivered to human populations has been increasing, and there is a concerted effort to reduce this radiation burden. For example, in nuclear cardiology, the initial attempt to reduce the radiation dose in myocardial perfusion imaging was to use a protocol in which the first image obtained was a low-dose stress image (2). Furthermore, the radiopharmaceutical dose has been reduced in the last 10 y by using advanced processing software such as Astonish (Philips) (3,4). Radiation dose reduction has also been possible through the use of solid-state detectors with better sensitivity, such as cadmium-zinc-telluride detectors (5).

As another example, the Society of Nuclear Medicine and Molecular Imaging and other societies have introduced the Image Wisely initiative to clinical practice (1). This initiative has resulted in studies demonstrating that images obtained with a decreased dose of a radiopharmaceutical can provide diagnostic information comparable to that from a full dose, such as <sup>99m</sup>Tc-meritide imaging for assessment of renal function and obstruction (6,7). The Image Wisely campaign was initially launched by the American College of Radiology and the Radiological Society of North America (1).

Decreasing the injected dose of radiopharmaceuticals will decrease not only the radiation dose delivered to the patient but also the dose received by the technologist who performs the study. In times of technetium shortage, which has been a recurrent problem in recent years, reducing the radiotracer dose may result in greater patient throughput (8).

<sup>99m</sup>Tc-methylene diphosphonate (<sup>99m</sup>Tc-MDP) planar bone scintigraphy is commonly used to evaluate malignant and benign conditions of the bone (9–11). Other bisphosphonate-derived radiotracers are used in other continents, although <sup>99m</sup>Tc-MDP is the most widely used in the United States. In the United States, the usual administered activity of <sup>99m</sup>Tc-MDP for bone scintigraphy in adults is 500–1,110 MBq (~13–30 mCi) (12); in Europe, a weight-based activity is customary and varies from 8 to 10 MBq/kg (11). In markedly obese adults, the administered activity could be increased to 11–13 MBq/kg (300–350  $\mu$ Ci/kg) (12).

In attempts to follow current optimal practices of patient-centered care by reducing the radiation dose in routine nuclear medicine examinations, our study aimed to prospectively evaluate the diagnostic value of half-time bone scans compared with standard-time scans. We obtained a

---

Received Feb. 21, 2021; revision accepted May 10, 2021.  
For correspondence or reprints, contact Valeria M. Moncayo (vmoncay@emory.edu).  
Published online July 30, 2021.  
COPYRIGHT © 2021 by the Society of Nuclear Medicine and Molecular Imaging.

full-dose scan in half the normal acquisition time, after obtaining a scan using the normal acquisition time. This stratagem allowed us to determine the clinical value of the standard-protocol scan while simultaneously obtaining a half-time scan for comparison, without the need to scan on different days and without increasing the radiation dose to the subjects.

## MATERIALS AND METHODS

This was an institutional review board–approved prospective study. Adult patients scheduled to receive an  $^{99m}\text{Tc}$ -MDP bone scan, who were over the age of 18 y and gave written informed consent, participated in this research study from May 2016 to December 2017. Fifty patients (37 male and 13 female; mean age, 62.5 y; SD, 8.7 y) were enrolled; their findings before this study were as follows: 47 had a malignancy (32 prostate cancer, 9 breast cancer, 1 thyroid cancer, 2 rectal cancer, 2 lung cancer, and 1 esophageal cancer) and 3 had benign bone lesions (2 Paget and 1 benign spinal lesion on MRI). The body mass index ranged from 17.5 to 43.2, with a mean of 28.2 and an SD of 7.9.

The patients were injected with 925–1,110 MBq (25–30 mCi) of  $^{99m}\text{Tc}$ -MDP intravenously, which is the standard for adults in the United States (12). Images were acquired after approximately 180–240 min. The standard-protocol whole-body planar images were acquired first (scan speed, 10 cm/min; acquisition time, ~20 min) and were followed immediately by the half-time protocol total-body planar images (scan speed, 20 cm/min; acquisition time, ~10 min). Philips  $\gamma$ -cameras (Bright View and Precedence) with low-energy high-resolution collimators were used.

Standard-protocol and half-time images were independently interpreted by 2 experienced nuclear medicine physicians, who were masked to the results of the other reviewer. The image interpretation was subjective as well as objective. Reviewer A had more than 30 y of experience, and reviewer B had 10 y of experience. Each reviewer, when reviewing the standard-protocol images, was self-masked to the result he or she had obtained when reviewing the half-time images, and vice versa. This self-masking was accomplished by allowing sufficient time (a minimum of 2 wk) to elapse between the 2 interpretations. The order in which the standard-protocol and half-time images were interpreted was random. The time of injection to the time of imaging was recorded for all patients in both protocols.

After this analysis, 1 reviewer then looked at the standard-protocol and half-time images side by side to assess whether there were any artifacts, noise, patient motion, or change in positioning between the two.

The reviewers used the following objective scoring scale for each lesion identified on the standard-protocol and half-time studies: 1, intensity hotter than background; 2, moderate intensity; 3, intensity similar to bladder or kidney; and 4, photopenic. In addition, the following lesion characterizations were used: D, degenerative; M, metastases; C, contamination; P, primary bone tumor; and O, other. To minimize bias, clinical information, results of the prior bone scans, or reports from other imaging modalities were not made available to the reviewers while they were interpreting for this study. The usual artifacts such as urine contamination, minor dose infiltration, or photopenic artifacts due to prostheses did not pose problems for either of the experienced readers.

## RESULTS

Figure 1 shows images for a subject with negative findings, with a comparison being made between the standard-protocol and half-time protocol anterior images and between the standard-protocol and half-time protocol posterior images. Figure 2 shows a similar comparison for a subject with extensive metastases.

Although our aim was to compare the results of the standard protocol with the half-time protocol, we also checked interobserver variability between the 2 reviewers. There was complete concordance between the 2 reviewers on the standard-protocol images; that is, both reviewers found the same 21 patients to have metastatic lesions and the same 29 patients to be without metastatic lesions. When the results of half-time images were compared between the 2 reviewers, the reviewers had different interpretations for only 1 patient, for whom reviewer A interpreted the foci to be degenerative and reviewer B did not mention the metastatic lesion. Except for this 1 lesion, all lesions were identified by both reviewers in the standard-protocol and half-time images. There were a few discordant interpretations between the 2 reviewers in categorizing degenerative versus metastatic disease; however, this discordance was similar between the standard and half-time protocols.

We used the  $\kappa$ -coefficient (13) to compare agreement between the standard-protocol results and the half-time results for the same reviewer. That is, the standard protocol and the half-time protocol were treated as separate reviewers. The comparison used 6 categories: D, one or more degenerate lesions found; M, one or more metastatic lesions found; T, trauma; D and M; T and M; and none, no lesion. For example, for 1 patient, the half-time review found only degenerative lesions whereas the standard-protocol review found both degenerative and metastatic lesions, and for 6 patients, both the standard-protocol review and the half-time review found both degenerative and metastatic lesions. For both reviewers,  $\kappa$  was 0.9390, the calculated SD was 0.0421, and the 95% CI was  $0.86 < \kappa < 1.0$ .

## DISCUSSION

Bone scintigraphy is one of the most common studies performed daily in nuclear medicine departments that have a high volume of oncologic patients. Although bone scintigraphy is considered to expose patients to only a modest amount of radiation, that amount is not to be underestimated. Bone scintigraphy is also done to evaluate for benign conditions, such as osteomyelitis, stress fractures, Paget disease, pain, fractures, and suspected infection of prosthetics (11).

Reducing radiation dose is important in all groups of patients, including those with cancer and those without cancer. Efforts in radiation dose reduction have been more intense in the area of nuclear cardiology.

This prospective study consisting of 50 adults found no statistical difference in diagnostic information between half-time and standard acquisitions.

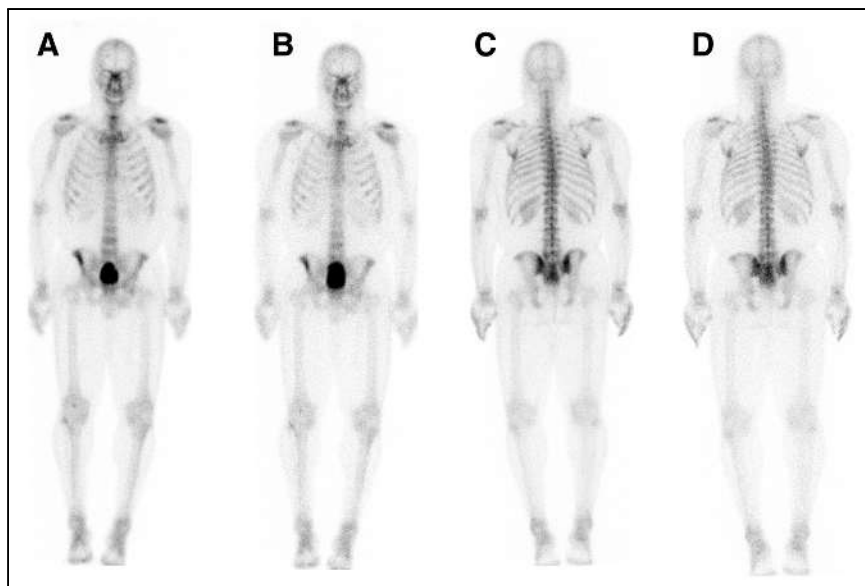


**FIGURE 1.** Planar anterior (A and B) and posterior (C and D) scintigraphic images of skeleton of patient being evaluated for prostate cancer metastasis. Images were obtained using standard (A and C) and half-time (B and D) protocols. Bladder is larger in B than in A because of time lapse between standard and half-time acquisitions. There were no findings suggestive of metastasis on this scan.

Factors such as poor renal function, poor hydration, dose infiltration, large body habitus, and patient motion can affect the quality of bone scintigraphy images. Poor renal

Some limitations of this study are that it used a relatively small number (50) of only adult subjects, all from a single institution, and that it used  $\gamma$ -cameras from a single vendor

function, poor hydration, and dose infiltration will have the same effect on both half-time and standard acquisitions.

A large body habitus can increase attenuation of photons and adversely affect the quality of the scan. Body mass index is a good indicator of body habitus, and the patient population we studied had a wide range of body mass index. There were no differences in quality or accuracy between the standard and half-time studies for the body mass index range of this study.

There were no large infiltrations of the injected dose in our study. However, the side-by-side comparison of the standard and half-time images, performed after the separate readings, showed 1 patient with head and pelvis motion between the 2 scans; this was the patient for whom the half-time protocol found only degenerative lesions but the standard protocol found both degenerative and metastatic lesions.

No camera-specific analysis was done to see whether the camera type influenced the results in some way, and this lack is also considered a limitation. The particulars of our patient population also led to some biases. Prostate cancer metastases are typically osteoblastic and show an increased tracer concentration, whereas multiple myeloma, renal disease, and thyroid disease usually demonstrate osteolytic lesions and avascular necrosis of the bone—conditions that present as photopenic defects on bone scintigraphy images. Since most patients in this study had prostate cancer, there were more instances of intense foci of uptake and very few of photopenic regions, and thus our study could not satisfactorily test the detection rates of osteolytic lesions presenting as photopenic lesions. Because we did not use weight-based doses, our results may not be applicable in countries—such as those in Europe—that do use weight-based doses. Finally, our time from injection to imaging was 2 h 30 min for

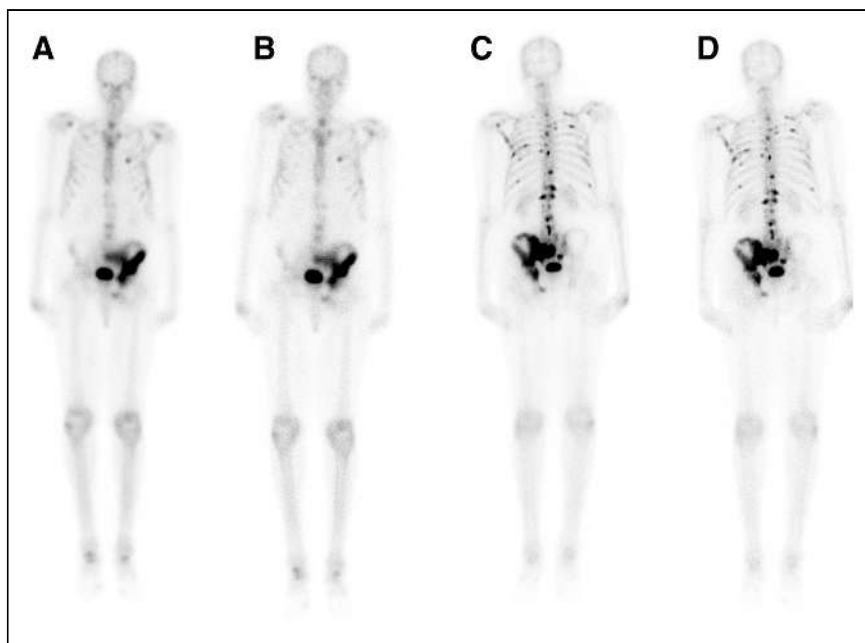


**FIGURE 2.** Planar scintigraphic images of skeleton of patient different from that in Figure 1, also being evaluated for prostate cancer metastasis. Planar anterior (A and B) and posterior (C and D) images were obtained using standard (A and C) and half-time (B and D) protocols. There is uptake throughout left iliac bone and within multiple ribs and vertebral bodies, better seen on posterior views, in pattern likely representing osseous metastasis. Degenerative uptake is noted in shoulders, ankles, and knees.



standard-protocol images and 2 h 55 min for the half-time images. Although this 25-min difference would not be expected to cause a significant change in the biodistribution of the isotope, an ideal research study might have acquired the half-time images first for 25 of our 50 patients. However, since the standard-protocol images were part of the standard clinical protocol for these patients, good clinical practices required that we obtain them first.

## CONCLUSION

We compared the diagnostic accuracy of our half-time image protocol with that of our standard-time image protocol, using the standard recommended radiation dose. We found that the diagnostic quality of half-time and standard-time images did not significantly differ. Since the half-time images have, on average, half the counts of the standard-time images, a reasonable assumption from these results is that by halving the original dose but maintaining the standard acquisition time (a procedure that would also result in half the counts), a clinically useful image will result. A multicenter, multivendor camera study is needed to determine whether our result would be true for patient populations different from the one in this study.

## DISCLOSURE

No potential conflict of interest relevant to this article was reported.

## REFERENCES

1. Brink JA. The art and science of medical guidelines: what we know and what we believe. *Radiology*. 2010;254:20–21.
2. Bateman TM, Heller GV, McGhie AI, et al. Multicenter investigation comparing a highly efficient half-time stress-only attenuation correction approach against standard rest-stress Tc-99m SPECT imaging. *J Nucl Cardiol*. 2009;16:726–735.
3. Slomka P, Germano G. Optimizing radiation dose and imaging time with conventional myocardial perfusion SPECT: technical aspects. *J Nucl Cardiol*. 2017;24:888–891.
4. Venero CV, Heller GV, Bateman TM, et al. A multicenter evaluation of a new post-processing method with depth-dependent collimator resolution applied to full-time and half-time acquisitions without and with simultaneously acquired attenuation correction. *J Nucl Cardiol*. 2009;16:714–725.
5. Duvall WL, Sweeny JM, Croft LB, et al. Reduced stress dose with rapid acquisition CZT SPECT MPI in a non-obese clinical population: comparison to coronary angiography. *J Nucl Cardiol*. 2012;19:19–27.
6. Taylor AT, Folks RD, Rahman A, et al. <sup>99m</sup>Tc-MAG3: Image Wisely. *Radiology*. 2017;284:200–209.
7. Hsiao EM, Cao X, Zurakowski D, et al. Reduction in radiation dose in mercaptoacetyl triglycerine renography with enhanced planar processing. *Radiology*. 2011;261:907–915.
8. Thomas GS, Maddahi J. The technetium shortage. *J Nucl Cardiol*. 2010;17:993–998.
9. Sureka SK, Maheshwari R, Agnihotri S, et al. Predictors for progression of metastatic prostate cancer to castration-resistant prostate cancer in Indians. *Indian J Med Res*. 2016;143(suppl):S68–S73.
10. Soloway MS, Hardeman SW, Hickey D, et al. Stratification of patients with metastatic prostate cancer based on extent of disease on initial bone scan. *Cancer*. 1988;61:195–202.
11. Van den Wyngaert T, Strobel K, Kampen WU, et al. The EANM practice guidelines for bone scintigraphy. *Eur J Nucl Med Mol Imaging*. 2016;43:1723–1738.
12. Bartel TB, Kuruva M, Gnanasegaran G, et al. SNMMI Procedure Standard for Bone Scintigraphy 4.0. *J Nucl Med Technol*. 2018;46:398–404.
13. Fleiss JL. *Statistical Methods for Rates and Proportions*. 2nd ed. John Wiley and Sons; 1981:218.

# Occupational Radiation Exposure of Radiopharmacy, Nuclear Medicine, and Surgical Personnel During Use of [ $^{99m}\text{Tc}$ ]Tc-PSMA-I&S for Prostate Cancer Surgery

Else A. Aalbersberg<sup>1</sup>, Desiree Verwoerd<sup>1,2</sup>, Chelvi Mylvaganan-Young<sup>1,2</sup>, Hilda A. de Barros<sup>3</sup>, Pim J. van Leeuwen<sup>3</sup>, Mariska Sonneborn-Bols<sup>2</sup>, and Maarten L. Donswijk<sup>1</sup>

<sup>1</sup>Department of Nuclear Medicine, Netherlands Cancer Institute, Amsterdam, The Netherlands; <sup>2</sup>Radiation Safety Department, Netherlands Cancer Institute, Amsterdam, The Netherlands; and <sup>3</sup>Department of Urology, Netherlands Cancer Institute, Amsterdam, The Netherlands

The aim of this study was to estimate and subsequently measure the occupational radiation exposure for all personnel involved in producing, administering, or performing imaging or surgery with [ $^{99m}\text{Tc}$ ]Tc-PSMA-I&S, which has been introduced for identification of tumor-positive lymph nodes during salvage prostate cancer surgery. **Methods:** The effective dose was estimated and subsequently measured with electronic personal dosimeters for the following procedures and personnel: labeling and quality control by the radiopharmacy technologist, syringe preparation by the nuclear medicine laboratory technologist, patient administration by the nuclear medicine physician, patient imaging by the nuclear medicine imaging technologist, and robot-assisted laparoscopic salvage lymph node dissection attended by an anesthesiology technologist, scrub nurse, surgical nurse, and surgeon. The dose rate of the patient was measured immediately after administration of [ $^{99m}\text{Tc}$ ]Tc-PSMA-I&S, after imaging, and after surgery. **Results:** The estimated dose per procedure ranged from  $1.59 \times 10^{-10}$   $\mu\text{Sv}$  (imaging technologist) to 9.74  $\mu\text{Sv}$  (scrub nurse). The measured effective dose ranged from 0 to 5  $\mu\text{Sv}$  for all personnel during a single procedure with [ $^{99m}\text{Tc}$ ]Tc-PSMA-I&S. The highest effective dose was received by the scrub nurse ( $3.2 \pm 1.3$   $\mu\text{Sv}$ ), whereas the lowest dose was measured for the surgical nurse ( $0.2 \pm 0.5$   $\mu\text{Sv}$ ). If a single scrub nurse were to perform as many as 100 procedures with [ $^{99m}\text{Tc}$ ]Tc-PSMA-I&S in a year, the total effective dose would be 320  $\mu\text{Sv/y}$ . Immediately after administration, the dose rate at 50 cm from the patient was  $18.5 \pm 1.6$   $\mu\text{Sv/h}$ , which dropped to  $1.8 \pm 0.3$   $\mu\text{Sv/h}$  after imaging the following day, reducing even further to  $0.56 \pm 0.33$   $\mu\text{Sv/h}$  after surgery. **Conclusion:** The effective dose for personnel involved in handling [ $^{99m}\text{Tc}$ ]Tc-PSMA-I&S is comparable to that of other  $^{99m}\text{Tc}$ -radiopharmaceuticals and therefore safe for imaging and radioguided surgery.

**Key Words:** genitourinary; radiation safety; occupational radiation exposure; PSMA-I&S; radioguided surgery; technetium-99m

J Nucl Med Technol 2021; 49:334–338

DOI: 10.2967/jnm.121.262161

Received Mar. 1, 2021; revision accepted May 27, 2021.  
For correspondence or reprints, contact Else A. Aalbersberg  
(e.aalbersberg@nki.nl).

Published online July 30, 2021.

COPYRIGHT © 2021 by the Society of Nuclear Medicine and Molecular Imaging.

Prostate cancer is the most common malignancy in men aged 50 y or older and is second only to lung cancer as the most frequent cause of cancer death among men (1). Local therapy, such as a radical prostatectomy and extended pelvic lymph node dissection, can be used to cure patients with intermediate- or high-risk (localized) prostate cancer (2). However, up to 25% of the prostate-draining pelvic lymph nodes are outside the standard extended pelvic lymph node dissection template and remain in vivo after extended pelvic lymph node dissection (3). Improvements in preoperative and intraoperative techniques for detection and removal of locoregional lymph node metastases may result in a shift toward increased cure rates in patients with prostate cancer.

Conventional preoperative lymph node imaging techniques, such as MRI and CT, are neither sensitive nor specific enough for accurate lymph node staging (4). In recent years, multiple PET tracers have been clinically introduced, targeting the prostate-specific membrane antigen (PSMA), a transmembrane glycoprotein that is overexpressed on most prostate cancer cells. Compared with conventional imaging, PSMA PET/CT has significantly improved the specificity and sensitivity of the detection of prostate cancer (5).

PSMA-based image-guided surgery has been proposed as a technique to prevent incomplete resections and to improve intraoperative detection and clearance of nodal metastases. However, intraoperative use of positron-emitting PSMA PET tracers is challenging because of the relatively short half-life, radiation dose to personnel, and lack of suitable positron-detecting surgical probes. To tackle this problem, [ $^{111}\text{In}$ ]In-PSMA radioguided surgery (RGS) was developed and proven feasible in localized and limited recurrent prostate cancer (6). Afterward, [ $^{99m}\text{Tc}$ ]Tc-PSMA-imaging and surgery ([ $^{99m}\text{Tc}$ ]Tc-PSMA-I&S) RGS was introduced (7). The good commercial availability and favorable radiation properties, with  $\gamma$ -emission and a half-life of 6.01 h for  $^{99m}\text{Tc}$ , make this isotope ideal for this application, allowing ample time for preoperative imaging followed by RGS with a  $\gamma$ -probe.

Imaging and RGS with [ $^{99m}\text{Tc}$ ]Tc-PSMA-I&S involves personnel in different departments of the hospital: production

takes place at the radiopharmacy department, patient syringes are prepared by the nuclear medicine laboratory, patient administration and imaging take place at the outpatient nuclear medicine department, and RGS is performed in the operating room. To ensure the radiation protection of all staff members, the radiation burden of the entire procedure with [<sup>99m</sup>Tc]Tc-PSMA-I&S must be known. Therefore, the aim of this study was to estimate and subsequently measure the occupational radiation exposure for all personnel involved in producing, administering, or performing imaging or surgery with [<sup>99m</sup>Tc]Tc-PSMA-I&S.

## MATERIALS AND METHODS

### Workflow of [<sup>99m</sup>Tc]Tc-PSMA RGS and Personnel

[<sup>99m</sup>Tc]Tc-PSMA is produced using an automated module by 2 radiopharmacy technologists as previously described (8). In short, the steps involve placing a cassette on the automated labeling module without the presence of radioactivity, attaching a syringe containing 2,000 MBq [<sup>99m</sup>Tc]pertechnetate and then immediately closing the lead shielding surrounding the labeling module, running an automated synthesis of [<sup>99m</sup>Tc]Tc-PSMA without personnel present, opening the lead shielding, removing the final product in the shielding, and removing and disposing of the cassette.

Subsequently, in a laminar flow hood with lead glass, the final vial is calibrated in a dose calibrator, and then a quality control syringe and a patient syringe are prepared by a nuclear medicine laboratory technologist. Quality control is then performed by the radiopharmacy technologist with instant thin-layer chromatography and high-performance liquid chromatography as previously described (8). After approval by the pharmacist, the nuclear medicine physician administers 550 MBq of [<sup>99m</sup>Tc]Tc-PSMA-I&S to the patient through an intravenous cannula.

The following day the patient returns to the nuclear medicine department for total-body planar imaging followed by a 1-bed-position SPECT/CT scan of the pelvis and abdomen performed by a nuclear medicine technologist 16 h after intravenous injection of the [<sup>99m</sup>Tc]Tc-PSMA-I&S. The SPECT/CT scan serves as a quality control scan for tracer injection and distribution. Afterward, a robot-assisted laparoscopic salvage lymph node dissection is performed using the da Vinci device (Intuitive Surgical Inc.). An intraoperative Drop-In probe prototype (Eurorad S.A.) is inserted through a trocar next to or through the port of the Alexis Laparoscopic System (Applied Medical Corp.) and is used to detect lymph node metastases with  $\gamma$ -tracing (9). After surgical removal of lymph nodes, ex vivo measurements are performed to confirm [<sup>99m</sup>Tc]Tc-PSMA-I&S uptake. During this procedure, an anesthesiology technologist is seated at the patient's head, a scrub nurse stands next to the patient, a surgeon is seated in the console several feet from the patient, and a surgical nurse is present in the room.

### Estimated Effective Dose

Before the first prepared patient dose, the estimated effective dose was calculated for all the steps described in the workflow according to Equation 1. This estimation assumes a worst case in which there is no biologic elimination but physical decay only:

$$E = A \times e^{-\ln 2 \times \frac{t}{t_{1/2}}} \times \Gamma \times t_s \times \frac{1}{l^2} \times e^{-\ln 2 \times \frac{d}{d_{1/2}}}, \quad (\text{Eq. 1})$$

in which  $E$  is the effective dose ( $\mu\text{Sv}$ ),  $A$  is the activity (MBq) at the start,  $t$  is the time between the beginning of

the entire procedure and the individual step ( $h$ ),  $t_{1/2}$  is the half-life ( $h$ ),  $\Gamma$  is the effective dose rate constant ( $\mu\text{Sv m}^2 \text{MBq}^{-1} \text{h}^{-1}$ ),  $t_s$  is the duration of the step based on prior measurements and experience ( $h$ ),  $l$  is the distance to the radioactive source ( $m$ ),  $d$  is the lead thickness ( $mm$ ), and  $d_{1/2}$  is the half-value layer of lead ( $mm$ ). For all steps, the  $t_{1/2}$  of <sup>99m</sup>Tc is 6.01 h, and the  $d_{1/2}$  of lead for <sup>99m</sup>Tc is 0.3 mm. All other values vary per step and are estimated in Table 1.

### Effective Dose Measurements

Actual dose measurements were performed with electronic personal dosimeters (DMC 2000 XB; MGP Instruments). The electronic personal dosimeters were worn at chest height by the following personnel: the radiopharmacy technologist during labeling and quality control of [<sup>99m</sup>Tc]Tc-PSMA-I&S; the nuclear medicine laboratory technologist during syringe preparation; the nuclear medicine physician during administration to a patient; the nuclear medicine imaging technologist during patient positioning and imaging; and, during surgery, by the anesthesiology technologist, scrub nurse, surgical nurse, and surgeon. The total dose received during the handling of [<sup>99m</sup>Tc]Tc-PSMA-I&S or of the patient and the total time were noted by the researchers. The minimum dose that can be reported by the electronic personal dosimeters is 1  $\mu\text{Sv}$ .

### Dose Rate Measurements

Dose rate measurements (Eberline ESM FH 40 G-L; Thermo Fisher Scientific) of the patient were performed immediately after administration of [<sup>99m</sup>Tc]Tc-PSMA at 30 cm, 50 cm, and 1 m and were repeated after the SPECT/CT imaging. Immediately after surgery, while still in the operating room, dose rate measurements were performed at 30 and 50 cm. After administration and imaging, these measurements were done while the technologist was standing in front of the patient at the height of the liver, while the patient was upright. After surgery, these measurements were performed while the technologist was standing by the side of the patient, who lying down with the arms at the sides. The minimum measurable dose rate is 0.1  $\mu\text{Sv/h}$ .

### Data Analysis

Data were analyzed in SPSS Statistics (version 25; IBM) and are represented as mean  $\pm$  SD.

## RESULTS

### Patients

For the evaluation of personnel dose, the first 5 consecutive [<sup>99m</sup>Tc]Tc-PSMA-I&S RGS procedures that were performed in the context of the prospective TRACE (<sup>99m</sup>Tc-Based PSMA-Radioguided Assisted Surgery for Prostate Cancer) feasibility study (NL68290.031.18) were measured to audit the estimated effective dose. The 5 patients involved in these procedures had provided informed consent for the TRACE study. The labeling started with  $2,123 \pm 854$  MBq, which resulted in  $1,284 \pm 473$  MBq of the final product, and  $567 \pm 26$  MBq were administered to the patients.

### Estimated Effective Dose

The estimated effective dose for each step is shown in Table 1. According to these calculations, the effective dose

**TABLE 1**  
Estimated Variables and Effective Dose for Personnel During Different Steps of [<sup>99m</sup>Tc]Tc-PSMA-I&S RGS Procedure

Location	Procedure	Step	Personnel	A (MBq)	I (m)	t <sub>s</sub> (min/s)	h	t (h)	d (mm)	Γ (μSv m <sup>2</sup> MBq <sup>-1</sup> h <sup>-1</sup> )	E (μSv)
Radiopharmacy	Labeling	Attaching [ <sup>99m</sup> Tc] pertechnetate	Technologist RP	2,000	0.3	10 s	0.003	0	3	0.023	1.50 × 10 <sup>-3</sup>
		Labeling	Technologist RP	2,000	2.0	30 min	0.500	0	55	0.023	3.72 × 10 <sup>-55</sup>
	Quality control	Removal final product	Technologist RP	2,000	0.3	10 s	0.003	0	50	0.023	1.03 × 10 <sup>-50</sup>
		Instant thin-layer chromatography	Technologist RP	100	0.3	1 min	0.017	0	2	0.023	4.28 × 10 <sup>-3</sup>
		High-performance liquid chromatography	Technologist RP	100	2.0	30 min	0.500	0	0	0.023	2.88 × 10 <sup>-1</sup>
Nuclear medicine	Syringe preparation	Calibration of vial	Technologist NML	2,000	0.4	10 s	0.003	0	50	0.023	5.81 × 10 <sup>-51</sup>
		Preparing syringes	Technologist NML	2,000	0.4	2 min	0.006	0	10	0.023	1.59 × 10 <sup>-10</sup>
	Patient administration	Patient administration	Physician NM	550	0.4	1 min	0.003	0	3	0.023	2.32 × 10 <sup>-4</sup>
		Care after administration	Physician NM	550	1.0	5 min	0.083	0	0	0.008	3.65 × 10 <sup>-1</sup>
	Imaging	Patient positioning	Technologist NM	550	0.5	3 min	0.050	17	0	0.008	1.24 × 10 <sup>-1</sup>
Operating room	Surgery	Patient imaging	Technologist NM	550	3.0	30 min	0.500	17	2	0.008	3.39 × 10 <sup>-4</sup>
		Surgery	Anesthesiology technologist	550	0.5	120 min	2.000	20	0	0.008	3.51 × 10 <sup>0</sup>
			Scrub nurse	550	0.3	120 min	2.000	20	0	0.008	9.74 × 10 <sup>0</sup>
			Surgical nurse	550	2.0	120 min	2.000	20	0	0.008	2.19 × 10 <sup>-1</sup>
			Surgeon	550	2.0	120 min	2.000	20	0	0.008	2.19 × 10 <sup>-1</sup>

RP = radiopharmacy; NM = nuclear medicine.

for a single procedure with [<sup>99m</sup>Tc]Tc-PSMA-I&S for the radiopharmacy technologist is 2.93 × 10<sup>-1</sup> μSv; the nuclear medicine laboratory technologist receives 1.59 × 10<sup>-10</sup> μSv, the nuclear medicine physician receives 3.75 × 10<sup>-1</sup> μSv, the nuclear medicine imaging technologist receives 1.24 × 10<sup>-1</sup> μSv, the anesthesiology technologist receives 3.51 μSv, the scrub nurse receives 9.74 μSv, the surgical nurse receives 2.19 × 10<sup>-1</sup> μSv, and the surgeon receives 2.19 × 10<sup>-1</sup> μSv. For all staff members, the estimated effective dose from [<sup>99m</sup>Tc]Tc-PSMA-I&S on a yearly basis (100 procedures) is below 1 mSv if that same staff member were to perform all procedures, well below the limit of 6 mSv/y for classified radiation worker category B as set by Dutch legislation (10).

#### Measured Effective Dose

The measured effective dose ranged from 0 to 5 μSv for all personnel during a single procedure with [<sup>99m</sup>Tc]Tc-PSMA-I&S. All results are shown in Table 2. The highest effective dose was received by the scrub nurse (3.2 ± 1.3 μSv), followed by the radiopharmacy technologist (1.6 ± 0.5 μSv). The lowest doses were measured for the surgical nurse (0.2 ± 0.5 μSv) and the nuclear medicine imaging technologist (0.8 ± 0.4 μSv). If a single scrub nurse were to perform all procedures with [<sup>99m</sup>Tc]Tc-PSMA-I&S in a year (100 procedures), the total effective dose would be 320 μSv/y.

#### Dose Rate Measurements

Immediately after administration, the dose rate at 50 cm was 18.5 ± 1.6 μSv/h, which dropped to 1.8 ± 0.3 μSv/

h after imaging the following day, reducing even further to 0.56 ± 0.33 μSv/h after surgery. All results for the dose rate measurements are shown in Table 3.

## DISCUSSION

RGS using [<sup>99m</sup>Tc]Tc-PSMA-I&S is designed to aid in the intraoperative detection of PSMA-positive lesions that contain prostate cancer metastases. The aim of this present analysis was to estimate and subsequently measure the occupational radiation dose of all personnel involved in producing, administering, and performing imaging or surgery with [<sup>99m</sup>Tc]Tc-PSMA-I&S.

#### Differences Between Estimated and Measured Effective Dose

The largest differences between the estimated and measured effective dose were seen for the radiopharmacy and nuclear medicine laboratory technologists on one hand and for all surgical staff on the other hand. For radiopharmacy and nuclear medicine laboratory personnel, the measured effective dose was higher than the estimated effective dose, probably because of the conditions under which the production is done. In both cases, multiple radioactive sources (e.g., <sup>68</sup>Ga-generator and <sup>18</sup>F-labeled tracers) are near the workers. These sources do contribute to the measured effective dose but are not considered when the effective dose from [<sup>99m</sup>Tc]Tc-PSMA-I&S alone is estimated. For most surgical personnel, the measured dose is lower than the estimated dose. The largest contributor to this difference is the fact that biologic excretion of [<sup>99m</sup>Tc]Tc-PSMA-I&S is not

**TABLE 2**  
Estimated, Measured, and Mean Effective Dose for Personnel During Different Steps of [ $^{99m}\text{Tc}$ ]Tc-PSMA-I&S RGS Procedure

Step	Personnel	<i>E</i> ( $\mu\text{Sv}$ )						Mean $\pm$ SD
		Estimated	Patient 1	Patient 2	Patient 3	Patient 4	Patient 5	
Labeling	Technologist RP	$1.50 \times 10^{-3}$	2	2	1	2	1	$1.6 \pm 0.5$
Quality control	Technologist RP	$2.91 \times 10^{-1}$	1	0	0	0	0	$0.2 \pm 0.4$
Syringe preparation	Technologist NML	$1.59 \times 10^{-10}$	0	0	0	0	1	$0.2 \pm 0.4$
Patient administration	Physician NM	$3.75 \times 10^{-1}$	1	1	1	0	1	$0.8 \pm 0.4$
Patient imaging	Technologist NM	$1.24 \times 10^{-1}$	0	0	0	0	0	0
Surgery	Anesthesiology technologist	$3.51 \times 10^0$	1	0	0	0	1	$0.6 \pm 0.5$
	Scrub nurse	$9.74 \times 10^0$	2	5	4	3	2	$3.2 \pm 1.3$
	Surgical nurse	$2.19 \times 10^{-1}$	0	0	0	1	0	$0.2 \pm 0.4$
	Surgeon	$2.19 \times 10^{-1}$	1	1	1	1	1	$1.0 \pm 0.0$

RP = radiopharmacy; NML = nuclear medicine laboratory; NM = nuclear medicine.

considered. For [ $^{177}\text{Lu}$ ]Lu-PSMA, it is known that 56% is excreted within 24 h (11), and it is expected that [ $^{99m}\text{Tc}$ ]Tc-PSMA-I&S follows a similar excretion pattern (12). For the surgeon, the measured dose was higher than the estimated dose. Because a robotic approach was used, the surgeon was estimated to be at a distance of 2 m from the patient. In practice, however, the surgeon was much closer to the patient both during the time-out procedure before surgery and while making incisions, placing trocars, and installing the robot.

#### Hand Dose

This study did not consider the hand dose (or extremity dose), which would have been the highest for the radiopharmacy technologist and nuclear medicine laboratory technologist. This dose was not considered for 2 main reasons. First, for the nuclear medicine laboratory technologist, preparing a patient syringe containing  $^{99m}\text{Tc}$  is daily practice. The effect of  $^{99m}\text{Tc}$ -syringe preparation has been well studied worldwide and reported. In a study with 32 European centers, the mean hand dose for preparation of a  $^{99m}\text{Tc}$  syringe was found to be  $320 \mu\text{Sv/GBq}$  (13). For a [ $^{99m}\text{Tc}$ ]Tc-PSMA syringe with 550 MBq, this mean hand dose would lead to an extremity dose of  $176 \mu\text{Sv}$ . Second, hand

(or finger) dosimeters that can be read after each procedure are not available at our institute. The additional radiation dose of the prepared 5 syringes over several months with  $^{99m}\text{Tc}$  is negligible compared with the total number of syringes that have been prepared with various isotopes during this period and could therefore not be determined from the monthly extremity dose reports.

#### Comparison with Other $^{99m}\text{Tc}$ - and PSMA Procedures

$^{99m}\text{Tc}$  is the most common isotope in nuclear medicine procedures worldwide. The radiation burden to personnel at nuclear medicine departments is therefore well known. Although the preparation of [ $^{99m}\text{Tc}$ ]Tc-PSMA-I&S differs from that of most  $^{99m}\text{Tc}$ -radiopharmaceuticals (labeling instead of kit preparation), the dose to radiopharmacy and nuclear medicine laboratory personnel for preparation lies well within that of other  $^{99m}\text{Tc}$ -radiopharmaceuticals (13,14).

For the surgical staff, a comparison is made with a sentinel node biopsy procedure (a common procedure with  $^{99m}\text{Tc}$  but a different pharmaceutical) and with [ $^{68}\text{Ga}$ ]Ga-PSMA (another isotope but a comparable peptide and distribution). For a sentinel lymph node biopsy procedure, the injected activity is much lower than that of [ $^{99m}\text{Tc}$ ]

**TABLE 3**  
Measured and Mean Dose Rate of Patient During Different Steps of [ $^{99m}\text{Tc}$ ]Tc-PSMA-I&S RGS Procedure

Step	Distance (cm)	Dose rate ( $\mu\text{Sv/h}$ )					Mean $\pm$ SD
		Patient 1	Patient 2	Patient 3	Patient 4	Patient 5	
Administration	30	32.8	34.2	29.9	30.0	38.5	$33.1 \pm 3.5$
	50	17.3	18.8	16.6	19.3	20.5	$18.5 \pm 1.6$
	100	7.6	7.7	6.2	5.6	7.3	$6.9 \pm 0.9$
Imaging	30	3.4	3.1	3.2	3.9	4.5	$3.6 \pm 0.6$
	50	1.8	2.1	1.4	1.5	2.1	$1.8 \pm 0.3$
	100	1.2	0.74	0.41	0.31	1.1	$0.74 \pm 0.39$
Surgery	30	0.50	0.58	0.80	0.21	1.4	$0.69 \pm 0.43$
	50	0.28	0.39	0.30	0.08	0.98	$0.56 \pm 0.33$

Tc-PSMA, ranging from approximately 20 to 240 MBq, depending on the time between injection and surgery. Furthermore, the activity is injected locally instead of intravenously. The dose to the surgeon in this procedure is reported to be 2–10  $\mu\text{Sv}$  (15,16). The values found for surgical staff during [ $^{99\text{m}}\text{Tc}$ ]Tc-PSMA-I&S RGS fell well within this range. Another comparison can be made with [ $^{68}\text{Ga}$ ]Ga-PSMA for Cerenkov luminescence imaging. In this case, patient administration is always on the same day as surgery because of the shorter half-life of  $^{68}\text{Ga}$  (68 min). Additionally, less activity is injected ( $\sim 100$  MBq), and the energy emitted by the isotope is much higher. In this case, the scrub nurse standing next to the patient receives 16  $\mu\text{Sv}$ /procedure, whereas other staff members present obtain 1–5  $\mu\text{Sv}$ /procedure (17). In this study, all surgeries were performed with a robotic approach. Although no data were collected during an open or laparoscopic approach, it is assumed that the dose to the surgeon would be comparable to that to the scrub nurse in this study. In summary, the radiation burden to surgical staff from [ $^{99\text{m}}\text{Tc}$ ]Tc-PSMA-I&S is comparable to that from other surgical procedures with  $^{99\text{m}}\text{Tc}$  and is lower than that from intraoperative Cerenkov luminescence imaging procedures with [ $^{68}\text{Ga}$ ]Ga-PSMA.

## CONCLUSION

[ $^{99\text{m}}\text{Tc}$ ]Tc-PSMA-I&S has been introduced for identification of tumor-positive lymph nodes during salvage prostate cancer surgery. The effective dose for all involved personnel (radiopharmacy technologist, nuclear medicine laboratory technologist, nuclear medicine physician, nuclear medicine imaging technologist, scrub nurse, surgical nurse, anesthesiology technologist, and surgeon) is comparable to that of other  $^{99\text{m}}\text{Tc}$ -radiopharmaceuticals. [ $^{99\text{m}}\text{Tc}$ ]Tc-PSMA-I&S RGS can therefore be performed safely by all staff members.

## DISCLOSURE

No potential conflict of interest relevant to this article was reported.

## REFERENCES

1. Ferlay J, Colombet M, Soerjomataram I, et al. Cancer incidence and mortality patterns in Europe: estimates for 40 countries and 25 major cancers in 2018. *Eur J Cancer*. 2018;103:356–387.
2. Wilkins LJ, Tosoian J, Sondi D, et al. Surgical management of high-risk, localized prostate cancer. *Nat Rev Urol*. 2020;17:679–690.
3. Mattei A, Fuechsel F, Dhar N, et al. The template of the primary lymphatic landing sites of the prostate should be revisited: results of a multimodality mapping study. *Eur Urol*. 2008;53:118–125.
4. Sankineni S, Brown AM, Fascelli M, et al. Lymph node staging in prostate cancer. *Curr Urol Rep*. 2015;16:30.
5. Hoffmann MA, Wieler HJ, Baues C, Kuntz NJ, Richardsen I, Schreckenberger M. The impact of  $^{68}\text{Ga}$ -PSMA PET/CT and PET/MRI on the management of prostate cancer. *Urology*. 2019;130:1–12.
6. Rauscher I, Düwel C, Wirtz M, et al. Value of  $^{111}\text{In}$ -prostate-specific membrane antigen (PSMA)-radioguided surgery for salvage lymphadenectomy in recurrent prostate cancer: correlation with histopathology and clinical follow-up. *BJU Int*. 2017;120:40–47.
7. Maurer T, Robu S, Schottelius M, et al.  $^{99\text{m}}\text{Tc}$ -based prostate-specific membrane antigen–radioguided surgery in recurrent prostate cancer. *Eur Urol*. 2019;75:659–666.
8. Aalbersberg EA, van Andel L, Geluk-Jonker MM, Beijnen JH, Stokkel MPM, Hendriks JJMA. Automated synthesis and quality control of [ $^{99\text{m}}\text{Tc}$ ]Tc-PSMA for radioguided surgery (in a [ $^{68}\text{Ga}$ ]Ga-PSMA workflow). *EJNMMI Radiopharm Chem*. 2020;5:10.
9. Meershoek P, van Oosterom MN, Simon H, et al. Robot-assisted laparoscopic surgery using DROP-IN radioguidance: first-in-human translation. *Eur J Nucl Med Mol Imaging*. 2019;46:49–53.
10. Bader S. Guideline for risk analysis radiation applications [in Dutch]. Rijksinstituut voor Volksgezondheid en Milieu website. <https://www.rivm.nl/publicaties/leidraad-risicoanalyse-stralingstoepassingen>. Published 2010. Accessed September 13, 2021.
11. Kabasakal L, Toklu T, Yeyin N, et al. Lu-177-PSMA-617 prostate-specific membrane antigen inhibitor therapy in patients with castration-resistant prostate cancer: stability, bio-distribution and dosimetry. *Mol Imaging Radionucl Ther*. 2017;26:62–68.
12. Robu S, Schottelius M, Eiber M, et al. Preclinical evaluation and first patient application of  $^{99\text{m}}\text{Tc}$ -PSMA-I&S for SPECT imaging and radioguided surgery in prostate cancer. *J Nucl Med*. 2017;58:235–242.
13. Sans Merce M, Ruiz N, Barth I, et al. Extremity exposure in nuclear medicine: preliminary results of a European study. *Radiat Prot Dosimetry*. 2011;144:515–520.
14. Bayram T, Yilmaz AH, Demir M, Sonmez B. Radiation dose to technologists per nuclear medicine examination and estimation of annual dose. *J Nucl Med Technol*. 2011;39:55–59.
15. Klausen TL, Chakera AH, Friis E, Rank F, Hesse B, Holm S. Radiation doses to staff involved in sentinel node operations for breast cancer. *Clin Physiol Funct Imaging*. 2005;25:196–202.
16. Burrah R, James K, Poonawala S. Evaluation of radiation exposure during sentinel lymph node biopsy in breast cancer: a retrospective study. *World J Surg*. 2019;43:2250–2253.
17. Olde Heuvel J, de Wit-van der Veen BJ, van der Poel HG, et al.  $^{68}\text{Ga}$ -PSMA Cerenkov luminescence imaging in primary prostate cancer: first-in-man series. *Eur J Nucl Med Mol Imaging*. 2020;47:2624–32.



# Establishing a Local Diagnostic Reference Level for Bone Scintigraphy in a Nigerian Tertiary Hospital

Musa Y. Dambele<sup>1</sup>, Sikiru G. Bello<sup>2</sup>, Umar F. Ahmad<sup>3</sup>, Maryam Jessop<sup>4</sup>, Nasiru F. Isa<sup>5</sup>, and Kenneth K. Agwu<sup>6</sup>

<sup>1</sup>Department of Medical Radiography, Bayero University, Kano, Nigeria; <sup>2</sup>Nuclear Medicine Centre, University College Hospital, Ibadan, Nigeria; <sup>3</sup>Centre for Renewable Energy Research, Bayero University, Kano, Nigeria; <sup>4</sup>Brighton and Sussex University Hospitals NHS Trust, Department of Imaging, Royal Sussex County Hospital, Brighton, United Kingdom; <sup>5</sup>Department of Physics, Bayero University, Kano, Nigeria; and <sup>6</sup>Department of Radiography and Radiological Sciences, University of Nigeria Enugu Campus, Enugu, Nigeria

It is of vital importance to optimize the radiation dose to patients undergoing radionuclide bone scanning. This is one of the most common nuclear medicine procedures in many parts of the world, including Nigeria, and the current study was performed as part of a national survey to establish diagnostic reference levels (DRLs) for common nuclear medicine procedures in Nigeria in order to optimize their use. Nuclear medicine was only recently introduced to the health-care system in Nigeria, with only 2 centers presently conducting these procedures. **Methods:** A retrospective, cross-sectional study was performed in the nuclear medicine department of a tertiary hospital in southwest Nigeria to determine the preliminary local DRL for radionuclide bone scanning. One hundred and nine patients who met the study criteria were included. Data were obtained from June 2017 to March 2019 and were analyzed to obtain the third quartile of the distributed administered activity and achievable dose (anthropometric variables and radiation dose to bone surface). **Results:** The mean administered activity, achievable dose, and DRL were  $833.98 \pm 106.93$ , 832.5, and 895.4 MBq, respectively. The calculated preliminary local DRL was larger than values reported in studies done in Sudan, the United Kingdom, and Australia or by the International Commission on Radiological Protection. **Conclusion:** The preliminary DRL from this first-of-its-kind study in Nigeria was high because of practitioners' lack of experience. However, the values were still within the international best-practice range, which when optimized will go a long way toward reducing medical exposure without compromising image quality.

**Key Words:** administered activity; diagnostic reference level; nuclear medicine; bone scintigraphy; image quality

**J Nucl Med Technol 2021; 49:339–343**

DOI: 10.2967/jnmt.121.262084

**I**n medical imaging, protecting patients from exposure to radiation is a major concern calling for intervention, prompting the International Commission on Radiological

Protection (ICRP) to recommend principles to justify use, optimize protection, and limit doses. In medical exposure, however, dose limits are not applicable per se, as they would defeat the purpose of justifying the practice (1).

The significant increase in the use of radiation for medical purposes has led to a concomitant increase in the exposure of patients, relatives, and the environment to radiation (2). In the early 1990s, the ICRP introduced the concept of diagnostic reference levels (DRLs) to optimize doses (3,4) and minimize the amount of applied radiation. According to Council Directive 97/43/Euratom, DRLs are dose levels in medical radiodiagnostic practices for typical examinations of standard-sized patients or in standard phantoms for broadly defined types of equipment (4).

The establishment of DRLs and achievable doses has proven to be an effective tool in optimizing protection in medical imaging (5). DRLs and achievable doses are as defined in ICRP publication 135, the former being the level that protects patients from exposure during diagnostic and interventional procedures and the latter being the DRL achievable by standard, widespread techniques without compromising image quality (i.e., the value set at the median [50th percentile] DRL determined in a departmental survey). DRLs define the lower and upper limits of administered activities in nuclear medicine and radiology and can be applied to the most common nuclear medicine procedure in Nigeria, bone scintigraphy (a sensitive diagnostic imaging method that uses a radiopharmaceutical to evaluate the distribution of bone formation relating to physiologic processes, in addition to malignant and benign disease). The examinations chosen for the DRL process should be those performed most often in the region and for which dose assessment is practicable (6).

DRLs help avoid delivering, to a patient, excess radiation that does not contribute to the clinical purpose of the medical imaging task. This goal is met by comparing the DRL (derived from relevant regional, national, or local data) with the mean value observed in practice for a reference group of patients (e.g., similar in height, weight, and age) or a suitable reference phantom (6). When a procedure consistently exceeds the DRL, that procedure and its equipment

Received Feb. 16, 2021; revision accepted May 21, 2021.  
For correspondence or reprints, contact Musa Y. Dambele (mydambele.rdg@buk.edu.ng).

Published online July 30, 2021.

COPYRIGHT © 2021 by the Society of Nuclear Medicine and Molecular Imaging.

**TABLE 1**  
Anthropometric Variables

Index	Age (y)	Weight (kg)	Height (m)	Body mass index (kg/m <sup>2</sup> )
Mean	57.9 ± 14	71.6 ± 6.7	1.63 ± 0.5	29.9 ± 3.0
Minimum	34	58.9	1.54	19.95
Maximum	87	85	1.77	37.99

should be locally reviewed for adequate optimization, and dose-reduction measures should be taken if necessary (7). DRLs are based on the activities that need to be administered to normal-sized patients (typically with a body weight of 70 ± 15 kg) to achieve good image quality during a standard procedure (8).

The role of nuclear medicine in patient management is as impactful in a developing nation as in other regions of the world. However, in developing nations the practice of nuclear medicine faces a myriad of challenges; these, though, can easily be avoided (9).

The “Bonn Call for Action” in 2012 (10) increased global awareness of the need to strengthen radiation protection in medicine. Despite the huge progress in protecting patients from radiation in most developed countries (10), the situation in most developing countries is still far from ideal. Nigeria does not have a local or national nuclear medicine dose registry, which is important for establishing dose reference levels, and a literature search could find no previous studies in Nigeria to establish DRLs for radionuclide bone scanning. Therefore, optimization of protection is doubtful, and establishing DRLs in Nigeria is vital (11).

The current study addressed this challenge by establishing a preliminary DRL for bone scintigraphy, the most requested procedure in Nigeria, and by determining the role that achievable dose plays in reducing dose while maintaining diagnostic image quality.

## MATERIALS AND METHODS

This was a retrospective and cross-sectional study performed in the nuclear medicine department of a tertiary hospital in southwest Nigeria. The data were collected from 2017 to 2019 and included 109 adults who were selected (using purposive sampling) (mean age, 57.9 ± 14 y [range, 34–87 y]; mean weight, 71.6 ± 6.7 kg; mean height, 1.63 ± 0.5 m; mean body mass index, 29.9 ± 3.0 kg/m<sup>2</sup>) (Table 1). The center was chosen because it had the imaging modality of choice and the facilities for the study.

## Equipment Specifications

The radioisotope dose calibrator was a CRC-ISR (Capintec), with 100–240 V, 50/60 Hz, and 120 mA. The  $\gamma$ -camera was a model 4369372 SPECT device (Siemens) manufactured in November 2005, with 200 V, 50/60 Hz, 30 mA, and a line single phase.

## Ethical Clearance

Ethical approval was obtained from the Research Ethics Committee of the Oyo State Ministry of Health. Also, data were anonymized and kept confidential in a personal computer, and the results did not contain any information that would allow the patients or center to be identified.

## Procedure

Departmental documents and records were made available to the researcher, who was a former staff member of the center and one of the pioneer radiographers in its imaging unit. Data were generated and sorted to capture the needed details. The departmental protocol for bone scintigraphy included preparing the radiopharmaceutical (<sup>99m</sup>Tc-methylene diphosphate), measuring it with a dose calibrator in the radiopharmacy hot lab, administering it intravenously to referred patients while they lay supine on the SPECT  $\gamma$ -camera, and acquiring planar images using the window and persistence routinely applied in the department. The activity administered and other anthropometric parameters were recorded for each patient.

## Method of Measurement

DOSIRAD software was used to automatically calculate the absorbed dose to organs and the effective dose from the administered activity of the radiopharmaceutical (12). This software is based on the ICRP values, and the calculation was specific to the type of imaging study, clinical indication, patient's weight, type of radiopharmaceutical, and administered activity (MBq).

## Data Analysis

The data were saved in a Microsoft Excel spreadsheet and categorized for the examination parameters and anthropometric parameters. SPSS software (version 23.0; IBM) was used to analyze the mean and SD of the administered activity, anthropometric

**TABLE 2**  
Administered Activities and Critical-Organ Doses

Index	Administered activity (MBq)	Critical-organ dose (mGy)
Mean	833.98 ± 106.93	52.54 ± 6.31
Minimum	632.7	39.86
Maximum	1124.8	70.86
Achievable dose (second quartile)	832.5	52.45
DRL (third quartile)	895.4	56.41

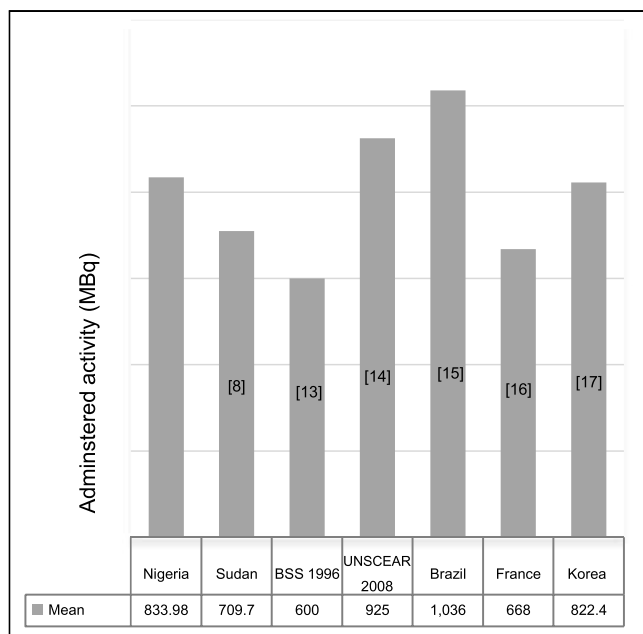


**FIGURE 1.** Comparison of mean administered activity (MBq). BSS = basic safety standard; UNSCEAR = United Nations Scientific Committee on the Effects of Atomic Radiation.

variables, and radiation dose to the critical organ (bone surface). The achievable dose and DRL were obtained from the distribution of the administered activity for radionuclide bone scanning. Parametric testing was suitable because there was a normal distribution at a 95% CI after using the Kolmogorov–Smirnov method to test for the normality of data distribution. Statistical significance was set at a *P* value of less than 0.05.

## RESULTS

Table 2 shows mean, minimum, maximum, achievable dose (second quartile), and DRL (third quartile) data for administered activity and critical-organ dose.

The mean administered activity,  $833.98 \pm 106.93$  MBq, translated to a mean dose of  $52.54 \pm 6.31$  mGy to the bone surface. Figure 1 compares this mean administered activity with the mean values in Sudan (8), Brazil (13), France (14), and Korea (15) and with the 1996 basic safety standard (16) and the 2008 standard of the United Nations Scientific Committee on the Effects of Atomic Radiation (17). The Nigerian mean value was lower than the United Nations standard and the Brazilian mean value but higher than the other mean values and standard.

The maximum activity administered was quite high, at 1,124.8 MBq; only Brazil had a higher value (1,480 MBq).

At 832.5 MBq, the achievable dose in this study was lower than the mean administered activity of 833.98 MBq (Table 2). However, the difference was not significant.

The DRL (895 MBq) was within the European Union range of 500–1,110 MBq (Table 3) but below the Brazilian DRL (1,110 MBq (13)) and the Australian DRL of 920 MBq (18) and above the Sudanese of 777 MBq and U.K. of 600 MBq DRLs (19).

## DISCUSSION

This study established preliminary DRLs for bone scintigraphy in a tertiary hospital in southwest Nigeria, the only teaching hospital that offered nuclear medicine services at that time.

### Anthropometric Variables

The high mean body mass index indicates that many of the patients being scanned for the various indications were overweight. The maximum body mass index fell within the severely obese class, at  $37.99 \text{ kg/m}^2$  (reference range for severe obesity,  $35\text{--}40 \text{ kg/m}^2$ ), a value that increases the risk of many types of cancer, such as cancers of the breast, colon, and endometrium.

### Maximum Administered Activity

The high maximum administered activity may stem from a lack of standardized protocols and may indicate use of an unnecessarily high radiation dose. Hence, there is a need to audit, regulate, and optimize doses. The minimum and maximum administered activities for the same type of procedure have been observed to range widely, by 44% (20). Nonstandardization of activities administered for the same type of procedure can denote a deficiency in controlling for radiation exposure.

### Mean Administered Activity

The mean administered activity in Nigeria, though within the international range, clearly points toward use of an unnecessarily high activity, which in turn increases the radiation dose to the patient. This finding indicates that neither a guideline nor a reference value is in place to guide personnel in optimizing medical exposure while retaining diagnostic image quality.

### Achievable Dose

Achievable dose represents the 50th percentile (median) (21) of the dose distribution, as defined by the ICRP and the International Atomic Energy Agency, and is recommended as a reference to prevent excessive ionizing radiation. Figure 2 shows that our calculated value was within

**TABLE 3**  
Comparison Between Local DRL and International Standard Values

Radiopharmaceutical	Current study	Sudan (8)	Australia (20)	United Kingdom (21)	European Union (10)	Brazil (15)
$^{99\text{m}}\text{Tc}$ -methylene diphosphate (MBq)	895.4	777	920	600	500–1,110	1,110

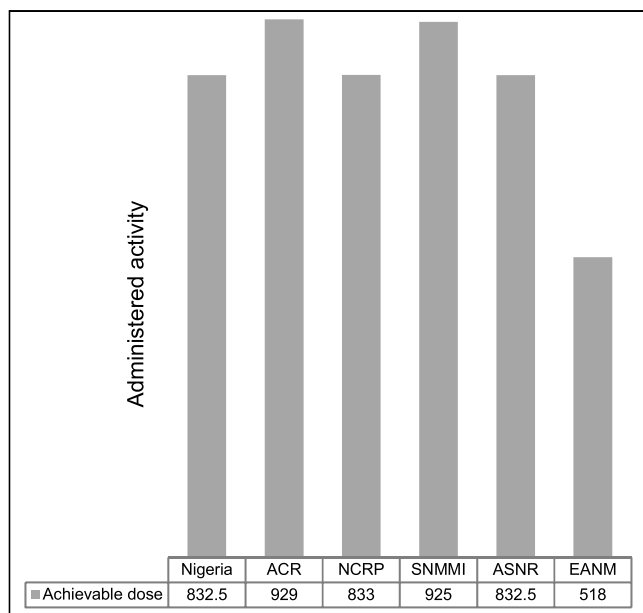


**FIGURE 2.** Comparison of achievable dose (19) with others indicated in literature. ACR = American College of Radiology; ASNR = American Society of Neuroradiology; EANM = European Association of Nuclear Medicine; NCRP = National Council on Radiological Protection; SNMMI = Society of Nuclear Medicine and Molecular Imaging.

the range reported by the Society of Nuclear Medicine and Molecular Imaging, the American Society of Neuroradiology, and the European Association of Nuclear Medicine but fell below the ranges reported by the American College of Radiology and the National Council on Radiological Protection. Achievable dose has an additional role in optimization, as some degree of patient dose reduction can be attained without affecting image quality. Extrapolation of this value into current practice for radionuclide bone scintigraphy could reduce the dose by approximately 26%, a highly significant degree of optimization.

#### Preliminary DRL

If the DRL is consistently being exceeded, the procedures and equipment should be reviewed to determine whether further optimization is needed to protect patients and, if so, dose-reduction measures taken (7). Our findings during this developmental phase in Nigeria showed a moderate level of safety, even though doses were sometimes administered without considering whether both patient protection and image quality had been optimized. Application of DRLs will help avoid administering an unwarranted radiation dose that does not add clinical information to the images. Establishing a national DRL will provide a dose-optimization tool to guide other nuclear medicine centers in Nigeria.

#### Limitations

The study, being retrospective, had some outliers too small or large for the age and weight ranges. Caution is therefore advised in applying the values.

## CONCLUSION

Optimization of protection in Nigeria is doubtful, as no reference records are kept in daily practice, and a literature search could find no previous studies to establish DRLs for radionuclide bone scanning, the most common nuclear medicine procedure in southwest Nigeria. This first study to determine local DRLs and achievable doses for bone scintigraphy found values higher than those in some other countries and international bodies. Application of these DRLs in subsequent studies will significantly reduce unnecessary exposure of patients to medical radiation. In determining the minimum practicable radiation dose, one should use sound judgment and have a clear reason to administer the radiation. Inconsistency in the activity administered for the same procedure calls for concern, as wide differences in administered dose were noted without additional image quality, signifying a lack of local regulations, evidence-based protocols, and standard operating procedures.

## DISCLOSURE

No potential conflict of interest relevant to this article was reported.

## ACKNOWLEDGMENTS

For their support, we thank Muideen Isa; Wasiu Lamidi; Ezinma Micheal (Deputy Director of Radiography and Nuclear Medicine Radiographer, University College Hospital, Ibadan); Idris Garba (HOD, Radiography, Bayero University, Kano); Prof. Tijjani H. Darna (Department of Physics, Bayero University, Kano); the Radiation Protection Research Group, University of Nigeria, Nsukka, headed by Prof. Kenneth K. Agwu; and HOD, Nuclear Medicine Centre, University College Hospital, Ibadan.

## REFERENCES

1. Watanabe H, Ishii K, Hosono M, et al. Report of a nationwide survey on actual administered radioactivities of radiopharmaceuticals for diagnostic reference levels in Japan. *Ann Nucl Med*. 2016;30:435–444.
2. Schauer DA, Linton OW. National Council on Radiation Protection and Measurements Report Shows Substantial Medical Exposure Increase. *Radiology*. 2009;253:293–296.
3. ICRP Publication 60: 1990 Recommendations of the International Commission on Radiological Protection. Pergamon Press; 1991:1–211.
4. Radiological protection and safety in medicine (publication 73). *Ann ICRP*. 1996;26:1–31.
5. Radiation Protection 109: Guidance on Diagnostic Reference Levels (DRLs) for Medical Exposures. Office for Official Publications of the European Communities; 1999:1–26.
6. Vañó E, Miller DL, Martin CJ, et al. ICRP publication 135: diagnostic reference levels in medical imaging. *Ann ICRP*. 2017;46:1–144.
7. McCollough CH. Diagnostic reference levels. Image Wisely website. <https://www.imagewisely.org/Imaging-Modalities/Computed-Tomography/Diagnostic-Reference-Levels>. Accessed September 9, 2021.
8. Ali WM, Elawad RM, Ibrahim MAA. Establishment of dose reference levels for nuclear medicine in Sudan. *Open J Radiol*. 2016;6:258–263.
9. Adedapo KS, Onimode YA, Ejeh JE, Adepoju AO. Avoidable challenges of a nuclear medicine facility in a developing nation. *Indian J Nucl Med*. 2013;28:195–199.
10. RP 180 medical radiation exposure of the European population, part 1 & part 2. European Commission website. <https://ec.europa.eu/energy/content/rp-180->

- medical-radiation-exposure-european-population-part-1-part-2\_en. Accessed September 9, 2021.
11. Joseph DZ, Nzotta CC. The need to establish national dose reference levels for radiological examinations in Nigeria: radiographer's role. *Niger J Med Imaging Radiat Ther.* 2016;5:25–40.
  12. Gomez-Perales JL, Garcia-Mendoza A. A software for automatic calculation of radiation dose to patients from radiopharmaceuticals [abstract]. *Eur J Nucl Med Mol Imaging.* 2011;38(suppl):S434.
  13. Radiation protection 109: guidance on diagnostic reference levels (DRLs) for medical exposures. European Commission website. [https://ec.europa.eu/energy/sites/ener/files/documents/109\\_en.pdf](https://ec.europa.eu/energy/sites/ener/files/documents/109_en.pdf). Published 1999. Accessed September 9, 2021.
  14. Miller DL, Martin CJ, Rehani MM. The mandate and work of ICRP committee 3 on radiological protection in medicine. *Ann ICRP.* 2018;47:142–151.
  15. Willegaignon J, Braga LFEF, Sapienza MT, et al. Diagnostic reference level: an important tool for reducing radiation doses in adult and pediatric nuclear medicine procedures in Brazil. *Nucl Med Commun.* 2016;37:525–533.
  16. Roch P, Celier D, Dessaud C, Etard C. Patient exposure from nuclear medicine in France: national follow-up and influence of the technology through diagnostic reference levels data analysis. *Radiat Prot Dosimetry.* 2018;179:87–94.
  17. Song HC, Na MH, Kim J, Cho SG, Park JK, Kang KW. Diagnostic reference levels for adult nuclear medicine imaging established from the national survey in Korea. *Nucl Med Mol Imaging.* 2019;53:64–70.
  18. Australian radiation protection and nuclear safety: national diagnostic reference level fact sheet. Study Resource website. <https://studyres.com/doc/1546990/national-diagnostic-reference-levels-factsheet#>. Published 2011. Accessed October 19, 2021.
  19. Hart D, Wall BF. UK Nuclear Medicine Survey 2003-2004. *Nucl Med Commun.* 2005;26:937–946.
  20. Becker MD, Butler PF, Siam M, et al. U.S. PET/CT and gamma camera diagnostic reference levels and achievable administered activities for noncardiac nuclear medicine studies. *Radiology.* 2019;293:203–211.
  21. Dambele MY, Abdulkarim MS, Agwu KK. Diagnostic reference level for common nuclear medicine studies in National Hospital, Abuja, Nigeria. *Niger J Med Imaging Radiat Ther.* 2019;8:115–118.

# Decay Correction for Quantitative Myocardial PET Perfusion in Established PET Scanners: A Potentially Overlooked Source of Errors

Robert Bober

*John Ochsner Heart and Vascular Institute, Department of Cardiovascular Diseases, and Ochsner Clinical School, Queensland University School of Medicine, New Orleans, Louisiana*

Quantitative myocardial PET perfusion requires decay correction (DC) of the dynamic datasets to ensure that measured activity reflects true physiology and not radiotracer decay or frame duration. DC is typically performed by the PET camera system, and the exact algorithm is buried within the settings and assumed to be correct for quantitative perfusion data. For quantitative myocardial perfusion, sequential dynamic images should be decay-corrected to the activity at the midpoint of the first scan in the sequence. However, there are different DC algorithms that can be implemented depending on the needs and expertise of the laboratory. As such, before quantitative myocardial perfusion is performed, the DC technique of a camera system should be tested.

**Key Words:** image processing; PET; decay correction; myocardial blood flow; positron emission tomography; arterial input function

**J Nucl Med Technol 2021; 49:344–349**

DOI: 10.2967/jnmt.121.262320

Quantification of absolute myocardial blood flow (MBF) with PET has become mainstream and is now reimbursed through the Centers for Medicare and Medicaid services. The literature describing the technical requirements for accurate reproducible MBF is extensive (1–4). An essential but commonly overlooked function is decay correction (DC), particularly for older or refurbished 2-dimensional (2D) or 3-dimensional (3D) scanners already in use. Since these are assumed to be working properly for quantification of MBF, the literature offers little information for practical, simple testing in order to assess the DC of an installed PET scanner or an older refurbished scanner under consideration for purchase.

The goals of this article are 2-fold. The first is to explain the rationale and methods for DC for assessment of MBF. The second is to report an easy method by which technologists can assess DC when there is no onsite physicist or technical expert.

Received Mar. 15, 2021; revision accepted May 5, 2021.  
For correspondence or reprints, contact: Robert Bober (rbober@ochsner.org).

Published online July 30, 2021.

COPYRIGHT © 2021 by the Society of Nuclear Medicine and Molecular Imaging.

## BASICS OF QUANTITATIVE PET PERFUSION

Measuring MBF requires 2 primary data: the concentration of radiotracer in the arterial blood over time (also known as arterial input [ $A_0$ ] or the early blood pool phase) and the concentration of radiotracer in the myocardium (also known as myocardial uptake [ $M$ ] or the late myocardial phase). For all PET scanners, radionuclides, acquisition protocols, flow models, and list mode or binned data, accurate DC of these datasets is essential but often buried from the end user and assumed to be correct for MBF studies. Different DC algorithms may be appropriate for different types of imaging (brain, cardiac, oncology), half-lives of the radiotracer, or questions asked (drug metabolism, scanner performance, MBF) (5). Consequently, each established PET scanner that is to be used for MBF should be checked for correct DC.

## RATIONALE FOR DC ON QUANTIFICATION OF MBF

Why is DC necessary for accurate and precise quantification of MBF? Although the various kinetic models correct for partial-volume loss, spillover, extraction, and exit from myocardium, in the simplest conceptual form MBF derives from the ratio of  $M$  to  $A_0$  (6,7).

The  $A_0$  images quantify the change in concentration of radiotracer in the blood pool over time, before myocardial extraction, due to dilution by circulating blood and lung volume after intravenous injection. The  $M$  images quantify the average concentration of radiotracer trapped in the myocardium after clearance from the blood pool. As a potassium analog,  $^{82}\text{Rb}$  does not leak from myocardium except in cases of severe cell injury wherein intracellular potassium is not maintained. The slow leakage of  $^{13}\text{N}$  ammonia from myocardium after initial uptake is accounted for in its flow model. The simplistic inverse relationship between MBF and  $A_0$  shows how erroneous MBF may be due to too high or too low an  $A_0$  or  $M$ , all of which may be due to incorrect DC.

For quantitative perfusion studies, the radiotracer concentrations of  $A_0$  and  $M$  should be dictated solely by physiology and not by radiotracer decay, image duration, or acquisition parameters (number of frames in an acquisition). If  $A_0$



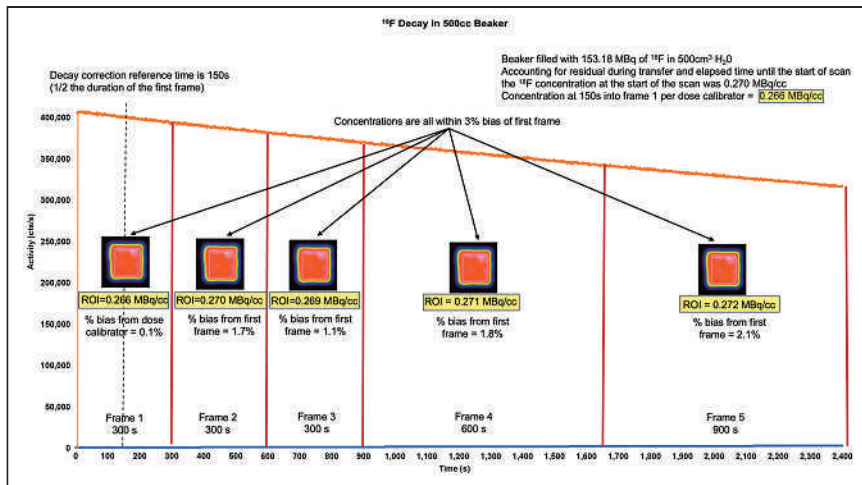


**FIGURE 1.** Decay of  $^{18}\text{F}$  in 500-cm $^3$  beaker. A detailed  $^{18}\text{F}$  protocol (“Fluorine Decay Correction.docx”) and worksheet (“F18 Decay Correction Worksheet.xlsx”) can be found in the supplemental materials. With syringe, 153.18 MBq of  $^{18}\text{F}$  were placed in beaker containing 500 cm $^3$  of H $_2$ O. Accounting for residual activity in transfer syringe and elapsed time between dose calibrator measurement and start of scan, concentration of  $^{18}\text{F}$  at start of scan was 0.270 MBq/cm $^3$ . Scanner performed 2,400-s (40 min) list-mode acquisition. Twenty-four hours later, after all activity decayed, attenuation scanning was performed and 5 serial frames were generated at intervals of 300, 300, 300, 600, and 900 s. ROIs were placed, avoiding beaker boundaries. Activity at time  $t$  equaled initial activity  $\times e^{(-0.693 \times t / \text{half-life of radiotracer})}$ . Therefore, with starting activity of 0.270 MBq/cm $^3$ , expected activity at 150 s into scan (midpoint of first frame) is 0.266 MBq/cm $^3$ . Half-life of  $^{18}\text{F}$  is 6,600 s, and  $0.270 \text{ MBq/cm}^3 \times e^{(-6.93 \times 150 \text{ s} / 6,600 \text{ s})} = 0.266 \text{ MBq/cm}^3$ . Concentration of ROI in first frame was 0.266 MBq/cm $^3$ , which is 0.1% bias from dose calibrator. Concentrations in each subsequent frame were nearly identical to first frame, with biases all within 3% window. There are several conclusions. First, scanner decay-corrects activity to midpoint of first frame. Second, scanner also corrects for duration of each frame, giving activity in MBq/cm $^3$ . Third, in biologic systems, only variation in quantitative activity after first frame would be due to physiologic changes and not imaging timing, duration, or decay. Bias from dose calibrator of first frame, also known as efficiency, is inconsequential to measurements of MBF as it cancels out in numerator and denominator of flow equations (6). Bias does inform us on whether test was performed with accurate timing, random, scatter, and dead-time corrections and also on whether camera system was internally calibrated for isotope against standard. If timing of beaker decay test is not precise or camera has not been calibrated, measured concentration could be significantly different from dose calibrator; however, if DC is performed correctly, bias of subsequent frames will be uniform.

images are not decay-corrected, the downstream impact would lead to erroneously reduced  $A_0$  and thus falsely high MBF. In addition, there is also a differential impact of incorrect DC between rest and stress datasets, thereby causing errors in stress mL/min/g and coronary flow reserve over and above the physiologic effects of cardiac output, heart rate, and blood pressure during stress compared with rest.

With the short-lived  $^{82}\text{Rb}$  having rapid decay over 75 s, an erroneous DC will particularly degrade quantitative data in both  $A_0$  and M phases. Because of the physiologic rapidly changing high blood concentrations of the  $A_0$  phase,  $A_0$  data are more prone to cause errors in MBF than are M data. The impact of incorrectly reduced  $A_0$  and M data will yield inaccurate elevation in absolute MBF ranging from 10% to 40% (1,6,8).

## UNDERSTANDING PET SCANNER DC

As a thought experiment, imagine a radiotracer X with a half-life approaching infinity. If 185 MBq (5 mCi) of X, as measured in a dose calibrator, is placed in a beaker filled with exactly 500 cm $^3$  of H $_2$ O, the concentration of X would be 0.37 MBq/cm $^3$  (10  $\mu\text{Ci/cm}^3$ ) at time 0. Because this imaginary radiotracer’s half-life is infinite, there is essentially a stable concentration of 0.37 MBq/cm $^3$  (10  $\mu\text{Ci/cm}^3$ ) over time. For each cm $^3$ , the beaker is emitting  $3.70 \times 10^5$  disintegrations per second, or 0.37 MBq (10  $\mu\text{Ci}$ ). If this beaker is now placed into an ideal camera system that captures every disintegration and an image is acquired over 10 s, what is the camera doing? In a sample volume of 1 cm $^3$ , the camera receives  $3.70 \times 10^5$  counts in the first second and  $3.70 \times 10^5$  counts in each second afterward. Therefore, over 10 s, the scanner has received  $3.7 \times 10^6$  counts. The units are integrated activity multiplied by time (count/cm $^3 \times \text{s}$ ). The total cumulative activity increases over time depending on the count/s coming from the beaker sample volume. This total cumulative integrated activity divided by the total image duration gives the average count/s emitted by the beaker sample volume. In this example,  $3.70 \times 10^6 \text{ counts/cm}^3/\text{s} \times \text{s}$  divided by 10 s gives the original target concentration of  $3.70 \times 10^5 \text{ counts/s per cm}^3$  or 0.37 MBq/cm $^3$  (10  $\mu\text{Ci/cm}^3$ ).

However, in the real clinical world—where decay occurs rapidly, scanners do not capture all disintegrations, and biologic processes influence the concentration of radiotracer—how does the camera operate such that the measured activity reflects the true activity of the biologic process? The main function of DC is to recalculate measured activity for each time frame into values that would be measured if decay did not occur, thus ensuring accurate arterial and myocardial activity essential for MBF.

The mathematic description of radioactive decay is

$$R(t) = R_i e^{-\lambda t} \quad (\text{Eq. 1})$$

where  $R(t)$  is the amount of radiotracer at time  $t$ ,  $R_i$  is the initial amount of radiotracer at the start of the scanning period, and  $\lambda$  is the decay constant of the radiotracer. With

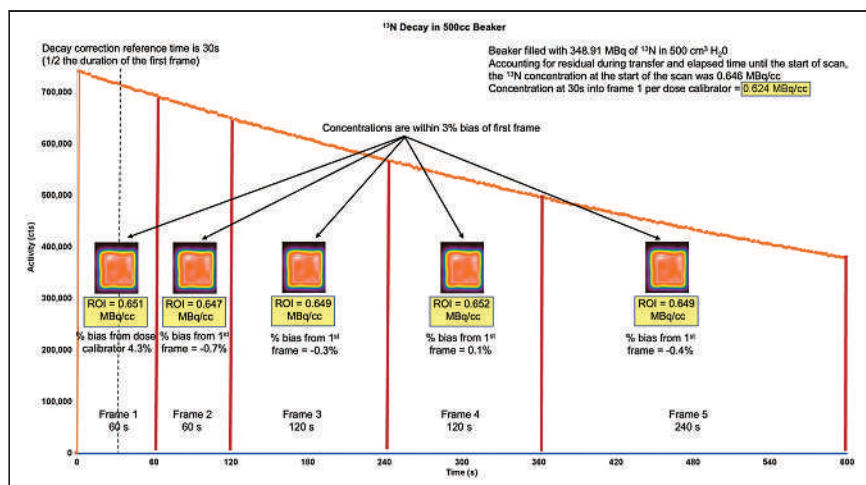


**FIGURE 2.** Decay of  $^{13}\text{N}$  in 500-cm<sup>3</sup> beaker. A detailed  $^{13}\text{N}$  protocol (“Nitrogen Decay Correction.docx”) and worksheet (“ $^{13}\text{N}$  Decay Correction Worksheet.xlsx”) can be found in the supplemental materials. Similar to Figure 1, 348.91 MBq of  $^{13}\text{N}$  were placed a beaker containing precisely 500 cm<sup>3</sup> of H<sub>2</sub>O. Scanner performed 600-s (10 min) list-mode acquisition. Two hours later, after all activity decayed, attenuation scanning was performed and 5 serial frames were generated at intervals of 60, 60, 120, 120, and 240 s. Calculations and measurements were as shown in Figure 1. There are several conclusions. First, scanner decay-corrects activity to midpoint of first frame. Second, scanner also corrects for duration of each frame, giving activity in MBq/cm<sup>3</sup>. Third, in biologic systems, only variation in quantitative activity after first frame would be due to physiologic changes and not imaging timing, duration, or decay.

regard to quantitative perfusion with PET, there are 2 methodologic predicaments that can be deduced from this equation. First,  $R(t)$  is not actually measured. The PET scanner accumulates and integrates counts over a time interval. Thus,  $R(t)$  equals  $\int_{t_1}^{t_2} R(t)dt$ , where  $t_1$  and  $t_2$  are the time duration of the scan or frame. Second,  $\int_{t_1}^{t_2} R(t)dt$  is influenced by factors other than decay, such as myocardial extraction and retention. In other words, the activity of radiotracer in a scanner region of interest (ROI) will depend on the duration of the time interval, the decay of the radiotracer, and any biologic process that removes or adds radiotracer from the ROI. Hence, to accurately measure the activity of  $A_0$  and  $M$ , decay of the radiotracer must be corrected for the duration of the scanning intervals.

Many PET scanners offer different DC options to correct sequential images relative to the activity at some point during the scan (5,9,10). For dynamic processes or for imaging PET tracers with half-lives shorter than the acquisition period, the midpoint of the first scan is used (5). This correction confirms that any subsequent change in activity in later sequences is due to biologic change and not to image duration, interval between images, or radiotracer decay.

As an example, a beaker containing 470 cm<sup>3</sup> of H<sub>2</sub>O is mixed with 30 cm<sup>3</sup> of 370-MBq (10 mCi)  $^{82}\text{Rb}$  (half-life, 76 s), yielding 0.74 MBq/cm<sup>3</sup> (20  $\mu\text{Ci}/\text{cm}^3$ ) at time zero as confirmed with a dose calibrator. If serial images are captured every 20 s for 3 frames, frames 1, 2, and 3—because of decay and calculated using the equation  $R(t) = R_0 e^{-\lambda t}$ —have an

actual average concentration of 0.666, 0.562, and 0.470 MBq/cm<sup>3</sup> (18.3, 15.2, and 12.7  $\mu\text{Ci}/\text{cm}^3$ ), respectively. However, the camera system should decay-correct frames 2 and 3 using a reference time of 10 s into the scan (half the interval of the first frame). Corrected for decay, frames 2 and 3 will have an average concentration of approximately 0.666 MBq/cm<sup>3</sup> (18.3  $\mu\text{Ci}/\text{cm}^3$ ) and all 3 frames should yield nearly identical concentrations, despite the fact that counts/s and concentrations are decreasing with time. The difference between the concentration at time 0 and the actual measured average concentration of the first frame is due to decay during the 20-s acquisition and the lag time of the first few seconds of the scanner, hence the rationale for using the midpoint as the reference (5).

## TESTING DC

In practice, DC can easily be tested using a simple protocol that requires a graduated cylinder, dose calibrator,

500-cm<sup>3</sup> beaker, and stopwatch. A solution of precise volume and dose of radiotracer is created in the beaker. An aliquot is withdrawn and inserted into a dose calibrator, and the beaker is positioned in the scanner. The scanner is started at the very moment that the dose calibrator measures the activity of the aliquot at time 0. The beaker is then scanned over the duration in which significant decay occurs. For  $^{82}\text{Rb}$ , measurement from 3.5 to 7 min is adequate; for  $^{13}\text{N}$ , from 10 to 15; and for  $^{18}\text{F}$ , from 40 to 60 min. The acquisition should allow for several frames to be created over the duration of the scan. For established 2D or 3D scanners acquiring in list mode, the frames can be created after the acquisition; however, for non-list-mode cameras, the protocol should be prespecified. Most modern 3D scanners correct for decay automatically as the data are acquired and likely do not require such testing for DC. All images should also be attenuation-corrected. After the attenuation-corrected frames are created, ROIs are drawn around the radiotracer activity for each frame and the average concentration is recorded by the scanner. If DC is set up correctly for MBF studies, the average concentration should be nearly identical in each frame and fall within a  $\pm 3\%$  window from the first frame. Furthermore, the ratio of the calculated concentration of the first frame (based on the dose calibrator) to the measured concentration can be determined. This ratio should be about  $1.00 \pm 10\%$  if the timing of the testing protocol was performed accurately; has accurate random, scatter, and dead-time corrections; and is calibrated correctly for the radiotracer

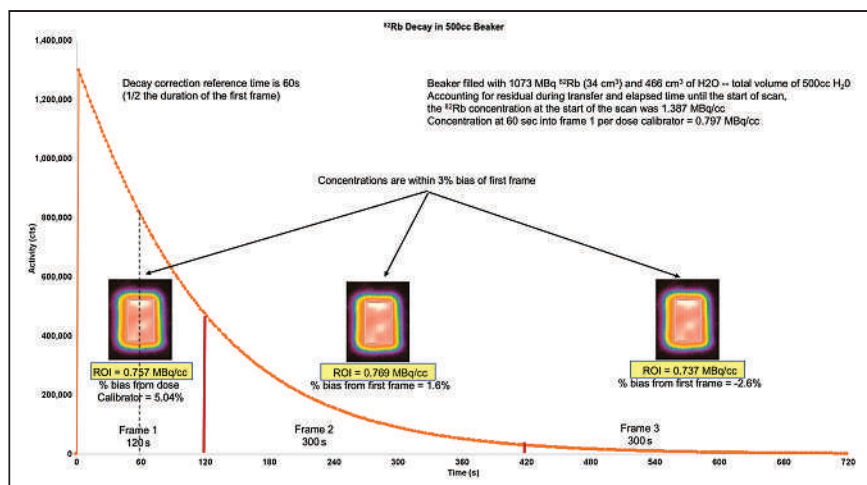


**FIGURE 3.** Decay of <sup>82</sup>Rb in 500 cm<sup>3</sup> beaker. A detailed <sup>82</sup>Rb protocol (“Rubidium Decay Correction.docx”) and worksheet (“<sup>82</sup>Rb Decay Correction Worksheet.xlsx”) can be found in the supplemental materials. Similar to Figures 1 and 2, 1,073 MBq of <sup>82</sup>Rb were placed in a beaker with a total volume precisely 500 cm<sup>3</sup> (H<sub>2</sub>O plus <sup>82</sup>Rb eluate). Scanner performed 720-s (12 min) list-mode acquisition. Ten minutes later, after all activity decayed, attenuation scanning was performed and 3 serial frames were generated at intervals of 120, 300, and 300 s. Calculations and measurements were as shown in Figure 1. There are several conclusions. First, scanner decay-corrects activity to midpoint of first frame. Second, scanner also corrects for duration of each frame, giving activity in MBq/cm<sup>3</sup>. Third, in biologic systems, only variation in quantitative activity after first frame would be due to physiologic changes and not imaging timing, duration, or decay.

being imaged. If not, further testing of other scanner function or calibration is needed. Distinct protocols for <sup>18</sup>F, <sup>13</sup>N, and <sup>82</sup>Rb that can be performed by one person, in addition to worksheets for <sup>18</sup>F, <sup>13</sup>N, and <sup>82</sup>Rb, can be found in the supplemental materials (available at <http://jnm.snmjournals.org>).

correct and incorrect DC algorithms. However quantitative perfusion data were about 30% higher at rest and about 55% higher at stress with incorrect DC, because of a falsely reduced A<sub>0</sub>. Besides the obvious difference in MBF values, there are several conclusions that can be made. First, relative

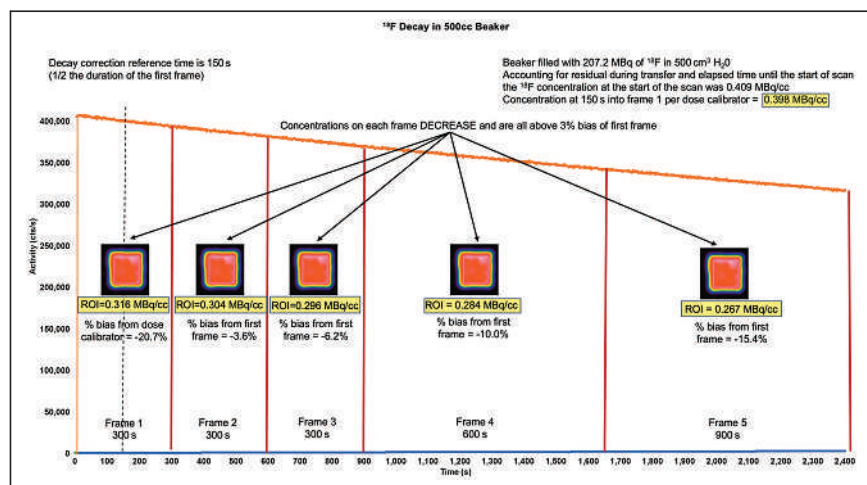


**FIGURE 4.** Similar to Figures 1–3, decay beaker testing, using <sup>18</sup>F, was performed on 2D refurbished PET camera when there was concern about accuracy of MBF data. Scanner performed 2,400-s (40 min) list-mode acquisition, and attenuation scans were obtained. Five serial frames were generated. ROI concentration continued to decrease over time and over varying frame durations. There are 2 conclusions. First, scanner does not decay-correct activity to midpoint of first frame or correct for frame duration. Second, in biologic systems, variation in quantitative activity is partly due to inadequate DC or frame duration, which cannot be differentiated from physiologic changes. Therefore, measurement of MBF will not be accurate.

## CASE EXAMPLES

Figures 1–3 illustrate beaker tests performed on an Attribus 2D PET scanner (Positron) that demonstrates accurate DC of <sup>18</sup>F, <sup>13</sup>N, and <sup>82</sup>Rb in a 500-mL beaker with a dose calibrator as the reference standard.

To investigate a refurbished 2D camera system for which absolute flow values were thought to be erroneously high, a DC beaker test using <sup>18</sup>F in a 500-cm<sup>3</sup> volume was performed. Figure 4 illustrates the results of inaccurate DC by the scanner. To confirm that this problem was not unique to the individual camera, a different camera from the same vendor was also tested and yielded similar results. Figure 5 demonstrates the relative and quantitative perfusion data from the refurbished 2D camera using the factory-installed incorrect DC algorithm and after the vendor corrected the DC algorithm. The relative images were normal and demonstrated no significant differences between the

correct and incorrect DC algorithms. However quantitative perfusion data were about 30% higher at rest and about 55% higher at stress with incorrect DC, because of a falsely reduced A<sub>0</sub>. Besides the obvious difference in MBF values, there are several conclusions that can be made. First, relative perfusion imaging is not impacted, and therefore incorrect DC can easily go unnoticed. Second, both sets of MBF values are physiologically plausible and therefore erroneous MBF values can easily go unnoticed, thus skewing site-specific reference datasets to higher MBF values. Third, prior testing on the performance of various camera systems did not specifically confirm correct DC but relied on “routine clinical practice at each institution” (3). Hence, although a camera’s performance with regard to peak counts, dead time, scatter, and randoms may be acceptable for MBF studies, inaccurate DC will still yield erroneous quantitative data. Finally, there is the possibility that clinicians or researchers who have older refurbished PET cameras with incorrect decay algorithms are making clinical decisions with erroneous MBF values.



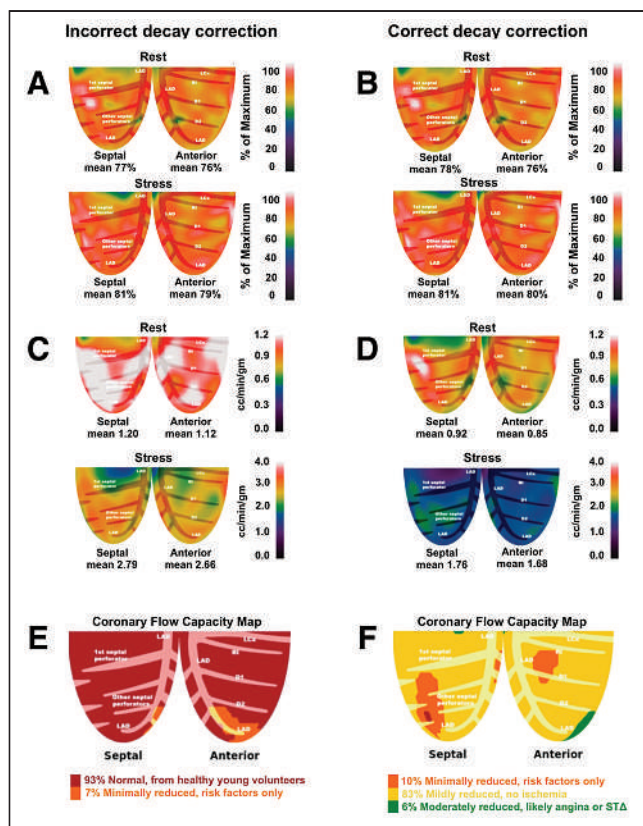


**FIGURE 5.** Figure demonstrates relative and quantitative perfusion data of the left anterior descending coronary artery (LAD) territory obtained from a refurbished 2D PET system where decay correction (DC), as part of the default settings within the camera, was performed incorrectly (left column). After recognition of the error, the DC algorithm was corrected and the study reprocessed. 5A and 5B represent rest and stress relative perfusion images, respectively. Both sets of relative images (incorrect and correct DC) are normal and appear nearly identical. 5C and 5D demonstrate inaccurate and accurate DC of rest and stress absolute perfusion in cc/min/g, respectively. With correct DC, rest and stress MBF are ~30% and ~55% lower, respectively. 5E and 5F demonstrate the coronary flow capacity (CFC) maps derived by the integration of absolute flow metrics of the incorrect and correct DC datasets, respectively. With incorrect DC, CFC maps suggest physiology consistent with healthy volunteers without risk factors. However, with correct DC, CFC maps are consistent with mild diffuse epicardial disease for which medical therapy is appropriate. Based on CFC maps, treatment would possibly be different based on the absolute perfusion metrics.

## THE RATIONALE FOR ALTERNATE DC ALGORITHMS

Most PET cameras are designed and manufactured with a focus on oncologic imaging using low-activity radiotracers ( $^{18}\text{F}$  and  $^{68}\text{Ga}$ ) with half-lives significantly longer than the duration of the acquisition. Over the course of a 10- to 15-min oncologic acquisition using these isotopes, loss of activity by radionuclide decay is insignificant such that an alternative DC algorithm could be used (5). Furthermore, in the clinic, SUVs are used instead of absolute quantification of activity. SUV is a ratio of the image-derived radiotracer

concentration to the whole-body concentration of injected dose. Provided the calibration time of the injected dose and the start of the acquisition are synchronized, alternative DC algorithms will not impact SUV or nonquantitative data (such as relative perfusion imaging), as whole-body and organ-specific activities are decaying at the same rate and with the same start time.

Therefore, unless the end user tests the scanner specifically for DC for MBF studies, alternative DC algorithms could inadvertently be used, thereby yielding an erroneous MBF. In fact, alternative DC algorithms will pass routine quality control tests when systems are designed for long-lasting radiotracers such as  $^{18}\text{F}$ .

However, non-DC datasets could be exported to software that performs DC, as might be used by research laboratories with expertise, but this option is not optimal for primarily clinical services. Finally, in more advanced or research applications, one could apply different DC algorithms based on specific needs since quantitative cardiac imaging is significantly different from oncologic imaging. The half-lives of the approved perfusion tracers are significantly shorter than the duration of the acquisition. Over the course of a myocardial perfusion scan, radiotracer activity decreases about 4-fold for  $^{13}\text{N}$  and about 64-fold for  $^{82}\text{Rb}$ , hence requiring correct DC.

## CONCLUSION

Accurate and precise quantitative myocardial perfusion requires correction for radiotracer decay. DC confirms that changes in activity over the scan duration are due to physiologic changes and not to radiotracer decay, image duration, or framing interval. Testing for correct DC is straightforward and can be performed by onsite technologists with instruments commonly found in a standard PET lab.

## DISCLOSURE

Robert Bober is a consultant for Bracco. No other potential conflict of interest relevant to this article was reported.

## ACKNOWLEDGMENT

Special thanks are given to Barbara Siede for medical illustrations.

## REFERENCES

1. Bui L, Kitkungvan D, Roby AE, Nguyen TT, Gould KL. Pitfalls in quantitative myocardial PET perfusion II: arterial input function. *J Nucl Cardiol.* 2020;27:397–409.
2. Lance Gould K, Bui L, Kitkungvan D, et al. Pitfalls in quantitative myocardial PET perfusion I: myocardial partial volume correction. *J Nucl Cardiol.* 2020;27:386–396.
3. Renaud JM, Yip K, Guimond J, et al. Characterization of 3-dimensional PET systems for accurate quantification of myocardial blood flow. *J Nucl Med.* 2017;58:103–109.
4. Murthy VL, Bateman TM, Beanlands RS, et al. Clinical quantification of myocardial blood flow using PET: joint position paper of the SNMMI Cardiovascular Council and the ASNC. *J Nucl Cardiol.* 2018;25:269–297.

5. Chen K, Reiman E, Lawson M, Dagan F, Sung-Cheng H. Decay correction methods in dynamic PET studies. *IEEE Trans Nucl Sci.* 1995;42:2173–2179.
6. Yoshida K, Mullani N, Gould KL. Coronary flow and flow reserve by PET simplified for clinical applications using rubidium-82 or nitrogen-13-ammonia. *J Nucl Med.* 1996;37:1701–1712.
7. Lortie M, Beanlands RS, Yoshinaga K, Klein R, Dasilva JN, DeKemp RA. Quantification of myocardial blood flow with  $^{82}\text{Rb}$  dynamic PET imaging. *Eur J Nucl Med Mol Imaging.* 2007;34:1765–1774.
8. Vasquez AF, Johnson NP, Gould KL. Variation in quantitative myocardial perfusion due to arterial input selection. *JACC Cardiovasc Imaging.* 2013;6:559–568.
9. Fitzgerald R. Corrections for the combined effects of decay and dead time in live-timed counting of short-lived radionuclides. *Appl Radiat Isot.* 2016;109:335–340.
10. Dawood M, Jiang X, Schäfers K. *Correction Techniques in Emission Tomography.* CRC Press; 2012:69–70.

## Erratum

In the article “Accuracy Assessment of SUV Measurements in SPECT/CT: A Phantom Study,” by Fatin Halim et al. (*J Nucl Med Technol.* 2021;49:250–255), the fundamental grant scheme number (203/CIPPT/6711730) was incorrectly stated in the Disclosure. The correct fundamental grant scheme number should be *FRGS/1/2019/SKK08/USM/03/4*. The authors regret the error.

# Root Cause Analysis of Na<sup>131</sup>I Contamination

Jitesh Dhingra<sup>1</sup>, Cesar Santana<sup>1</sup>, John Harvey<sup>2</sup>, Amelia Miller<sup>2</sup>, Ariel Benton<sup>1</sup>, Meguewell Childs<sup>1</sup>, and Raghuveer Halkar<sup>1</sup>

<sup>1</sup>Grady Memorial Hospital, Atlanta, Georgia; and <sup>2</sup>West Physics, Atlanta, Georgia

Establishing a cause-and-effect relationship for an adverse event is one of the key steps in preventing them and involves multiple people, resources, and steps, thus requiring a root cause analysis. Here, we describe a root cause analysis performed in the nuclear medicine department for an event involving Na<sup>131</sup>I contamination. Oral administration of Na<sup>131</sup>I in a capsule minimizes the risk of contamination and spills. However, the patient must be able to swallow a capsule. Na<sup>131</sup>I in capsule form is currently in widespread use for treatment of hyperthyroidism and thyroid cancer. Na<sup>131</sup>I in liquid form is rarely available immediately on demand and must be ordered at least 24–48 h in advance of the planned administration. The events leading to the incident, immediate remedial steps taken, and subsequent root cause analysis are described. The corrective actions taken after the root cause analysis, as well as the subsequent effectiveness of these actions, are mentioned. There may be one or multiple causes for an adverse event. It is important to identify the root cause. Corrective actions derived from the root cause can help prevent similar adverse events in the future. Therapeutic procedures in nuclear medicine involve unsealed radioactive sources, further adding a separate layer of immediate steps and reporting to the root cause analysis itself.

**Key Words:** root cause analysis; Na<sup>131</sup>I contamination; radioiodine therapy; hyperthyroidism

**J Nucl Med Technol 2021; 49:350–353**  
DOI: 10.2967/jnmt.121.262492

**S**aul Hertz first administered radioiodine (Na<sup>131</sup>I) to a patient in 1941 at Massachusetts General Hospital as a treatment for hyperthyroidism (1). For a long period, Na<sup>131</sup>I was available only in liquid form, but by the 1970s, Na<sup>131</sup>I was available in capsule form (2). Oral administration of Na<sup>131</sup>I in a capsule minimizes the risk of contamination and spills. However, the patient must be able to swallow a capsule. Na<sup>131</sup>I in capsule form is currently in widespread use for treatment of hyperthyroidism and thyroid cancer. Na<sup>131</sup>I in liquid form is rarely available immediately on demand and must be ordered at least 24–48 h in advance of the planned administration.

Here, we describe an adverse event in which a hot lab and radioisotope dosing room were contaminated with Na<sup>131</sup>I because of an attempt to break open the capsule to dissolve the contents in a cup of water. We also describe the events leading to the incident, the immediate remedial steps taken, the subsequent root cause analysis, corrective actions developed after the root cause analysis, and the subsequent effectiveness of the corrective actions. There may be one or multiple causes for an adverse event, and unless a root cause is determined, a comprehensive corrective action to prevent a similar adverse event in the future is not possible (3,4).

**Quality Event.** The Na<sup>131</sup>I contamination event occurred on October 15, 2019, in the radioisotope dosing room and hot lab of a large community hospital where around 30 patients per year are treated for hyperthyroidism. The facility performs around 6,000 nuclear medicine (NM) procedures per year and has 5 NM technologists and a supervisor. Three NM physicians cover different days of the week. The policy of the hospital regarding patients who are to undergo a radioactive iodine scan and subsequent therapy is to perform a consultation using a checklist (5). Figure 1 shows the policy and protocol for radioiodine therapy for hyperthyroidism.

A 48-y-old woman presented to the NM department for Na<sup>131</sup>I therapy for hyperthyroidism. When the authorized user (AU) physician and a resident physician were about to administer the 1.11-GBq (30 mCi) Na<sup>131</sup>I capsule in the dosing room, the patient told them that she was unable to swallow the capsule as she had oropharyngeal thrush due to an underlying immunodeficiency.

The AU called the radiopharmacy to obtain Na<sup>131</sup>I in liquid form, but it would not be available for another 3 d because the request was being made on a weekend. Since the patient was not willing to return after 3 d, the AU decided to open the Na<sup>131</sup>I capsule in the dosing room and empty the contents into a cup of water for the patient to drink. The AU and resident first tried to open the capsule with gloved hands over a cup of water placed on a counter in the treatment room. The Na<sup>131</sup>I capsules supplied by the vendor have Na<sup>131</sup>I solution injected directly into a small capsule, which is enclosed within a larger capsule. Figure 2 demonstrates the preparation and configuration of these Na<sup>131</sup>I capsules.

Received Aug. 6, 2021; revision accepted Sep. 30, 2021.  
For correspondence or reprints, contact Jitesh Dhingra (jitesh.dhingra@emory.edu).  
COPYRIGHT © 2021 by the Society of Nuclear Medicine and Molecular Imaging.



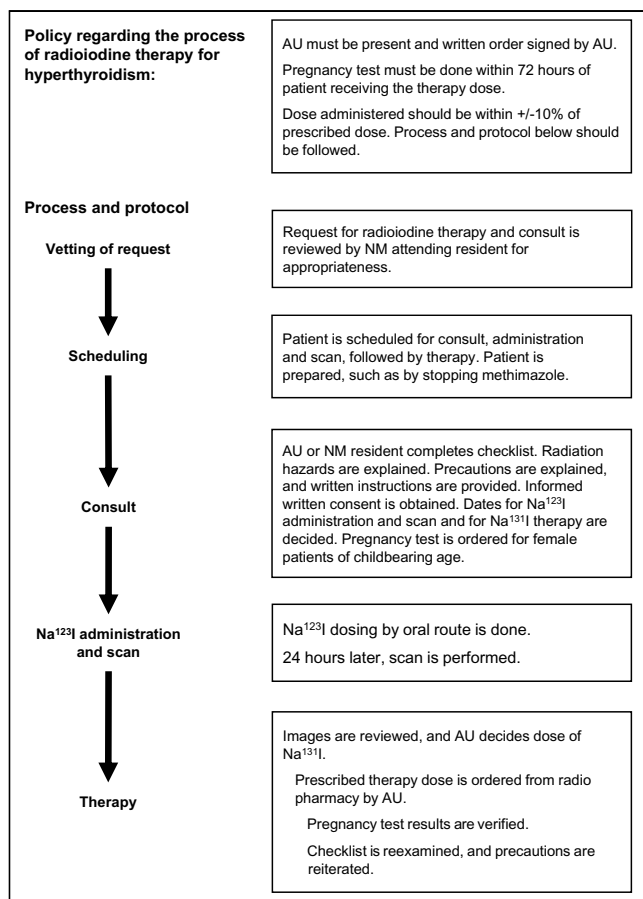


**FIGURE 1.** Policy and protocol for radioiodine therapy for hyperthyroidism.

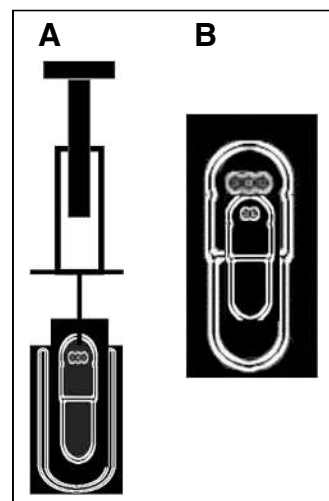


**FIGURE 2.** (A) Injecting Na<sup>131</sup>I into center of inner small capsule. (B) Slipping upper half of large capsule over bottom half to completely cover small capsule, which is then gently pushed down until locked.

Unaware that the capsule had this configuration, the resident and AU opened the outer capsule but could not open the inner capsule. They transported both into the hot lab and, placing them behind a lead glass shield, tried to puncture the inner capsule with a needle. A technologist passing through the area overheard the physicians talking about the attempt to puncture the capsule. She raised concern about contamination and contacted the radiation safety team. The radiation safety officer and an assistant radiation safety officer surveyed the hot lab and dosing room and found

that Na<sup>131</sup>I contamination was present on the floor, as well as on the countertop in the dosing room. The radiation levels from the floor contamination were quite high (over 20 mR/h at a distance of 1 m), whereas the levels on the countertop were lower (5 mR/h at 5 cm). An attempt to clean the floor contamination was not successful. The patient did not receive Na<sup>131</sup>I therapy, was surveyed for contamination, and was sent home with a plan to reschedule her treatment with liquid Na<sup>131</sup>I.

The radiation safety officer surveyed the AU, resident, and technologist and found that the shoes and white coats of all three were contaminated. The shoes and white coats were stored in the radioactive waste room, and the hot lab and dosing room were posted with warning signs for a total of 80 d, the equivalent of 10 half-lives of Na<sup>131</sup>I. The facility had a second dosing room and another hot lab that could be used in the interim, and operation of the department was resumed with little interruption. On the next day, the AU, resident, and technologist underwent bioassays to measure radioactivity in the thyroid, and none was found. The radiation safety officer contacted the state nuclear materials regulator within 24 h and provided a detailed report within 30 d. An unbiased team consisting of a NM physician, a technologist supervisor, and another technologist (none of whom were involved in the incident) performed a root cause analysis.

The contamination event and immediate actions are summarized in Figure 3.

## QUALITY ANALYSIS

The team asked “why” until the answers guided them toward corrective actions.

### Why Did AU and Resident Try to Open Capsule?

The patient could not swallow the capsule, and the radio-pharmacy could not provide Na<sup>131</sup>I in liquid form on that day. The policy folder did not specifically mention “do not tamper with the radioiodine capsule.”

Suggested corrective action: The policy will specifically forbid tampering with Na<sup>131</sup>I capsules.

### Why Was Treating Team Not Aware That Patient Could Not Swallow Capsule?

The patient was in the department on the previous day to undergo a Na<sup>123</sup>I scan. Another technologist had opened the Na<sup>123</sup>I capsule, dissolved the contents in a cup of water, and given it to the patient. He also informed the AU about taking these measures. The Na<sup>123</sup>I capsule contained granules and could be twisted open to release the contents. Even though the contents can be emptied into a glass of water, this method of administration is not correct because it is not possible to assay the dose and there is a possibility of contamination.

Suggested corrective action: All AUs and technologists are to be provided with additional training.

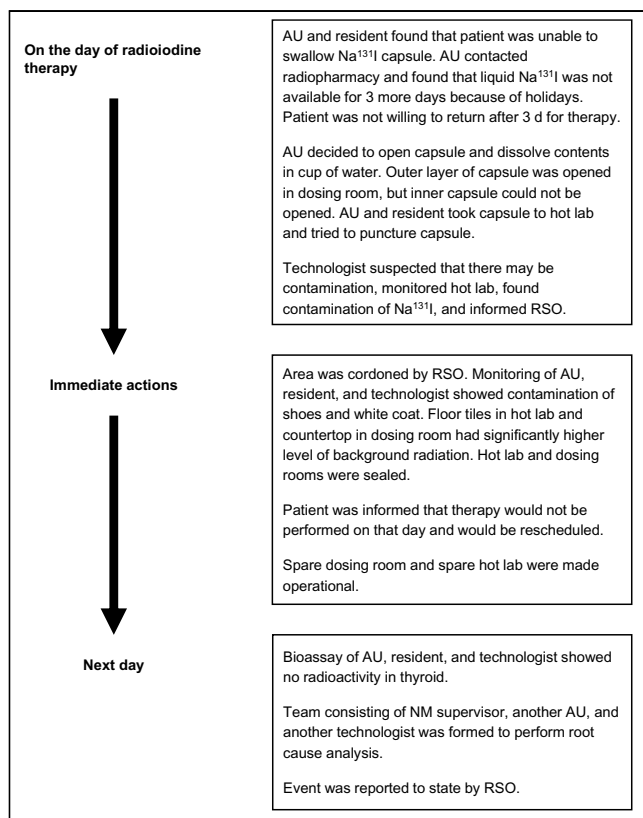


**FIGURE 3.** Sequence of events on day of radioiodine therapy contamination.

#### Why Was Inability to Swallow Capsule Not Identified Before Na<sup>123</sup>I or Na<sup>131</sup>I Capsules Were Ordered?

The checklist used for patient consultations before Na<sup>123</sup>I scanning and Na<sup>131</sup>I therapy did not include a check of whether the patient can swallow the capsule.

Suggested corrective action: A question about capacity to swallow the capsule is to be added to the checklist.

#### Why Was Floor Contamination Not Removable?

The floor of the hot lab and dosing room had 30-cm square tiles. The Na<sup>131</sup>I had seeped into the gaps between the tiles. The hot lab was designed almost 2 decades before the incident.

Suggested corrective action: The flooring of the hot lab, dosing areas, and bathrooms in the NM department is to be replaced with continuous linoleum.

#### CORRECTIVE ACTION

The NM staff, consisting of all technologists, NM physicians, and NM residents, comprehensively reviewed the incident and were retrained within a week afterward. The training was done by a team of experienced AUs, including the directors of the NM departments of 2 major hospitals.

The corrective actions suggested in the root cause analysis were added to the policy and checklist. The consultation form was updated with a line specifically directing that the capsule should not be tampered with under any circumstances.

Continuous linoleum flooring was installed in the renovated hot lab, dosing room, and bathrooms.

The corrective actions for each cause and effect are summarized in Figure 4.

#### VERIFICATION OF EFFECTIVENESS

Between May 1, 2020, and April 31, 2021, more than 50 hyperthyroid patients have been treated with Na<sup>131</sup>I. During that time, no adverse events have been recorded.

Cause-and-effect analysis is needed to prevent errors. Finding a cause is easy and straightforward in a procedure that involves a single step and a single person. Providing health care has become a team effort involving multiple people and steps. When an adverse event takes place during or because of a procedure that involves multiple steps and people, it is necessary to perform a root cause analysis to prevent such events in the future.

In our case, if we had looked at the apparent cause we would have ended up retraining only the AU, resident, and technologist involved. The root cause analysis revealed that multiple additional team members were also misinformed and had—contrary to recommendations—opened Na<sup>123</sup>I capsules. The root cause analysis exposed deficiencies in the policy and in the checklist used in the protocol. Thus, the root cause analysis resulted in a comprehensive corrective-action plan.

Reporting the exact sequence of events honestly is the critical factor in root cause analysis. Honest reporting is possible when there is no fear of reprisal if unintended human error or deficiency is found in the policy or protocol. Analysis of the event and finding the causes that led to it also depend on having an unbiased team perform the analysis and make the

Event	Why	Corrective action
Radioiodine contamination on day of therapy.	Why was there Na <sup>131</sup> I contamination?  Patient was not able to swallow capsule, liquid Na <sup>131</sup> I was not available, and AU decided to open capsule so as to dissolve contents in water. Policy did not specifically mention that capsule should not be opened.	Add to policy: "do not tamper with radioiodine capsule," and train the AU involved.
Na <sup>123</sup> I dosing for administration and scan	Why was patient able to swallow Na <sup>123</sup> I capsule on previous day?  Patient was not able to swallow Na <sup>123</sup> I capsule. It was opened, and content was dissolved in water by another technologist and another AU.	Retrain whole team, since other technologist and AU opened Na <sup>123</sup> I capsule.
Consult	Why was inability to swallow capsule not known before scan or therapy?  Consult checklist did not check for ability to swallow a capsule.	Add to checklist: "determine whether patient can swallow a capsule; if not, order liquid radioiodine."
Radioiodine contamination	Why could contamination not be removed?  Tiles were used for flooring in hot lab and dosing room. Iodine powder was in cracks between tiles.	Change flooring of hot lab, dosing room, and bathroom to continuous linoleum sheet.

**FIGURE 4.** Sequential corrective actions taken for each cause and effect identified while performing root cause analysis.

corrective recommendations. Continuous monitoring after the recommendations are implemented is the way to measure continuous quality improvement. The reported event and subsequent root cause analysis in our case resulted in comprehensive corrective actions, achieving desired outcomes in procedures for over a year of subsequent follow-up.

## DISCLOSURE

No potential conflict of interest relevant to this article was reported.

## REFERENCES

1. Hertz S, Roberts A. Radioactive iodine in the study of thyroid physiology; the use of radioactive iodine therapy in hyperthyroidism. *J Am Med Assoc.* 1946;131:81–86.
2. Halpern S, Alazraki N, Littenberg R, et al.  $^{131}\text{I}$  thyroid uptakes: capsule versus liquid. *J Nucl Med.* 1973;14:507–510.
3. Rooney JJ, Vanden Heuvel LN. Root cause analysis for beginners. *Quality Process.* 2004;37:45–53.
4. Croteau RJ, Schyve PM. Proactively error-proofing health care processes. In Spath PL, ed. *Error Reduction in Health Care: A Systems Approach to Improving Patient Safety.* Jossey Bass; 2000:179–198.
5. Moncayo VM, Applegate KE, Duszak R Jr, et al. The nuclear medicine therapy care coordination service: a model for radiologist-driven patient-centered care. *Acad Radiol.* 2015;22:771–778.

# A Case of $^{177}\text{Lu}$ -DOTATATE Therapy Without the Use of Antiemetics

Justin G. Peacock<sup>1,2</sup>, Brendan O'Sullivan<sup>3</sup>, and Michael R. Povlow<sup>1</sup>

<sup>1</sup>Department of Radiology, Brooke Army Medical Center, San Antonio, Texas; <sup>2</sup>Department of Radiology, Uniformed Services University of the Health Sciences, Bethesda, Maryland; and <sup>3</sup>Chicago College of Osteopathic Medicine, Midwestern University, Downers Grove, Illinois

Recommended  $^{177}\text{Lu}$ -DOTATATE treatment regimens involve prophylaxis with antiemetics to counteract the emetogenic properties of the nephroprotective amino acid solution infusion. We describe a 58-y-old woman treated with  $^{177}\text{Lu}$ -DOTATATE for metastatic small-bowel carcinoid, who was allergic to many classes of antiemetics. Therefore, she was treated with  $^{177}\text{Lu}$ -DOTATATE without antiemetic prophylaxis. She tolerated the compounded amino acid infusion of lysine and arginine, followed by  $^{177}\text{Lu}$ -DOTATATE, without significant nausea or any vomiting. We hypothesize that aggressive antiemetic prophylaxis may not be necessary if a  $^{177}\text{Lu}$ -DOTATATE patient receives compounded lysine/arginine amino acid solutions. The omission would decrease overall health-care costs and limit possible medication side effects.

**Key Words:** LUTATHERA; antiemetics; amino acid; nausea; vomiting

**J Nucl Med Technol 2021; 49:354–355**

DOI: 10.2967/jnmt.121.261996

**D**OTATATE with  $^{177}\text{Lu}$  (LUTATHERA; Advanced Accelerator Applications SA) is a peptide receptor radionuclide therapy used in gastroenteropancreatic neuroendocrine tumors. The regimen includes pretreatment with positively charged amino acids (AA) to prevent possible nephrotoxicity from  $^{177}\text{Lu}$ -DOTATATE retention. Nausea and vomiting are unfortunate side effects of the AA solution (1). Historically, commercial AA solutions resulted in significant nausea; however, new data suggest that compounded L-arginine and L-lysine AA solutions are significantly less emetogenic (2). Because of historic severe nausea and vomiting with commercial AA solutions, aggressive pretreatment with antiemetics is recommended (3). We present a case of a patient allergic to many antiemetic drugs, who successfully underwent  $^{177}\text{Lu}$ -DOTATATE therapy without the use of antiemetics.

## CASE REPORT

The typical prophylactic antiemetic at our institution for  $^{177}\text{Lu}$ -DOTATATE patients is a combination of netupitant

and palonosetron (Akynzeo; Helsinn Healthcare SA). We administer this drug 30 min before the AA infusion, followed by  $^{177}\text{Lu}$ -DOTATATE infusion 30 min later. For the AA renal-protective solution, we use a compounded solution of lysine and arginine, rather than the commercial AA solutions.

A 58-y-old woman presented to our clinic for her first  $^{177}\text{Lu}$ -DOTATATE cycle for metastatic small-bowel carcinoid that was progressive despite chronic long-acting octreotide therapy (Fig. 1). She had undergone resection of a low-grade ileal carcinoid tumor in 2005, followed by long-acting octreotide therapy. During consultation for the first treatment dose, the patient reported severe allergies to



**FIGURE 1.**  $^{68}\text{Ga}$ -DOTATATE PET/CT maximum-intensity projection demonstrating multiple radiotracer-avid abdominopelvic lymph nodes (solid arrows). Incidental mediastinal and hilar nodal uptake (dashed arrows) were felt to be due to underlying inflammatory condition, such as sarcoidosis.

Received Jan. 23, 2021; revision accepted Apr. 13, 2021.  
For correspondence or reprints, contact Justin G. Peacock (justin.g.peacock@gmail.com).  
Published online July 30, 2021.  
COPYRIGHT © 2021 by the Society of Nuclear Medicine and Molecular Imaging.

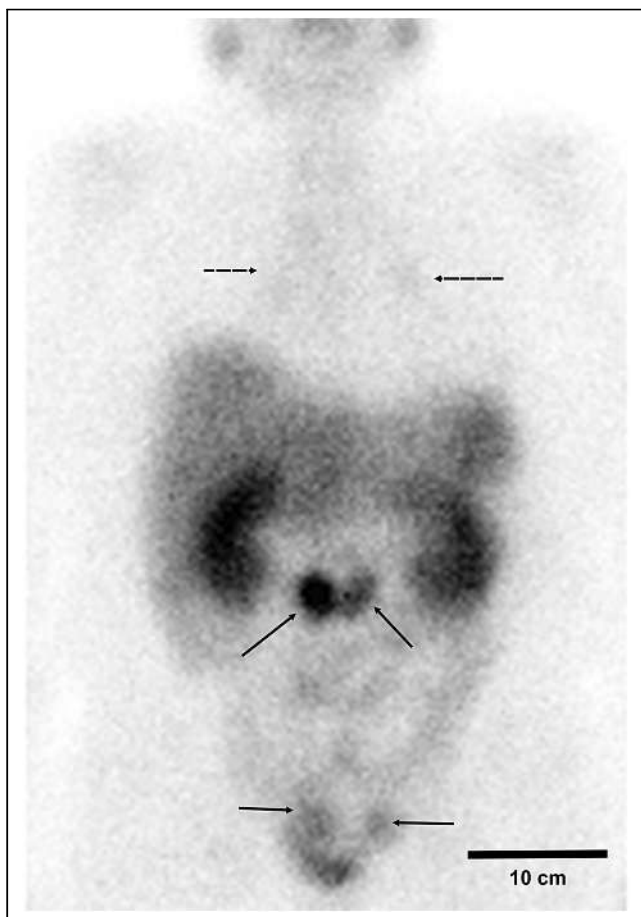


**FIGURE 2.**  $^{177}\text{Lu}$ -DOTATATE (7.3 GBq) posttreatment anterior planar  $\gamma$ -image demonstrating pattern of uptake similar to that seen on prior  $^{68}\text{Ga}$ -DOTATATE PET/CT (Fig. 1), with abdominopelvic (solid arrows) and incidental mediastinal and hilar (dashed arrows) nodal uptake again noted.

many classes of antiemetics, including the antiserotonergic class that we typically give to patients. After a discussion with the patient on the risks of not administering antiemetics, we decided to proceed with standard AA and  $^{177}\text{Lu}$ -DOTATATE (7.3 GBq) infusion without antiemetic prophylaxis. The  $^{177}\text{Lu}$ -DOTATATE infusion was performed using the standard technique outlined by the manufacturer. The patient denied experiencing any significant nausea or vomiting at any time during her infusion or at any time (checked at approximately 2-h intervals) during her overnight hospital admission. We imaged the patient the next morning per the standard protocol and allowed her to return home (Fig. 2). She denied experiencing nausea the next morning as well.

## DISCUSSION

Although omitting the antiemetic placed our patient at a higher risk for developing symptoms of nausea and vomiting, the compounded AA solution of lysine and arginine likely lowered the likelihood of symptoms (2). She was monitored closely but did not develop any significant nausea or vomiting symptoms at any time during her clinical course.

The recommended  $^{177}\text{Lu}$ -DOTATATE treatment regimen includes aggressive and potentially expensive antiemetic prophylaxis. The cash-paying cost (i.e., insurance costs of medications often differ from out-of-pocket cash costs from the manufacturer) of a single dose of the combination antiemetic Akynzeo is \$683. Another possible problem with these antiemetics are side effects, including headache and fatigue.

## CONCLUSION

Our patient with metastatic small-bowel carcinoid underwent  $^{177}\text{Lu}$ -DOTATATE therapy successfully despite the fact that, because of allergies, she did not receive antiemetics. We hypothesize that aggressive and potentially expensive antiemetic prophylaxis may not be necessary when infusing patients with a compounded AA solution of lysine and arginine. Further research into this matter is important to improve patient care and to reduce treatment costs.

## DISCLOSURE

The views expressed here are those of the authors and do not reflect the official policy or position of Brooke Army Medical Center, the U.S. Army Medical Department, the U.S. Army Office of the Surgeon General, the Department of the Army, the Department of the Air Force, the Department of Defense, the Defense Health Agency, or the U.S. Government. No potential conflict of interest relevant to this article was reported.

## REFERENCES

1. Lapa C, Werner RA, Bluemel C, et al. Influence of the amount of co-infused amino acids on post-therapeutic potassium levels in peptide receptor radionuclide therapy. *EJNMMI Res*. 2014;4:46.
2. Alonzo N, Seyer M, Kim E-J, Keshavarzi R, Yee K, Kunz PL. Evaluation of the incidence of acute nausea and vomiting after administration of an amino acid solution containing only arginine and lysine with lutetium Lu-177 dotatate [abstract]. *J Clin Oncol*. 2020;38(suppl):12113.
3. Hope TA, Abbott A, Colucci K, et al. NANETS/SNMMI procedure standard for somatostatin receptor-based peptide receptor radionuclide therapy with  $^{177}\text{Lu}$ -DOTATATE. *J Nucl Med*. 2019;60:937-943.

# Artifact from $^{131}\text{I}$ -Contaminated Mask in Postradioiodine Therapy Scintigraphy

Francesca Betti, Luca Antonacci, and Duccio Volterrani

Nuclear Medicine Unit, University Hospital of Pisa, Pisa, Italy

A patient wearing the mandatory face mask because of the ongoing coronavirus disease 2019 pandemic underwent postradioiodine therapy scintigraphy. The spot view of the neck showed an area of uptake that was later demonstrated to be caused by contamination of the mask. This finding has led to updating the scan procedure for posttherapy scintigraphy by replacing the patients' masks before the scan acquisition.

**Key Words:**  $^{131}\text{I}$ ; artifact; face mask; posttherapy scintigraphy

**J Nucl Med Technol 2021; 49:356–357**

DOI: 10.2967/jnmt.121.262438

**G**uidelines for radioiodine therapy (RAIT) of differentiated thyroid cancer recommend that whole-body scintigraphy be performed after every RAIT. The aim of post-RAIT scintigraphy is not only to characterize the extent of the thyroid remnant but also to detect unknown lesions. Areas of focal iodine uptake outside the physiologic ones are suggestive of metastatic disease, although radioactive contamination artifacts in  $^{131}\text{I}$  imaging after RAIT are a known issue (1).

## CASE REPORT

A patient treated with 2,960 MBq of  $^{131}\text{I}$  to ablate a thyroid remnant was referred for posttherapy scintigraphy 5 d after RAIT administration. Because of the ongoing coronavirus disease 2019 pandemic, the patient was required to wear a face mask during his time in the hospital. The mask was kept on during the whole imaging acquisition procedure.

After the whole-body scan, an anterior spot view of the neck, including the laterocervical region and part of the chest, was acquired as required by the protocol in use. Iodine uptake was found in the residual thyroidal tissue in the neck, as well as in the mucosae of the nose and mouth. An area of intense iodine uptake below the right corner of the patient's mouth was also present (Fig. 1). Given the unusual appearance of the iodine distribution pattern, the technologist suspected a possible artifact due to iodine contamination of the mask.

Therefore, the patient was given a new mask to wear and the scan was repeated.

The newly acquired spot view showed the disappearance of the high-activity area (Fig. 2). Lateral views also demonstrated a physiologic distribution of radioiodine.

## DISCUSSION

Contamination artifacts in  $^{131}\text{I}$  imaging are often due to body secretions, perspiration, or saliva (2,3). In particular, radioactive iodine can be detected in patients' saliva up to 2 wk after RAIT (4).

In a recently reported artifact linked to a contaminated face mask, the abnormal iodine distribution was considered to be due to the presence of  $^{131}\text{I}$  in the exhaled air remaining in the mask (5). In our case, given the intense activity shown on the scintigraphy, our finding more likely refers to salivary imbibition after prolonged use of the same mask than to exhalation only.

If not recognized as an artifact, further characterization of the area of uptake would have been required. The differential diagnosis should have included increased uptake in the right sublingual or submandibular glands, a metastatic lymph node, or a bone metastasis of the mandible.

## CONCLUSION

Unusual patterns of iodine distribution on post-RAIT scintigraphy must be evaluated accurately. Patients undergoing post-RAIT scintigraphy in our hospital are currently asked to wear a new mask just before the scan begins. Used masks are disposed of as radioactive waste.

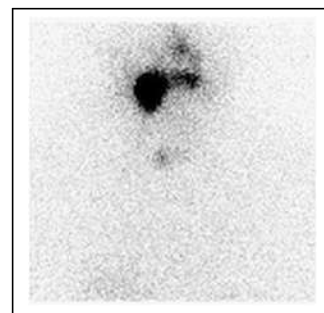


**FIGURE 1.** Post-RAIT spot view of neck shows hot spot below right corner of patient's mouth.

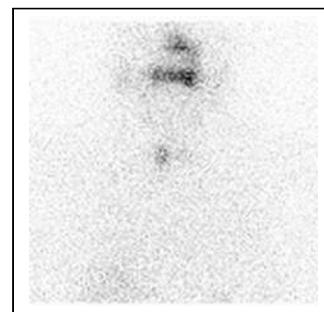


**FIGURE 2.** Spot view of neck acquired while patient was wearing new mask. Hot spot has disappeared.

Received Apr. 15, 2021; revision accepted May 27, 2021.  
For correspondence or reprints, contact Francesca Betti (francesca.betti@med.unipi.it).

Published online July 30, 2021.

COPYRIGHT © 2021 by the Society of Nuclear Medicine and Molecular Imaging.



## DISCLOSURE

No potential conflict of interest relevant to this article was reported.

## REFERENCES

1. Ozcan Kara P, Gunay EC, Erdogan A. Radioiodine contamination artifacts and unusual patterns of accumulation in whole-body I-131 imaging: a case series. *Int J Endocrinol Metab*. 2014;12:e9329.
2. Park HM, Tarver RD, Schauwecker DS, Burt R. Spurious thyroid cancer metastasis: saliva contamination artifact in high dose iodine-131 metastases survey. *J Nucl Med*. 1986;27:634–636.
3. Gritters LS, Wissing J, Gross MD, Shapiro B. Extensive salivary contamination due to concurrent use of chewing tobacco during I-131 radioablative therapy. *Clin Nucl Med*. 1993;18:115–117.
4. Rakha A, Rehman K, Shadid M, Jahan N, Babar Imran M. Salivary flow rate and radioactivity in saliva, blood and serum of benign and malignant thyroid patients after <sup>131</sup>I therapy. *Int J Radiat Res*. 2021;19:197–203.
5. Kawabe J, Yoshida A, Higashiyama S. False-positive I-131 distribution caused by residual I-131 in the face mask. *Jpn Archive Cases Conference Clin Nucl Med*. 2020;2:10–14.

# Rare Multisystem Histiocytic Sarcoma on $^{18}\text{F}$ -FDG PET/CT

Matthew Harwood<sup>1</sup>, Fiona E. Craig<sup>2</sup>, and Ming Yang<sup>1</sup>

<sup>1</sup>Department of Radiology, Mayo Clinic Arizona, Scottsdale, Arizona; and <sup>2</sup>Laboratory of Medicine and Pathology, Mayo Clinic Arizona, Scottsdale, Arizona

Histiocytic sarcoma (HS) is a rare malignancy with morphologic and immunophenotypic features indicating histiocytic differentiation. We present a case of HS with multisystem involvement, including an obstructing mass in the pancreatic head.  $^{18}\text{F}$ -FDG PET/CT is a valuable tool in staging this rare entity and in assessing the response to therapy. Knowing the diverse metastatic pattern of HS will help avoid imaging pitfalls on clinical  $^{18}\text{F}$ -FDG PET/CT scans.

**Key Words:** histiocytic sarcoma; FDG; PET/CT; pancreas

**J Nucl Med Technol 2021; 49:358–359**  
DOI: 10.2967/jnmt.121.262247

**H**istiocytic sarcoma (HS) is a rare neoplasm of myeloid-derived macrophages. The exact etiology is unclear. It occurs predominantly in adults and is associated with poor survival (1). HS may involve lymph nodes and many organs and is hypermetabolic on  $^{18}\text{F}$ -FDG PET/CT. Diagnosis of HS relies on demonstration of histopathologic evidence of histiocytic differentiation, that is, CD68 and CD163, and exclusion of other malignancies, including large B-cell lymphoma, T/NK-cell lymphoma, and other histiocytic and dendritic neoplasms.

## CASE REPORT

A 51-y-old woman presented with progressively worsening back pain. Thoracic spine MRI demonstrated a large mass centered at the T7 level and bilaterally infiltrating the T7 and T8 neural foramen, as well as adjacent ribs. The patient underwent T6–T8 decompression and tumor debulking to relieve back pain. Histopathologic evaluation of the intraspinal, extradural mass lesion demonstrated large anaplastic cells, mitotic activity, and admixed lymphocytes and eosinophils. Immunohistochemical stains showed the large tumor cells to be positive for CD4, CD10, CD45, CD68, and CD163 and negative for markers of a plasma cell neoplasm (CD138 immunoglobulin light-chain–negative), Hodgkin lymphoma (CD30 and CD15), Langerhans cell sarcoma (CD1a), and dendritic cell sarcoma (CD21 and CD35). A diagnosis of HS was established.

Shortly after surgery, the patient presented with acute pain in the right upper quadrant and around the stomach, which worsened after meals, as well as jaundice and pruritus. Contrast-enhanced CT showed an ill-defined mass in the pancreatic head, with dilation of the bile duct and the main pancreatic duct. On  $^{18}\text{F}$ -FDG PET/CT, there were multiple hypermetabolic lesions, including the mass in the pancreatic head (Fig. 1). The patient underwent 3 cycles of chemotherapy under the CHOP regimen (cyclophosphamide, doxorubicin, vincristine, and prednisolone) and demonstrated a favorable response to therapy.

## DISCUSSION

HS is a rare histiocyte disorder with a slight male predominance (2). Since HS may involve multiple systems, its clinical manifestation varies and may present as multifocal hypermetabolic extranodal disease on  $^{18}\text{F}$ -FDG PET/CT (2–4). Pancreatic involvement in HS is extremely rare and may mimic other pancreatic malignancies. Ultimate diagnosis of HS relies on histopathologic evidence of histiocytic differentiation within involved tissue and exclusion of other malignancies, including large B-cell lymphoma and other histiocytic and dendritic neoplasms (5). There is no standard treatment for HS, and the CHOP regimen might be acceptable

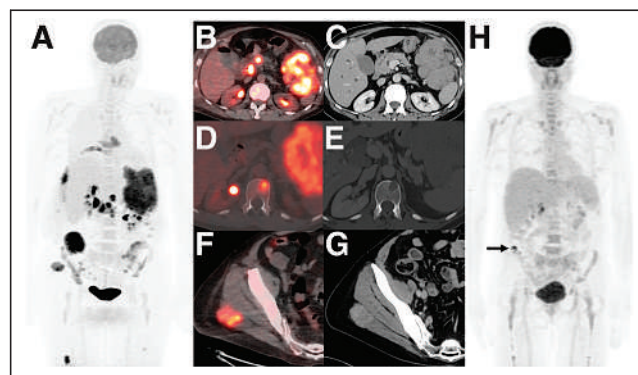


**FIGURE 1.** (A–G) On staging  $^{18}\text{F}$ -FDG PET/CT maximum-intensity projection (A), PET/CT fusion, and corresponding contrast-enhanced diagnostic CT images, there are multiple hypermetabolic metastases, including obstructive mass in pancreatic head and large mass lesion in left upper quadrant (B and C), lytic lesion in T12 vertebral body (D and E), and lesion in right gluteus maximus muscle (F and G). (H) After 3 cycles of chemotherapy, follow-up  $^{18}\text{F}$ -FDG PET/CT showed near-complete response and small, residual tracer-avid focus in right iliac wing (arrow).

Received Mar. 5, 2021; revision accepted Apr. 15, 2021.  
For correspondence or reprints, contact Ming Yang (yang.ming@mayo.edu).

Published online July 30, 2021.

COPYRIGHT © 2021 by the Society of Nuclear Medicine and Molecular Imaging.

for multifocal disease. Although HS might exhibit a favorable response to chemotherapy, the long-term survival rate is poor (1). <sup>18</sup>F-FDG PET/CT may allow us to delineate the extent of HS, guide biopsy, and assess treatment response.

## CONCLUSION

It is important to be familiar with the widespread multi-system pattern of HS. <sup>18</sup>F-FDG PET/CT is a valuable tool in staging and surveillance of this rare entity.

## DISCLOSURE

No potential conflict of interest relevant to this article was reported.

## REFERENCES

1. Takahashi E, Nakamura S. Histiocytic sarcoma: an updated literature review based on the 2008 WHO classification. *J Clin Exp Hematop*. 2013;53:1–8.
2. Saboo SS, Krajewski KM, Shinagare AB, Jagannathan JP, Hornick JL, Ramaiya N. Imaging features of primary extranodal histiocytic sarcoma: report of two cases and a review of the literature. *Cancer Imaging*. 2012; 12:253–258.
3. Fernández-Aceñero MJ, Pérez Alonso P, Díaz del Arco C. Histiocytic sarcoma with bladder involvement: case report and literature review. *Rev Esp Patol*. 2018; 51:23–26.
4. Makis W, Ciarallo A, Derbekyan V, Lisbona R. Histiocytic sarcoma involving lymph nodes: imaging appearance on gallium-67 and F-18 FDG PET/CT. *Clin Nucl Med*. 2011;36:e37–e38.
5. Swerdlow SH, Campo E, Harris NL, et al. *WHO Classification of Tumours of Haematopoietic and Lymphoid Tissues*. 4th ed. World Health Organization; 2011: 468–470.

# <sup>18</sup>F-FDG PET/CT Imaging Features of Cardiac Arrhythmia in a Patient Treated with Panitumumab

Pokhraj P. Suthar, Jagadeesh S. Singh, and Khushboo Gupta

Department of Diagnostic Radiology and Nuclear Medicine, Rush University Medical Center, Chicago, Illinois

Panitumumab is a new humanized antiepidermal growth factor receptor monoclonal antibody (mAb) approved for the treatment of advanced colorectal cancer. There is an increase in the use of this drug due to a good response rate and possible secondary resection in advanced colorectal cancer. Here, we present <sup>18</sup>F-FDG PET/CT imaging findings of cardiac arrhythmia in a patient receiving panitumumab for the treatment of metastatic infiltrating rectal adenocarcinoma. Cardiotoxicity is a known adverse effect associated with panitumumab. So far, to our knowledge, no documented imaging findings for the same are available in the literature.

**Key Words:** PET; PET/CT; cardiac arrhythmia; PET/CT; panitumumab

**J Nucl Med Technol 2021; 49:360–361**

DOI: 10.2967/jnmt.121.262216

**P**anitumumab is used as a targeted immunotherapy for metastatic colorectal carcinoma as a first-line or second-line treatment (1). The adverse effects of this drug include skin-related toxicity as well as cardiotoxicity. The following case represents imaging features of newly diagnosed cardiac arrhythmia in a patient treated with panitumumab.

## CASE REPORT

A 68-y-old nonsmoker man presented with intermittent hematochezia of 6-mo duration. He underwent colonoscopy, which showed a large fungating, ulcerated, and non-obstructing mass in the rectum. Biopsy from the lesion revealed infiltrating adenocarcinoma of the rectum. The carcinoembryonic antigen level was high and KRAS/NRAS/BRAF wild-type was positive. The patient underwent staging <sup>18</sup>F-FDG PET/CT, which showed an <sup>18</sup>F-FDG-avid hepatic lesion in the right lobe, in addition to an <sup>18</sup>F-FDG-avid rectal wall thickening and perirectal lymph nodes. The myocardium demonstrated diffuse blood-pool tracer activity without any distinct abnormal focal tracer uptake (Fig. 1). Biopsy from the liver lesion was positive for adenocarcinoma metastasis. The patient was staged as advanced colorectal adenocarcinoma (stage IV) and was

started on the FOLFOX regimen (folinic acid, fluorouracil, and oxaliplatin) with panitumumab. There was interim microwave thermal ablation of the hepatic lesion. After 8 cycles of combination chemotherapy, follow-up <sup>18</sup>F-FDG PET/CT was performed 9 mo after the prior imaging. It demonstrated a reduction in the metabolic activity of primary rectal mass lesion and resolution of <sup>18</sup>F-FDG avidity in the metastatic hepatic lesion. There was an incidental finding of intense <sup>18</sup>F-FDG uptake in bilateral atrial walls with relatively intense uptake in the left atrium, maximum metabolic activity (SUV<sub>max</sub>) of 9.2 (Fig. 2). The patient underwent cardiac evaluation with electrocardiography, which showed an irregular rhythm, with changes of left-axis deviation, atrial fibrillation, and a rapid ventricular response (Fig. 3). Echocardiography showed normal systolic function, with an ejection fraction of 55% and no evidence of thrombus. Comprehensive metabolic panel, including electrolytes, was within the reference range. A clinical diagnosis of cardiac arrhythmia secondary to cardiotoxicity from the antiepidermal growth factor receptor (EGFR) inhibitor panitumumab was postulated. The panitumumab was discontinued, and the patient was treated with diltiazem, with consideration of future abdominoperineal resection of the rectal tumor mass.

## DISCUSSION

Colorectal cancer is one of the most common cancers worldwide. Median survival in metastatic colorectal cancer

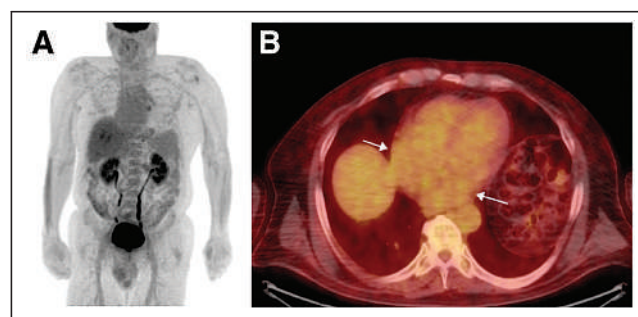


**FIGURE 1.** (A) Maximum-intensity projection of whole-body <sup>18</sup>F-FDG PET/CT pretherapy staging scan in patient with colorectal cancer. Imaging was performed 62 min after intravenous injection of 362.6 MBq (9.8 mCi) of <sup>18</sup>F-FDG. (B) Transaxial <sup>18</sup>F-FDG PET/CT image demonstrating diffuse blood-pool <sup>18</sup>F-FDG activity in myocardium (arrows), with SUV<sub>max</sub> of 3.3 and SUV<sub>min</sub> of 1.8.

Received Mar. 1, 2021; revision accepted May 20, 2021.  
For correspondence or reprints, contact Pokhraj P. Suthar (pokhraj89@gmail.com).  
Published online July 30, 2021.  
COPYRIGHT © 2021 by the Society of Nuclear Medicine and Molecular Imaging.

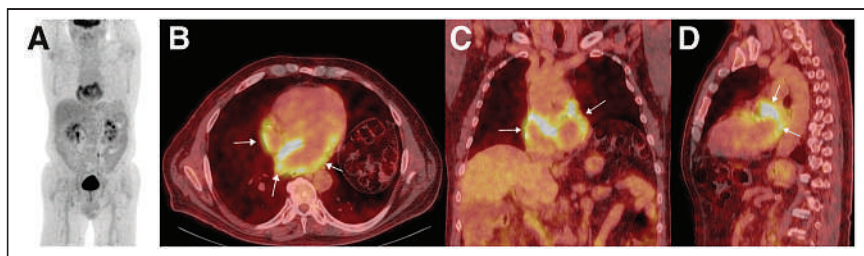


**FIGURE 2.** (A) Maximum-intensity projection of whole-body  $^{18}\text{F}$ -FDG PET/CT scan in patient who had received combination therapy (FOLFOX regimen plus panitumumab) for colorectal cancer. Imaging was performed 66 min after intravenous injection of 436.6 MBq (11.8 mCi) of  $^{18}\text{F}$ -FDG. (B–D) Transaxial (B), coronal (C), and sagittal (D)  $^{18}\text{F}$ -FDG PET/CT images demonstrating intense  $^{18}\text{F}$ -FDG uptake in bilateral atrial walls (white arrows). Uptake is more intense in left atrium, with  $\text{SUV}_{\text{max}}$  of 9.2 and  $\text{SUV}_{\text{min}}$  of 5.9.

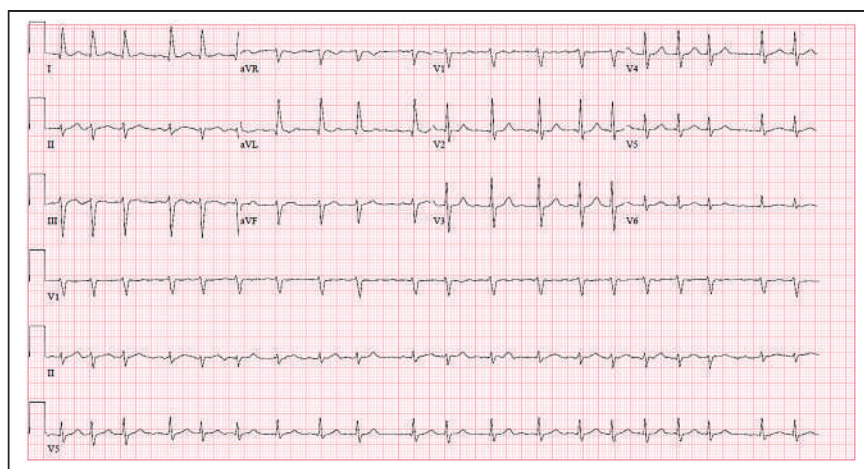


**FIGURE 3.** Electrocardiography demonstrating irregular rhythm, with changes consisting of left axis deviation, atrial fibrillation, and rapid ventricular response.

has improved because of combined use of chemotherapy and targeted agents (1) such as antivascular endothelial growth factor and anti-EGFR therapies. Panitumumab is a human immunoglobulin G2 monoclonal antibody against EGFR. It binds with the EGFR, reduces cell proliferation, and induces apoptosis (2). There are adverse effects associated with panitumumab, such as skin-related toxicities and cardiac arrhythmias. Preexisting cardiac disease and hypertension are assumed to increase the risk of developing cardiac arrhythmia (3). Qi et al. reported an overall 8.4% increase in the incidence of cardiac events with panitumumab combination therapy, as compared with 6.8% with chemotherapy alone (3).  $^{18}\text{F}$ -FDG PET/CT usually demonstrates variable tracer uptake in the myocardium, a finding that is presumed to be due to shifting of metabolism between glucose and fatty acids (4). In cases of cardiac arrhythmia, there may be distinct abnormal increase in myocardial  $^{18}\text{F}$ -FDG uptake (5). According to a study published by Sinigaglia et al. (6), diffuse increased  $^{18}\text{F}$ -FDG uptake in the atrium was seen in one third of patients with atrial fibrillation, and the intensity of  $^{18}\text{F}$ -FDG uptake

was associated with underlying heart rhythm. The article also suggested an association between an increased risk of stroke and a detectable abnormality in atrial  $^{18}\text{F}$ -FDG uptake. Though  $^{18}\text{F}$ -FDG uptake in the myocardium is considered nonspecific on  $^{18}\text{F}$ -FDG PET scans performed for oncology purposes, for the above-mentioned reason the reading physician should be aware of certain patterns of tracer uptake indicative of the underlying disease process. As seen in this case, the patient treated with panitumumab had new atrial fibrillation with increased atrial wall  $^{18}\text{F}$ -FDG activity, findings that were attributed to possible cardiotoxicity, known to be associated with anti-EGFR immunotherapy.

## CONCLUSION

Incidental findings on whole-body  $^{18}\text{F}$ -FDG PET/CT scans performed for oncological purpose may point toward underlying metabolic abnormalities. Although cardiac uptake on whole-body  $^{18}\text{F}$ -FDG PET scans is nonspecific, an abnormal myocardial  $^{18}\text{F}$ -FDG uptake pattern may occasionally warrant further investigation. Cardiotoxicity associated with panitumumab may present as an abnormal finding on  $^{18}\text{F}$ -FDG PET scans, as demonstrated in this case. Knowledge about such pat-

terns of tracer uptake will improve diagnostic efficiency and contribute to holistic patient care.

## DISCLOSURE

No potential conflict of interest relevant to this article was reported.

## REFERENCES

1. Cremolini C, Schirripa M, Antoniotti C, et al. First-line chemotherapy for mCRC: a review and evidence-based algorithm. *Nat Rev Clin Oncol*. 2015;12:607–619.
2. Anandappa G, Cunningham D. Panitumumab alone for maintenance treatment in advanced colorectal cancer. *JAMA Oncol*. 2019;5:1262–1264.
3. Qi WX, Zhao S, Chen J. Risk factors for developing cardiac toxicities in cancer patients treated with panitumumab combination therapy. *Future Oncol*. 2020;16:1359–1370.
4. Fujii H, Ide M, Yasuda S, Takahashi W, Shohitsu A, Kubo A. Increased FDG uptake in the wall of the right atrium in people who participated in a cancer screening program with whole-body PET. *Ann Nucl Med*. 1999;13:55–59.
5. Gupta K, Jadhav R, Prasad R, Virmani S. Cardiac uptake patterns in routine  $^{18}\text{F}$ -FDG PET-CT scans: a pictorial review. *J Nucl Cardiol*. 2020;27:1296–1305.
6. Sinigaglia M, Mahida B, Piekarski E, et al. FDG atrial uptake is associated with an increased prevalence of stroke in patients with atrial fibrillation. *Eur J Nucl Med Mol Imaging*. 2019;46:1268–1275.



# Bone Scanning Findings in a Patient with Heat Stroke–Induced Rhabdomyolysis

Jitesh Dhingra and Yoram Baum

Emory University Hospital, Atlanta, Georgia

We present a case that caused a diagnostic dilemma on a bone scan. We also review the broad spectrum of nonmalignant findings that can impact the interpretation of a bone scan and the value of correlative imaging using SPECT/CT for exact localization and characterization of lesions. The imaging features of important benign pathologies—that is, metastatic mimics—are elaborated so that the reader can avoid misinterpretations when reporting them. We elucidate 4 uncommon benign findings on a bone scan. Rhabdomyolysis is a result of lysis of skeletal muscle with release of cell contents, such as myoglobin and muscle enzymes, and is diagnosed mostly through a combination of clinical appearance and laboratory values. Myositis ossificans is the most common form of heterotopic ossification, usually occurring within large muscles. Its importance stems largely from its ability to mimic more aggressive pathologic processes. Myositis ossificans is one of the skeletal “do not touch” lesions. Such bone lesions are defined by characteristic imaging features, the identification of which precludes the need for additional diagnostic tests or biopsies, thereby avoiding unnecessary interventions. Acute tubular necrosis is kidney injury caused by damage to the kidney tubule cells (kidney cells that reabsorb fluid and minerals from urine as it forms). Common causes are low blood flow to the kidneys, drugs that damage the kidneys, or a severe underlying infection.

**Key Words:** renal; SPECT/CT; nonmalignant; bone scan; renal failure; rhabdomyolysis

**J Nucl Med Technol 2021; 49:362–363**

DOI: 10.2967/jnmt.121.262501

**B**one scanning continues to be the second most commonly used nuclear imaging procedure after nuclear cardiac scans, offering the advantage of total-body examination, low cost, and high sensitivity not only for metastatic lesions but also for benign conditions. Its power rests in the physiologic uptake and pathophysiologic behavior of  $^{99m}\text{Tc}$ -diphosphonates (1). Radiotracers localize in damaged skeletal muscles because calcium builds up in them and, when combined with phosphate, provides a site for radiotracer deposition (1).

In a case of suspected rhabdomyolysis, not only is bone scintigraphy a sensitive indicator of muscle damage but also the amount of uptake is proportional to the extent of myonecrosis (2–5). Specifically, in sports medicine, bone scintigraphy could be a valuable tool in discriminating bone trauma from muscle trauma (6).

We present an unusual case of a 19-y-old woman who experienced heat stroke and whose bone scan presented several unusual findings; this case demonstrates important teaching points.

## CASE REPORT

As per our institute protocol, the patient was injected with 925 MBq of  $^{99m}\text{Tc}$ -methylidiphosphonate, and after 2.5 h whole-body anterior and posterior images of the entire skeleton were obtained using a  $\gamma$ -camera with gantry motion of 10 cm/min, a matrix size of  $256 \times 1024$ , and no magnification. Subsequently, for better visualization of related

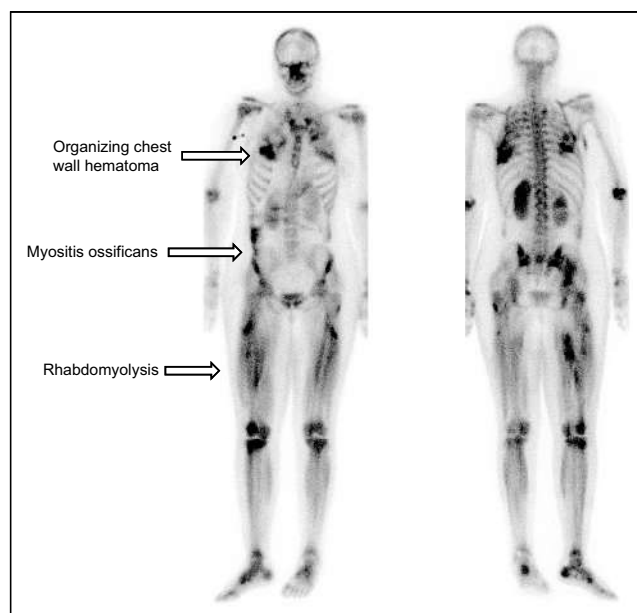


**FIGURE 1.** Whole-body  $^{99m}\text{Tc}$ -methylidiphosphonate SPECT/CT image demonstrating abnormally increased uptake in organizing chest hematoma, myositis ossificans, and rhabdomyolysis. Increased bilateral uptake in several locations in lower extremities along length of muscle corresponds to pattern of rhabdomyolysis.

Received Apr. 27, 2021; revision accepted Jun. 10, 2021.  
For correspondence or reprints, contact Jitesh Dhingra (jitesh.dhingra@emory.edu).

Published online July 30, 2021.

COPYRIGHT © 2021 by the Society of Nuclear Medicine and Molecular Imaging.



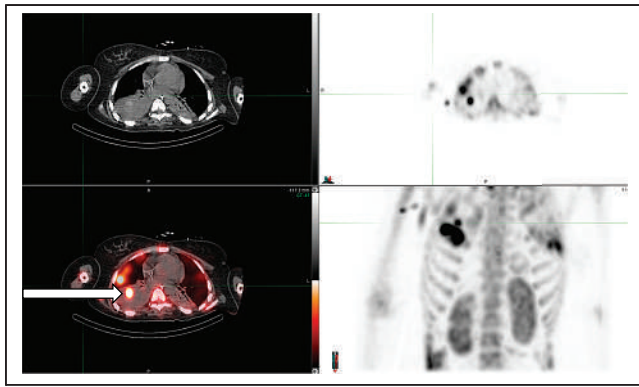


**FIGURE 2.** SPECT/CT images demonstrating abnormally increased radiotracer uptake in organizing chest wall hematoma. (Top left) CT image of chest demonstrating chest wall hematoma. (Top right) SPECT image demonstrating abnormally increased uptake within hematoma. (Bottom left) SPECT/CT image demonstrating abnormally increased radiotracer uptake (arrow) corresponding to underlying chest wall hematoma. (Bottom right) Rotating maximum-intensity projection SPECT image demonstrating focal region of uptake in right chest. Also seen is faint focus of uptake in left chest (additional site of hematoma).

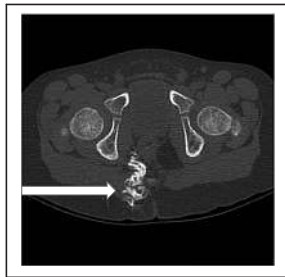


**FIGURE 3.** CT images in bone window demonstrating focus of myositis ossificans (new bone formation, arrow) in pelvis.

pathologies, SPECT images of the chest and upper abdomen were obtained using a 360° rotation, noncircular step-and-shoot mode, 128 steps, 20 s per step, a matrix size of 128 × 128, and no magnification.

The whole-body planar and SPECT/CT images demonstrated abnormal radiotracer uptake suggestive of rhabdomyolysis in the muscles of the lower extremity, abnormal bilateral cortical uptake suggestive of acute tubular necrosis

within the kidneys, greater abnormal uptake in the right than the left pleural space suggestive of organizing hematoma, and abnormal uptake within the abdominal musculature suggestive of myositis ossificans.

## DISCUSSION

Rhabdomyolysis is a complex medical condition leading to disruption of skeletal muscle integrity. This disruption can lead to the direct release of intracellular muscle components such as myoglobin, creatine kinase, aldolase, and lactate dehydrogenase into the bloodstream and extracellular space (2–4).

Bone scans are a sensitive way to visualize muscle injury and have been used with  $^{99m}\text{Tc}$ -diphosphonate and several similar agents in a wide variety of conditions, including exercise injuries (6), seizures, crush injuries, and polymyositis, and are a good indicator of acute rhabdomyolysis.



**FIGURE 4.** Planar image demonstrating abnormally increased bilateral cortical retention of radiotracer in kidneys in pattern of acute tubular necrosis.

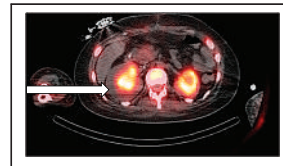


**FIGURE 5.** SPECT/CT image demonstrating abnormal bilateral cortical retention of radiotracer in kidneys, corresponding to acute tubular necrosis.

Myositis ossificans is essentially metaplasia of the intramuscular connective tissue resulting in extraosseous bone formation. Examination of the soft-tissue lesion using  $^{99m}\text{Tc}$ -diphosphonate bone scans has been helpful in establishing the diagnosis and in determining the full extent of the process early in its evolution (6).

Another important utility of  $^{99m}\text{Tc}$ -diphosphonate bone scans lies in evaluation of acute renal failure after exercise with flank pain and patchy renal vasoconstriction due to acute tubular necrosis. These findings have been shown in multiple reports, with a prominent example being one written by Watanabe et al. (7). We also found an organizing pleural hematoma with radiotracer uptake. Localization of bone-imaging  $^{99m}\text{Tc}$ -diphosphonate agents has previously been described in abdominal, chest wall, and pelvic hematomas (8,9).

## CONCLUSION

It is extremely important for all 4 benign conditions described above to be recognized on a bone scan. We hope this report educates the reader about the types of uncommon conditions that can be seen on bone scans.

## DISCLOSURE

No potential conflict of interest relevant to this article was reported.

## REFERENCES

- Brenner AI, Koshy J. The bone scan. *Semin Nucl Med.* 2012;42:11–26.
- Sanders JA. Rhabdomyolysis detected by bone imaging. *Clin Nucl Med.* 1989;14:431–432.
- Steuart RD, Morrison RT, Lot L. An incidental finding of rhabdomyolysis on bone scintigraphy: case report. *J Nucl Med Technol.* 1993;21:63–64.
- Torres PA, Helmstetter JA, Kaye AM, Kaye AD. Rhabdomyolysis: pathogenesis, diagnosis, and treatment. *Ochsner J.* 2015;15:58–69.
- Tyler JL, Derbekyan V, Lisbona R. Early diagnosis of myositis ossificans with  $^{99m}\text{Tc}$  diphosphonate imaging. *Clin Nucl Med.* 1984;9:256–258.
- Williamson MR, Archibeque F, Eisenberg B, Williamson S, Rosenberg R.  $^{99m}\text{Tc}$  pyrophosphate localization in chest wall muscles after bench pressing. *Clin Nucl Med.* 1989;14:546.
- Watanabe N, Shimizu M, Kageyama M, Kamei T, Seto H, Kakishita M. Diffuse increased renal uptake on bone scintigraphy in acute tubular necrosis. *Clin Nucl Med.* 1994;19:19–21.
- Park C, LaRoy L, Ali A, Fordham EW. Pelvic hematoma diagnosed on  $^{99m}\text{Tc}$  methylene diphosphonate bone imaging. *Clin Nucl Med.* 1989;14:139–140.
- Bhattacharya A, Prasad V, Mittal BR.  $^{99m}\text{Tc}$  MDP uptake in a soft tissue hematoma of the chest wall. *Clin Nucl Med.* 2004;29:454–455.

# The most powerful words you'll ever hear.


# **“Thank You.”**

With your contribution, our profession can continue efforts leading to critical advances in cancer treatments and care.

The **Value Initiative Transformative Leadership Campaign** is the cornerstone for making these efforts a reality for patients of all ages.

**The world needs more “thank you’s.”**

Help improve the life of a patient. Lend your support today.

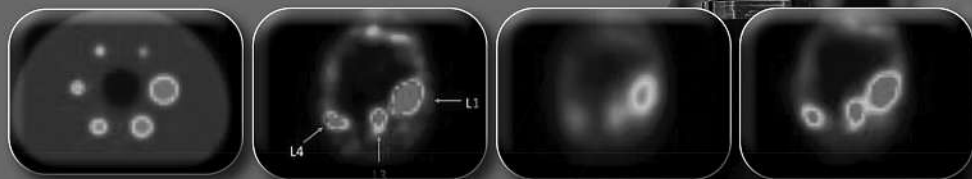


Make Your Tax-Deductible  
Donation by December 31

[www.snmmi.org/TransformativeLeadership](http://www.snmmi.org/TransformativeLeadership)

SNMMI is a 501 (c)(3) tax id 36-2496678. Your donation is tax deductible as per current IRS regulations. Please remember SNMMI in your estate plans.

**SNMMI** | Value Initiative  
**MI** |  
SOCIETY OF NUCLEAR MEDICINE & MOLECULAR IMAGING



Rue Bourbon  
**Bourbon**

## Explore the Latest Innovations and Clinical Applications in Radiopharmaceutical Therapy

Register now to attend the **SNMMI 2022 Therapeutics Conference**, taking place **March 10-12** in **New Orleans, LA**.

As an attendee, you'll have the opportunity to connect directly with an esteemed group of experts and learn more about the latest innovations and clinical applications in radiopharmaceutical therapy.

### Topics include:

- Operational Issues
- Radiation Safety and Research
- MIBG
- Dosimetry
- Lymphoma/Leukemia
- Neuroendocrine Cancer
- Prostate Cancer
- Thyroid
- Future Strategies for Radiopharmaceutical Therapy

Join us in New Orleans, reconnect with colleagues, and be part of the discussion on the future of personalized medicine. Register early. Space is limited.

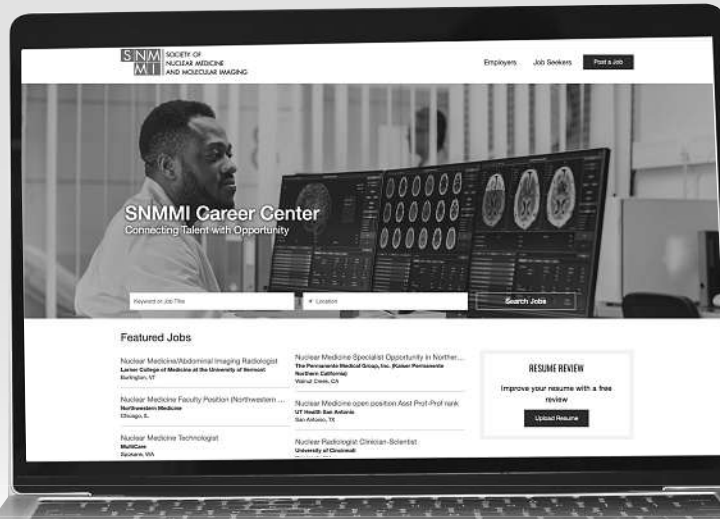


Learn more and register today!  
[www.snmmi.org/TC2022](http://www.snmmi.org/TC2022)

**Early-bird Deadline: January 20, 2022**

# Explore SNMMI's New Online Career Center!

SNMMI is proud to announce the launch of our new and improved SNMMI Career Center. Explore the benefits of our new career center by logging in or creating a new account today.



**careercenter.snmmi.org**

*\*Note: Single sign-on has been enabled for this platform and you can use your member login credentials to access the Career Center. If you are unsure of your password, to go to the SNMMI password reset link to create a new password.*



## Statement of Ownership, Management, and Circulation (All Periodicals Publications Except Requester Publications)

1. Publication Title <b>JOURNAL OF NUCLEAR MEDICINE TECHNOLOGY</b>	2. Publication Number <b>966 - 500</b>	3. Filing Date <b>10/1/2021</b>
4. Issue Frequency <b>QUARTERLY</b>	5. Number of Issues Published Annually <b>4</b>	6. Annual Subscription Price <b>\$237 US/Can; \$252 Intl</b>
7. Complete Mailing Address of Known Office of Publication (Not printer) (Street, city, county, state, and ZIP+4®) <b>1850 Samuel Morse Dr., Reston, VA 20190</b>		Contact Person <b>Rebecca Maxey</b> Telephone (Include area code) <b>703-652-6772</b>
8. Complete Mailing Address of Headquarters or General Business Office of Publisher (Not printer) <b>1850 Samuel Morse Dr., Reston, VA 20190</b>		
9. Full Names and Complete Mailing Addresses of Publisher, Editor, and Managing Editor (Do not leave blank) Publisher (Name and complete mailing address) <b>Society of Nuclear Medicine and Molecular Imaging, 1850 Samuel Morse Dr., Reston, VA 20190</b> Editor (Name and complete mailing address) <b>Kathy S. Thomas, 1850 Samuel Morse Dr., Reston, VA 20190</b> Managing Editor (Name and complete mailing address) <b>Rebecca Maxey, 1850 Samuel Morse Dr., Reston, VA 20190</b>		
10. Owner (Do not leave blank. If the publication is owned by a corporation, give the name and address of the corporation immediately followed by the names and addresses of all stockholders owning or holding 1 percent or more of the total amount of stock. If not owned by a corporation, give the names and addresses of the individual owners. If owned by a partnership or other unincorporated firm, give its name and address as well as those of each individual owner. If the publication is published by a nonprofit organization, give its name and address.) Full Name <b>Society of Nuclear Medicine and Molecular Imaging</b> Complete Mailing Address <b>1850 Samuel Morse Dr., Reston, VA 20190</b>		
11. Known Bondholders, Mortgagees, and Other Security Holders Owning or Holding 1 Percent or More of Total Amount of Bonds, Mortgages, or Other Securities. If none, check box <input checked="" type="checkbox"/> None Full Name <b>Society of Nuclear Medicine and Molecular Imaging</b> Complete Mailing Address <b>1850 Samuel Morse Dr., Reston, VA 20190</b>		
12. Tax Status (For completion by nonprofit organizations authorized to mail at nonprofit rates) (Check one) The purpose, function, and nonprofit status of this organization and the exempt status for federal income tax purposes: <input checked="" type="checkbox"/> Has Not Changed During Preceding 12 Months <input type="checkbox"/> Has Changed During Preceding 12 Months (Publisher must submit explanation of change with this statement)		

PS Form 3526, July 2014 [Page 1 of 4 (see instructions page 4)] PSN: 7530-01-000-9931

PRIVACY NOTICE: See our privacy policy on [www.usps.com](http://www.usps.com).

13. Publication Title <b>JOURNAL OF NUCLEAR MEDICINE TECHNOLOGY</b>	14. Issue Date for Circulation Data Below <b>SEPTEMBER 2021</b>
15. Extent and Nature of Circulation	
Average No. Copies Each Issue During Preceding 12 Months	
No. Copies of Single Issue Published Nearest to Filing Date	
a. Total Number of Copies (Net press run)	
2303	
2487	
b. Paid Circulation (By Mail and Outside the Mail)	
(1) Mailed Outside-County Paid Subscriptions Stated on PS Form 3541 (Include paid distribution above nominal rate, advertiser's proof copies, and exchange copies)	2124
(2) Mailed In-County Paid Subscriptions Stated on PS Form 3541 (Include paid distribution above nominal rate, advertiser's proof copies, and exchange copies)	0
(3) Paid Distribution Outside the Mails Including Sales Through Dealers and Carriers, Street Vendors, Counter Sales, and Other Paid Distribution Outside USPS®	46
(4) Paid Distribution by Other Classes of Mail Through the USPS (e.g., First-Class Mail®)	0
c. Total Paid Distribution (Sum of 15b (1), (2), (3), and (4))	
2170	
2345	
d. Free or Nominal Rate Distribution (By Mail and Outside the Mail)	
(1) Free or Nominal Rate Outside-County Copies included on PS Form 3541	0
(2) Free or Nominal Rate In-County Copies included on PS Form 3541	0
(3) Free or Nominal Rate Copies Mailed at Other Classes Through the USPS (e.g., First-Class Mail)	0
(4) Free or Nominal Rate Distribution Outside the Mail (Carriers or other means)	26
e. Total Free or Nominal Rate Distribution (Sum of 15d (1), (2), (3), and (4))	
26	
26	
f. Total Distribution (Sum of 15c and 15e)	
2196	
2371	
g. Copies not Distributed (See Instructions to Publishers #4 (page #3))	
107	
116	
h. Total (Sum of 15f and g)	
2303	
2487	
i. Percent Paid (15c divided by 15f times 100)	
98.81%	
98.99%	
* If you are claiming electronic copies, go to line 16 on page 3. If you are not claiming electronic copies, skip to line 17 on page 3.	
16. Electronic Copy Circulation	
Average No. Copies Each Issue During Preceding 12 Months	
No. Copies of Single Issue Published Nearest to Filing Date	
a. Paid Electronic Copies	
b. Total Paid Print Copies (Line 15c) + Paid Electronic Copies (Line 16a)	
c. Total Print Distribution (Line 15f) + Paid Electronic Copies (Line 16a)	
d. Percent Paid (Both Print & Electronic Copies) (16b divided by 16c x 100)	
<input checked="" type="checkbox"/> I certify that 50% of all my distributed copies (electronic and print) are paid above a nominal price.	
17. Publication of Statement of Ownership	
<input checked="" type="checkbox"/> If the publication is a general publication, publication of this statement is required. Will be printed in the <b>December 2021</b> issue of this publication.	
<input type="checkbox"/> Publication not required.	
18. Signature and Title of Editor, Publisher, Business Manager, or Owner	
Date <b>10/1/2021</b>	



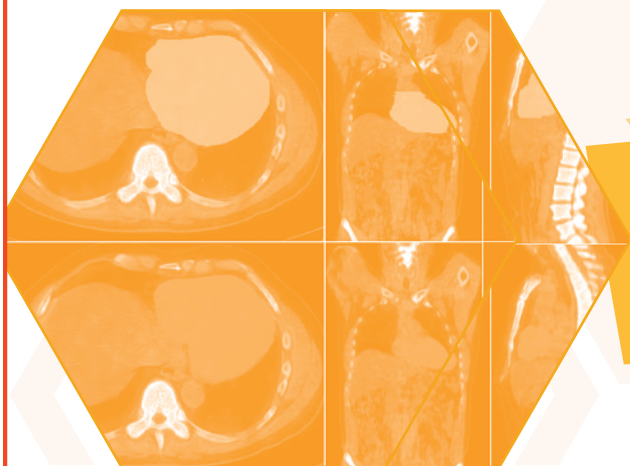
# Learn about the Latest Clinical Applications & Best Practices in Nuclear Cardiology

Make your plans to attend the **2022 SNMMI Mid-Winter and ACNM Annual Meeting**—January 27-29 in Orlando, Florida.

Featuring a dedicated track on nuclear cardiology, the 2022 meeting's intimate, focused setting provides you with an ideal environment to learn and collaborate with luminaries in the field and expand your knowledge on the latest clinical applications and best practices in cardiovascular imaging.

## Sessions include:

- ✓ Imaging Guided Management of CAD
- ✓ Blood Flow Quantification
- ✓ New Cardiac Radiotracers
- ✓ New Cardiac Instrumentation
- ✓ New Software/AI for Cardiac SPECT and PET
- ✓ Cardiac Hybrid Imaging
- ✓ Imaging of Cardiac Sarcoidosis
- ✓ Radionuclide Imaging in Cardiac Amyloidosis
- ✓ Clinical Controversies Relevant to Cardiac Imaging
- ✓ Cardiac Infection Imaging



EARLY-BIRD REGISTRATION ENDS:

**DECEMBER 16, 2021**

[www.snmmi.org/MWM2022](http://www.snmmi.org/MWM2022)

At this time, the 2022 SNMMI Mid-Winter and ACNM Annual Meeting is scheduled to be held in person in Orlando, Florida. We will continue to monitor the ongoing conditions in Florida and across the world and communicate any changes to the meeting should they arise. **Currently, there is no plan to offer a virtual or hybrid element for this meeting.**

Please note: SNMMI is committed to ensuring that appropriate and necessary health and safety protocols will be in place for this event. We will follow all Centers for Disease Control and Prevention (CDC) safety protocols and recommendations and will comply with all federal, state, and local regulations. **Attendees must be fully vaccinated for COVID-19 and masks will be required.**

January 27-29  
**2022**  
**SNMMI MID-WINTER &  
ACNM ANNUAL MEETING**

**HILTON ORLANDO  
LAKE BUENA VISTA  
ORLANDO, FLORIDA**



2022 *Mid-Winter*  
**Meeting**

**ACNM**  
ANNUAL MEETING



**RADQUAL**  
*Global Sources*

Quality Radioactive  
Sources:  
It's in our name!

## Ge-68 PET Cylinders & Transmission Rods



Available in lengths of 19cm, 27cm and 30cm

Contact a distributor today for pricing and availability.  
Mention this ad for free shipping

[www.radqual.com](http://www.radqual.com)

1(800)699-3108

[info@radqual.com](mailto:info@radqual.com)



